



2010

DEVELOPMENT OF NOVEL AHR ANTAGONISTS

Hyosung Lee

University of Kentucky, hyosung.f.lee@gmail.com

[Click here to let us know how access to this document benefits you.](#)

Recommended Citation

Lee, Hyosung, "DEVELOPMENT OF NOVEL AHR ANTAGONISTS" (2010). *University of Kentucky Doctoral Dissertations*. 103.
https://uknowledge.uky.edu/gradschool_diss/103

This Dissertation is brought to you for free and open access by the Graduate School at UKnowledge. It has been accepted for inclusion in University of Kentucky Doctoral Dissertations by an authorized administrator of UKnowledge. For more information, please contact UKnowledge@lsv.uky.edu.

ABSTRACT OF DISSERTATION

Hyosung Lee

The Graduate School

University of Kentucky

2010

DEVELOPMENT OF NOVEL AHR ANTAGONISTS

ABSTRACT OF DISSERTATION

A dissertation submitted in partial fulfillment of the requirements for the degree of Doctor of Philosophy in the College of Pharmacy at the University of Kentucky

By
Hyosung Lee

Lexington, Kentucky

Director: Dr. Kyung Bo Kim, Associate Professor of Pharmaceutical Sciences

Lexington, Kentucky

2010

Copyright © Hyosung Lee 2010

ABSTRACT OF DISSERTATION

DEVELOPMENT OF NOVEL AHR ANTAGONISTS

Aryl hydrocarbon receptor (AHR) is a sensor protein, activated by aromatic chemical species for transcriptionally regulating xenobiotic metabolizing enzymes. AHR is also known to be involved in a variety of pathogenesis such as cancer, diabetes mellitus, cirrhosis, asthma, etc. The AHR signaling induced by xenobiotics has been intensively studied whereas its physiological role in the absence of xenobiotics is poorly understood. Despite a number of ligands of AHR have been reported thus far, further applications are still hampered by the lack of specificity and/or the partially agonistic activity. Thus, a pure AHR antagonist is needed for deciphering the AHR cryptic as well as potential therapeutic agent. The Proteolysis Targeting Chimera (PROTAC) is a bi-functional small molecule containing a ligand and proteolysis inducer. PROTAC recruits the target protein to proteolysis machinery and elicits proteolysis. Thus far, a number of PROTAC have been prepared and demonstrated to effectively induce the degradation of targeted protein in cultured cells, validating PROTAC as a useful research tool. In the present study, PROTACs based on apigenin was prepared and demonstrated to induce the degradation of AHR, providing the proof of concept. To improve activity, a synthetic structure, CH-223191, was optimized for antagonistic activity by positional scanning identifying several AHR antagonists. PROTACs based on the optimal structure were prepared and assessed their biological activity. The products and synthetic scheme described hereby will be helpful for the further understanding on AHR biology as well as for developing therapeutic agents targeting AHR.

KEYWORDS: PROTAC, Aryl hydrocarbon Receptor, AHR, antagonist, positional optimization, ubiquitin proteasome system, UPS.

Hyosung Lee

February, 2010

DEVELOPMENT OF NOVEL AHR ANTAGONISTS

By

Hyosung Lee

Kyung Bo Kim, Ph. D.
Director of Dissertation

Robert Yokel, Ph. D.
Director of Graduate Studies

February, 2010

DISSERTATION

Hyosung Lee

The Graduate School

University of Kentucky

2010

DEVELOPMENT OF NOVEL AHR ANTAGONISTS

DISSERTATION

A dissertation submitted in partial fulfillment of
the requirements for the degree of Doctor of Philosophy in the
College of Pharmacy at the University of Kentucky

By
Hyosung Lee

Lexington, Kentucky

Director: Kyung Bo Kim, Ph.D., Associate Professor of Pharmaceutical Sciences

Lexington, Kentucky

2010

Copyright © Hyosung Lee 2010

ACKNOWLEDGEMENTS

I have met a lot of people who should be recognized. This dissertation would not be completed without their help. I would like to express my sincere appreciation to all the people who assisted, supported, inspired and encouraged me to complete my dissertation.

My first debt of gratitude must go to my dedicated advisor, Dr. Kyung Bo Kim. Without his guidance and support, the completion of this dissertation would not have been possible.

Special thanks to my committee, Dr. Jurgen Rohr, Dr. Hollie I. Swanson, Dr. Gragory Elliott for their insightful advices and valuable suggestions.

As well, special thanks go to my dear lab members, classmates and colleagues at UK PS DDD, especially to Dr. Sun-Hee Baek, Dr. Abby Ho, Dr. Kedra Cyrus, Marie Wehenkel, Kim Cornish, Jee Eun Kim, Domin Lee, Sung Hee Park, Eyob Adane, Lipeng Wang, Michael Smith, Madan Kharel and Pallab Pahari for their assistance, friendship, and support on the days of study. Additionally, the people who participated in my study also deserve the credit for their contribution.

Finally, I wish to offer my cordial gratitude to my parents, my brother, Soosung and my girl friend, Seoyoung Lee, for their tolerance and understanding during my graduate years. Their support and encouragement made it possible for me to overcome the anxieties and difficulties throughout the years.

TABLE OF CONTENTS

ACKNOWLEDGEMENTS	iii
LIST OF FIGURES	vi
CHAPTER 1 OVERVIEW	1
Specific Aims	2
CHAPTER 2 INTRODUCTION.....	4
2.1 Aryl hydrocarbon Receptor	4
2.1.1 Signaling pathway	5
2.1.2 The functions of AHR in cells.....	7
2.1.3 Clinical implication of AHR	8
2.2 Chemical approach to AHR biology	10
2.2.1 Agonistic ligands of AHR	10
2.2.2 Antagonists.....	15
2.3 PROTAC technology	17
2.4 The development of PROTAC as an antagonist of AHR signaling pathway ..	20
CHAPTER 3 PROTAC BASED ON NATURAL PRODUCT	22
3.1 Introduction.....	22
3.2 Apigenin and PROTAC.....	23
3.2.1 Optimization of coupling position	23
3.2.2 Synthesis of PROTACs based on apigenin	25
3.2.3 Biological assessment of PROTACs based on apigenin.....	27
3.2.4 Confirmation of biological activity of PROTAC2 (4, 128).....	29
3.2.5 Characterization of PROTAC2.....	31
3.3 Discussion.....	33

3.4 Materials and Methods	35
CHAPTER 4 IDENTIFICATION OF NOVEL AHR LIGANDS	45
4.1 Introduction.....	45
4.2 The construction of privileged library.....	46
4.2.1 C Ring optimization.....	47
4.2.2 A ring optimization.....	50
4.2.3 Ring B optimization and fine tuning.....	53
4.2.4 Antagonistic evaluation of diphenyldiazenyl amines	54
4.3 Discussion.....	56
4.4 Syntheses of compounds	57
CHAPTER 5 PROTAC BASED ON THE SYNTHETIC LIGAND	78
5.1 Introduction.....	78
5.2 Synthesis and biological evaluation of PROTAC4.....	78
5.3 C ring-linked PROTACs	81
5.4 Discussion.....	84
CHAPTER 6 CONCLUSION.....	100
6.1 Discussion.....	100
6.2 Summary.....	101
6.3 Conclusions.....	102
6.4. Future directions	102
REFERENCES.....	104
VITA	118

LIST OF FIGURES

Figure 2.1 Functional domains of Aryl hydrocarbon Receptor	4
Figure 2.2 Signaling pathway of AHR	6
Figure 2.3 Classic synthetic ligands of AHR	11
Figure 2.4 Non-classical ligands of AHR	13
Figure 2.5 Naturally occurring ligands and endogenous ligands of AHR.....	14
Figure 2.6 Antagonists of AHR.....	16
Figure 2.7 Structure of PROTAC	17
Figure 2.8 Mechanism of PROTAC	18
Figure 2.9 The AHR antagonism induced by PROTAC	21
Figure 3.1 Phytochemicals interacting with AHR.....	22
Figure 3.2 The synthesis of acetylated apigenins.....	23
Figure 3.3 The effect of apigenin and acetylated derivatives on the activation of AHR ..	24
Figure 3.4 Synthetic schemes for the preparation of apigenin-based PROTACs	25
Figure 3.5 Synthetic schemes for the preparation of E3 ligase recognition peptide	26
Figure 3.6 The structures and activities of apigenin-based PROTACs.....	28
Figure 3.7 PROTAC2 induces degradation of AHR	30
Figure 3.8 The characterization of PROTAC2	32
Figure 4.1 The structure of N-[2-methyl-4-[(2-methylphenyl)diazenyl]-phenyl]-1-Methyl- 1H-pyridiazenylle-5-carboxamide and the synthetic approach for combinatorial chemistry	46

Figure 4.2 Synthetic scheme and the resulting library of C ring substituted analogues of 2-methyl-4-[(2-methylphenyl)diazenyl]phenyl carboxamides.....	48
Figure 4.3 Biological activities of C ring substituted analogues.....	49
Figure 4.4 Synthetic scheme and the resulting library of C ring substituted analogues of 2-methyl-4-[(methylphenyl)diazenyl]phenyl picolinic carboxamides	50
Figure 4.5 Biological activities of A ring or B ring substituted analogues	52
Figure 4.6 Synthetic scheme and the resulting library of diphenyldiazenyl picolinic carboxamides	53
Figure 4.7 Synthetic scheme and the resulting library of diphenyldiazenyl amines	54
Figure 4.8 Biological activities of diphenyldiazenyl amines	55
Figure 5.1 Synthesis of PROTAC4	78
Figure 5.2 The Biological activity of PROTAC4	80
Figure 5.3 Synthetic scheme of C ring linked PROTACs	81
Figure 5.4 C Ring linked PROTACs with various spacer lengths	82
Figure 5.5 The effect of PROTAC8 on the cellular level of AHR.....	83
Figure 5.6 Mass spectrum for PROTAC4	87
Figure 5.7 Mass spectrum for PROTAC5	91
Figure 5.8 Mass spectrum for PROTAC6	93
Figure 5.9 Mass spectrum for PROTAC7	94
Figure 5.10 Mass spectrum for PROTAC8.....	96
Figure 5.11 Mass spectrum for PROTAC9.....	97
Figure 5.12 Mass spectrum for PROTAC10.....	99

CHAPTER 1 OVERVIEW

With the advent of the proteomics era, elucidation of protein function is of great importance in developing novel therapeutic agents and dissecting complex signaling pathways. While a number of useful approaches have been used to investigate the function of proteins, their applications are often limited due to difficulties with temporal and spatial control of protein function. Furthermore, these approaches are also constrained to a certain subset of signaling molecules.

Traditionally, small molecules have played a crucial role in the drug development process by providing lead compounds. In recent years, small molecules have been increasingly serving an additional purpose as a molecular probe in investigating principles underlying biology. Therefore, the development of novel chemical agents modulating protein function has become of more importance in elucidating the role of proteins in biological processes.

Proteolysis Targeting Chimera (PROTAC) is a novel class of small molecules that target proteins of interest for degradation. PROTACs recruit targeted proteins to E3 ubiquitin ligase complex for ubiquitination and subsequent degradation by the proteasome. Up to the present time, a number of proteins have been successfully targeted for degradation by the PROTAC approach (1-5), validating the PROTAC approach as a novel tool for perturbing protein function. AHR is a ligand-activated transcription factor, regulating the metabolism of xenobiotics (6). Even though considerable effort has been devoted to the study of the roles of AHR in human physiology, the knowledge gained from these studies is still limited due to the lack of appropriate molecular tools. In addition, emerging data suggest that AHR may play a role in disease development and progression. Furthermore, recent studies indicate that AHR is a potentially therapeutic target. Therefore, the development of novel molecular tool that can modulate AHR function is urgently needed to investigate the complex AHR biology as well as to validate the AHR as a therapeutic target. With these in mind, we envision that AHR-targeting PROTACs and the synthetic procedures will provide useful molecular tools as well as a lead compound to be used for further development of AHR-targeting therapeutic agents.

Specific Aims

The overall goal of this study is to develop a novel antagonist of the aryl hydrocarbon receptor (AHR) as a research tool to explore AHR biology as well as a potential therapeutic agent. The rationale underlying the proposed study was based on the fact that there is no pure AHR antagonist currently available for use of dissecting the complex AHR biology. Further, the PROTACs may provide potential therapeutic agents by targeting disease-promoting proteins. Taken together, we hypothesized that AHR-targeting PROTAC will provide a pure and specific antagonist of AHR. To test this, the following specific aims were set forth:

1) Determine whether the AHR is targeted by the PROTAC approach

A number of phytochemicals were identified as AHR antagonists. Among these, apigenin and kaempferol were selected for the synthesis of PROTAC. The SAR study of apigenin revealed that derivatization at hydroxyl groups of apigenin is tolerated for its AHR antagonistic activity. Thus, PROTACs were prepared by linking E3 ligase recognition residue at the 4' hydroxyl group of apigenin and tested for their activity of AHR degradation. Similarly, kaempferol-based PROTACs were prepared and tested for their activity.

2) Identify AHR additional antagonists by constructing and screening a chemical library

Despite the promising potential of the apigenin-based PROTAC, its target specificity is a major concern due to apigenin's multiple targets in cells. Therefore, we aim to develop specific AHR ligands and prepare PROTACs based on the specific AHR ligands. To develop specific AHR antagonists, we have built a small molecule library using the core structure of a known synthetic AHR antagonist, CH-223191 and have identified a number of AHR ligands.

3) Develop synthetic AHR antagonist-based PROTACs

Synthetic antagonist-based PROTACs were synthesized by introducing a ‘handle’ at the several positions of AHR ligands selected above. To optimize AHR degradation, several PROTACs with varying linker lengths were prepared.

4) Determine the activity of PROTACs in living cells.

Using Western blot, we investigated the ability of PROTACs to degrade the AHR. In addition, it was examined whether PROTACs inhibit TCDD-induced AHR transcriptional activation. Further, the transcription of downstream genes was investigated using RT-PCR.

CHAPTER 2 INTRODUCTION

2.1 Aryl hydrocarbon Receptor

AHR is a ligand activated transcription factor, which is classified as a member of the basic helix-loop-helix/Per-Arnt-Sim (bHLH/PAS) family (7). AHR has long been recognized to mediate the toxic effects of exogenous chemical agents, including polycyclic and halogenated aromatic hydrocarbons (8-13). Recently, additional functions of AHR have been reported. Recent data indicates that AHR is implicated in cell cycle regulation, reproduction, development, circadian rhythm, and immune response by playing a pivotal role in key signaling networks. Hence, it has been suggested that the perturbation of this network by this xenobiotic chemical agent may cause toxicity and diseases (14).

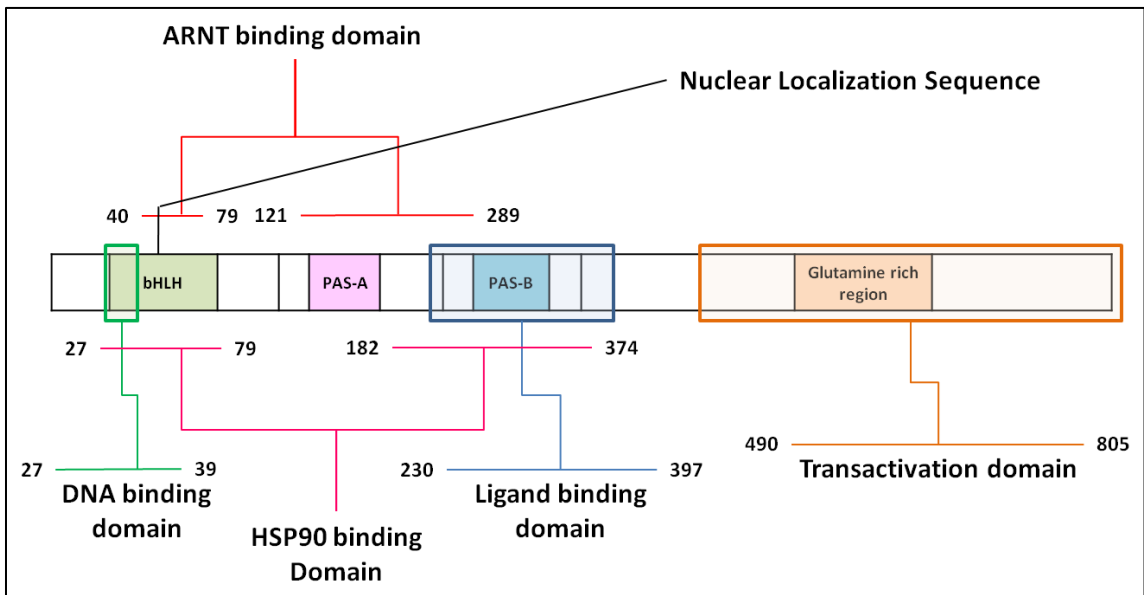


Figure 2.1 Functional domains of Aryl hydrocarbon Receptor

AHR protein is comprised of a number of functionally distinctive domains, the DNA binding domain in the N-terminal (15, 16), ligand binding domain in the middle (17,

18) and transactivational domain in the C-terminus (19). The DNA binding domain of AHR is contained within the bHLH region and PAS regions are responsible for the interaction with aryl hydrocarbon receptor nucleus translocator (ARNT) (20) (17, 18). AHR has two PAS consensus domains, PAS-A and PAS-B (17, 21). The PAS domains support the PAS-PAS interaction for dimerization with ARNT (17, 18). The PAS-B contains ligand binding site that initiates the signaling pathways transduction (22). The glutamine rich region (QRR) is located in the C-terminal region and supports recruitment of co-activator for transcriptional activation (23, 24). The nucleus localization sequence (NLS) is located in the bHLH motif and is responsible for the trafficking of AHR into nucleus (25-27).

2.1.1 Signaling pathway

In cells, an inactive AHR is bound to a chaperone complex consisting of a dimer of Heat Shock Protein 90 (HSP90), hepatitis B virus X-associated protein 2 (XAP2), aryl hydrocarbon receptor activated 9 (ARA9) and prostaglandin E synthase 3 (p23) (28). The complex protects AHR from proteolysis, prevents premature binding of ARNT and helps the ligand bind to AHR. Upon binding of ligand to an inactive AHR complex, XAP2 and ARA9 are released from the complex exposing the NLS, leading translocation of AHR into the nucleus (26, 29). Once in the nucleus, activated AHR is released from the complex exposing PAS domains resulting in dimerization with ARNT and binding to responsive elements for gene regulation (18, 30).

The recognition motif of the AHR/ARNT dimer is the xenobiotic responsive element (XRE). It is also referred to as TCDD responsive element (DRE) or AHR responsive element (AHRE). A large number of genes are regulated by the interaction of AHR with XRE resulting in a wide variety of end results, highlighting the importance of AHR in physiology. While XRE is extensively characterized, the second type of XRE (AHRE-II) is recently identified and is thought to regulate an additional set of genes (31).

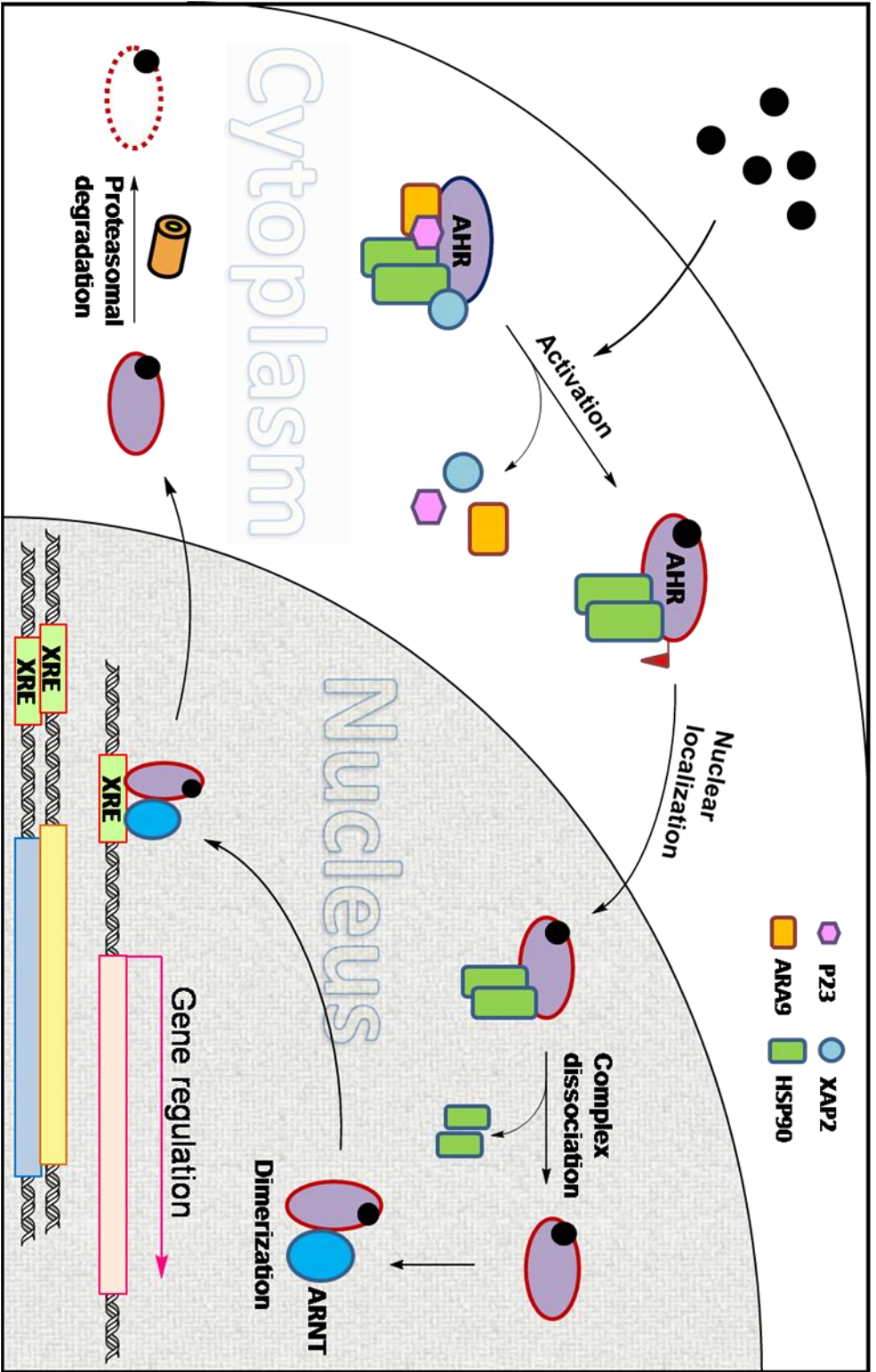


Figure 2.2 Signaling pathway of AHR

Though the ligand binding of AHR triggers the signaling pathways, other factors also contribute to the regulation of the AHR transcriptional activity. For example, protein kinase C activity is required for the transcriptional activity of AHR (32). In summary, the activation of AHR-mediated signaling pathways is regulated by several signaling factors, suggesting that various signaling pathways plausibly converge into the AHR-mediated gene regulation.

2.1.2 The functions of AHR in cells

The general role of AHR has long been known as a master regulator of xenobiotic metabolizing enzymes (XMEs). The activation of AHR pathway up-regulates the expression of genes involved in xenobiotic metabolism, such as cytochrome p450 1A1 (CYP1A1), cytochrome p450 1A2 (CYP1A2), cytochrome p450 1B1 (CYP1B1), aldehyde dehydrogenase 3A1 (ALDH3A1), NADPH-quinone-oxidoreductase (NQO), and the phase II conjugating enzymes glutathione-S-transferase A1 (GSTA1) and UDP-glucuronosyltransferase 1A2 (UGT1A2) (33).

AHR signaling pathway is triggered by a class of chemical agents, termed aryl hydrocarbons. Generally, the ligand which triggers AHR signaling pathway is the target of the AHR-regulated gene products, including XMEs. Therefore, it is thought that the metabolism of the ligand is the primary role of AHR. However, the identification of additional genes regulated by AHR, such as TGF α , p27^{Kip1}, COX-2 and an inhibitor of the TGF- β signaling pathway (latent TGF- β binding protein: LTBP-1) indicate that the AHR function is multifaceted (34-39). In addition, some mitogen-activated kinases (MAPKs) related to cell cycle regulation, such as extracellular signal-regulated kinases (ERKs), c-Jun N-terminal protein kinases (JNKs) and p38, have been shown to cross-talk with the AHR signaling pathway (40-42). In addition, un-anticipated functions of AHR have been reported, such as induction of estrogen receptor α (ER α) ubiquitination and degradation (43). The regulatory function of AHR with respect to the immune response has also been reported (44-46). Furthermore, the role of AHR is also reported in developmental process of the heart, brain, and liver (47-50). The level of AHR

culminates between postnatal day (PND) 3-10, this period is critical for the development of cerebellar granular neuroblasts (50). The complete closure of fetal specific shunts is important for the proper development of heart and liver. The cardiomyopathy and vascular hypertrophy were observed in AHR knocked-out animal and liver hypotrophy was observed as well. These anomalies are thought to be due to the incomplete closure of the fetal specific shunts, ductus arteriosus, foramen ovale, and ductus venosus (48, 51). Ductus arteriosus is a shunt connecting the pulmonary artery to aorta and foramen ovale is a hole between the right and left atriums. The fetus acquires the oxygenated blood from umbilical vein, hence the pulmonary circulation is not required and the fetus develops these shunts. They protect the lung and allow the left ventricle to strengthen. The failure to close these shunts elicits hypertrophic cardiomyopathy (52). Ductus venosus is a shunt bypassing the liver from the placenta to the inferior vena cava. It helps the nourished and oxygenated blood flow directly to the fetal brain. The incomplete closure of this shunt interrupts the liver development resulting in the liver hypotrophy (53). Various anomalies have been reported in AHR knock out animal such as the T cell deficiency and insulin resistance as well (48).

Taken together, it is clear that the role of AHR in tissue homeostasis and development process is diverse. However, the detailed mechanistic understanding underlying the role of AHR in cells is yet to be fully understood.

2.1.3 Clinical implication of AHR

As aforementioned, the AHR is involved in many crucial biological processes. Due to its ligand-activated nature, it is presumed that the dysregulation of AHR pathways will disrupt signaling network, resulting in pathophysiological conditions. Given that the AHR is widely known to mediate the toxicity of xenobiotics, the correlation between chemical compounds produced by human activities and their physiological consequences have been intensively studied. In this regard, many studies have shown that anomalies in AHR signaling pathway can result in cancer, hyperreactivity, hydronephrosis, diabetes

mellitus, cirrhosis, cleft palate, and the other developmental failures such as patent ductus arteriosus (53-58).

Cancer, hyperreactivity and hydronephrosis are thought to be arisen from inappropriate activation of AHR while other anomalies are caused by failure of AHR activation. The exposure to environmental factors are thought to be, at least in part, responsible for many cancers and a series of studies revealed that lung cancer is more prevalent in populations exposed to certain chemical agents, such as polycyclic, polychlorinated aromatic hydrocarbons that are commonly found in diet, tobacco smoke and outdoor air pollution (59).

The metabolism of exogenous chemicals has been extensively studied, showing the pivotal role of AHR in metabolic pathway and carcinogenesis. For example, the activation of proto-oncogene was observed upon the activation of AHR (60). In addition, it was reported that AHR-mediated formation of a reactive metabolite of benzo[a]pyrene provides initiation step of carcinogenesis by facilitating formation of a DNA adduct (61). Furthermore, inactivation of tumor suppressor p53 by these metabolites was also reported (62). Finally, the DNA-ligand adduct formation in carcinogenesis process was reported to be suppressed in AHR knock-out mice (63), indicating that the AHR may be a potential therapeutic target for the treatment of cancer.

The better understanding and the development of therapeutic agent for these diseases with respect to the abnormal activation of AHR are currently hampered mainly due to the lack of appropriate research tools. Novel antagonists developed in this study may be useful molecular probes that can be used to dissect complex AHR signaling pathways triggered by environmental carcinogens and in other pathogenesis. Further, the novel antagonists developed in the present study may be useful to test whether AHR is a clinical target not only for chemoprevention but also for treatment of related diseases.

2.2 Chemical approach to AHR biology

The XMEs and AHR signaling pathway are important for the adaptive response to exogenous chemicals. The promiscuous ligand binding of AHR has been playing a crucial role in deciphering the complex signaling pathway providing the key understandings on the fundamental principles underlying xenobiotic metabolism. Paradoxically, the promiscuity hampers the development of appropriate ligands with antagonistic activity. Since the pathway was immediately activated by a wide variety of aromatic chemicals for the gene regulation, studies on AHR have been focused on the effect of potent agonist which may veil the diverse consequences resulting from the weak, a perhaps more physiologically relevant activation of AHR. Currently, studies on AHR focus more on the effect of non-classic and relatively weak agonist and/or antagonist. Since the physiological consequence of AHR activation is divergent and specific to the ligand, the development of novel ligands with more diverse structures and novel antagonist without agonistic potency is essential to decipher the AHR cryptics.

2.2.1 Agonistic ligands of AHR

Thus far, a large number of chemical compounds have been identified as ligands interacting with AHR. Generally, these ligands are structurally related. They are environmentally and biologically persistent, induce a common spectrum of responses and have a common mechanism of action (64). The exogenous ligands, aryl hydrocarbons, are relatively well-analyzed due to the strong binding affinity, providing the structural understanding for binding and activation of AHR. Recent studies demonstrated that structurally diverse chemicals interact with AHR, suggesting that AHR presumably has a promiscuous binding site(s). Moreover, emerging studies demonstrated that physiological consequences of AHR activation are differentiated in a ligand-specific manner, highlighting the importance of understanding the structural specificity of AHR ligand binding.

AHR ligands can be categorized into two classes, synthetic and natural products. Most of the known ligands with high affinity belong to the first class. This class includes benzo[a]pyrene, polychlorinated dibenzo-*p*-TCDDs (PCDDs), polychlorinated dibenzofurans (PCDFs), polychlorinated biphenyls (PCBs) and related compounds, such as 2,3,7,8 tetrachlorodibenzo-*p*-TCDD (TCDD) comprising “classical ligands” as termed by Denison et Al (65). As the structures of recently identified ligands are substantially different from the classical ligands, these new synthetic AHR can be classified as “non-classical synthetic ligands” also termed by Denison et al (65). The overall biological activity and the binding affinity of non-classical ligands are not comparable to the classical ligands such as TCDD. However, the identification of these non-typical synthetic ligands have broadened the structural spectrum of ligands to a wide diversity, suggesting that the chemical structure of ligands should not be restricted to the rigid structure based on the observation in classical ligand.

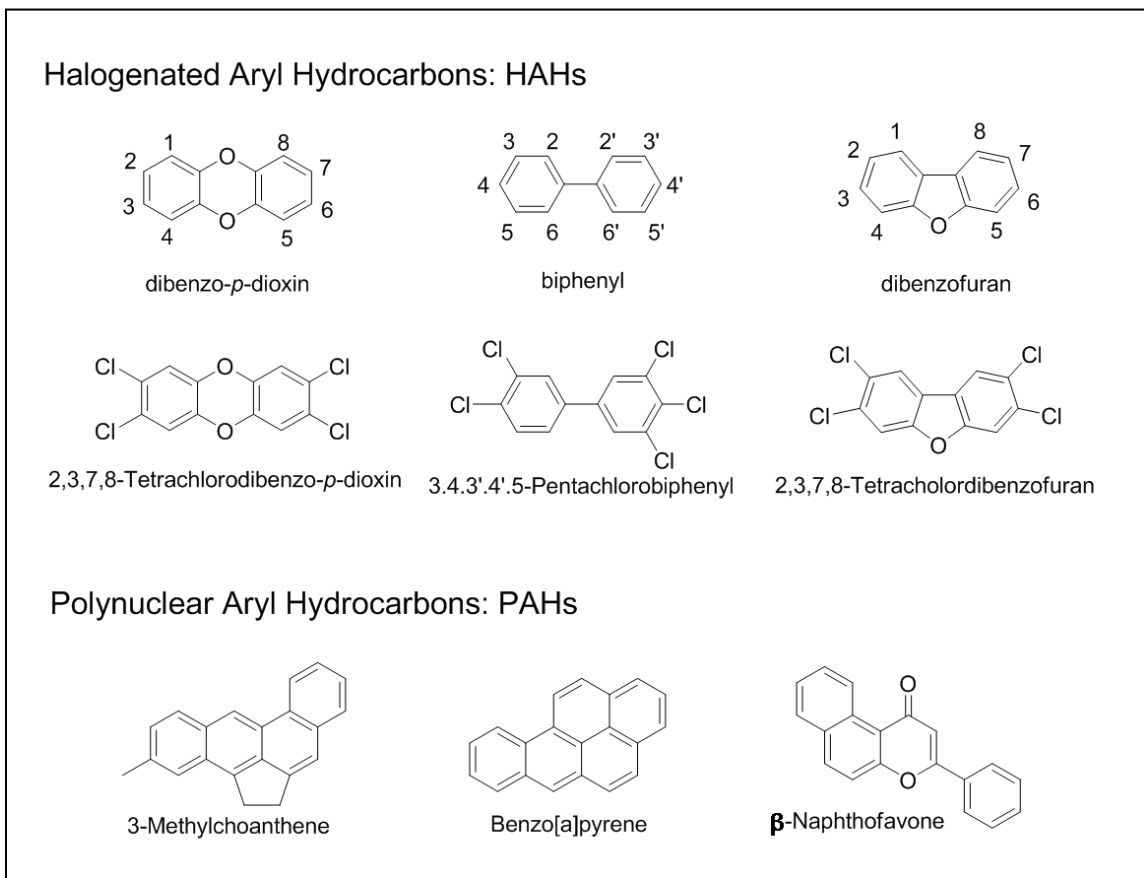


Figure 2.3 Classic synthetic ligands of AHR

AHR ligands can be categorized into two classes, synthetic and natural products. Most of known ligands with high affinity belong to the first class. This class includes benzo[a]pyrene, polychlorinated dibenzo-*p*-TCDDs (PCDDs), polychlorinated dibenzofurans (PCDFs), polychlorinated biphenyls (PCBs) and related compounds, such as 2,3,7,8 tetrachlorodibenzo-*p*-TCDD (TCDD) comprising “classical ligands” as termed by Denison et Al (65). As the structures of recently identified ligands are substantially different from the classical ligands, these new synthetic AHR can be classified as “non-classical synthetic ligands” also termed by Denison et al (65). The overall biological activity and the binding affinity of non-classical ligands are not comparable to the classical ligands such as TCDD. However, the identification of these non-typical synthetic ligands have broadened the structural spectrum of ligands to a wide diversity, suggesting that the chemical structure of ligands should not be restricted to the rigid structure based on the observation in classical ligand.

The classical ligands are the aryl hydrocarbons of coplanar, rigid plural aromatic ring structure. The structure gains more rigidity by the polynuclear aromatic ring structures or halogen substituents. The general ability inducing the activation of AHR resulting in the up- regulation of XRE-regulated gene products of these compounds and the binding affinity are enormously strong (65). The non-classical ligands, on the other hand, have divergent structures with less rigidity. These compounds are chemically labile, hence, relatively easy to be processed by XMEs (65). Their interaction with the AHR and potency for AHR activation are weak as a whole as compared to the classical ligands.

AHR ligands are easily misunderstood to be air-pollutants or the other environmental contaminants, since the classical ligands are usually generated from combustion or chemical synthesis. However, a substantial proportion of the total exposure to AHR ligands for humans comes from diet (65). Thus far, a wide variety of dietary AHR ligands have been identified from plants and characterized. A large majority of phytochemicals are antagonists of AHR with weak agonistic activity (65). However, the exposure to the dietary ligand of AHR continues throughout the life, hence, accumulating the effect of phytochemicals to the body. Therefore, the total effect of phytochemicals for AHR activation should not be overlooked.

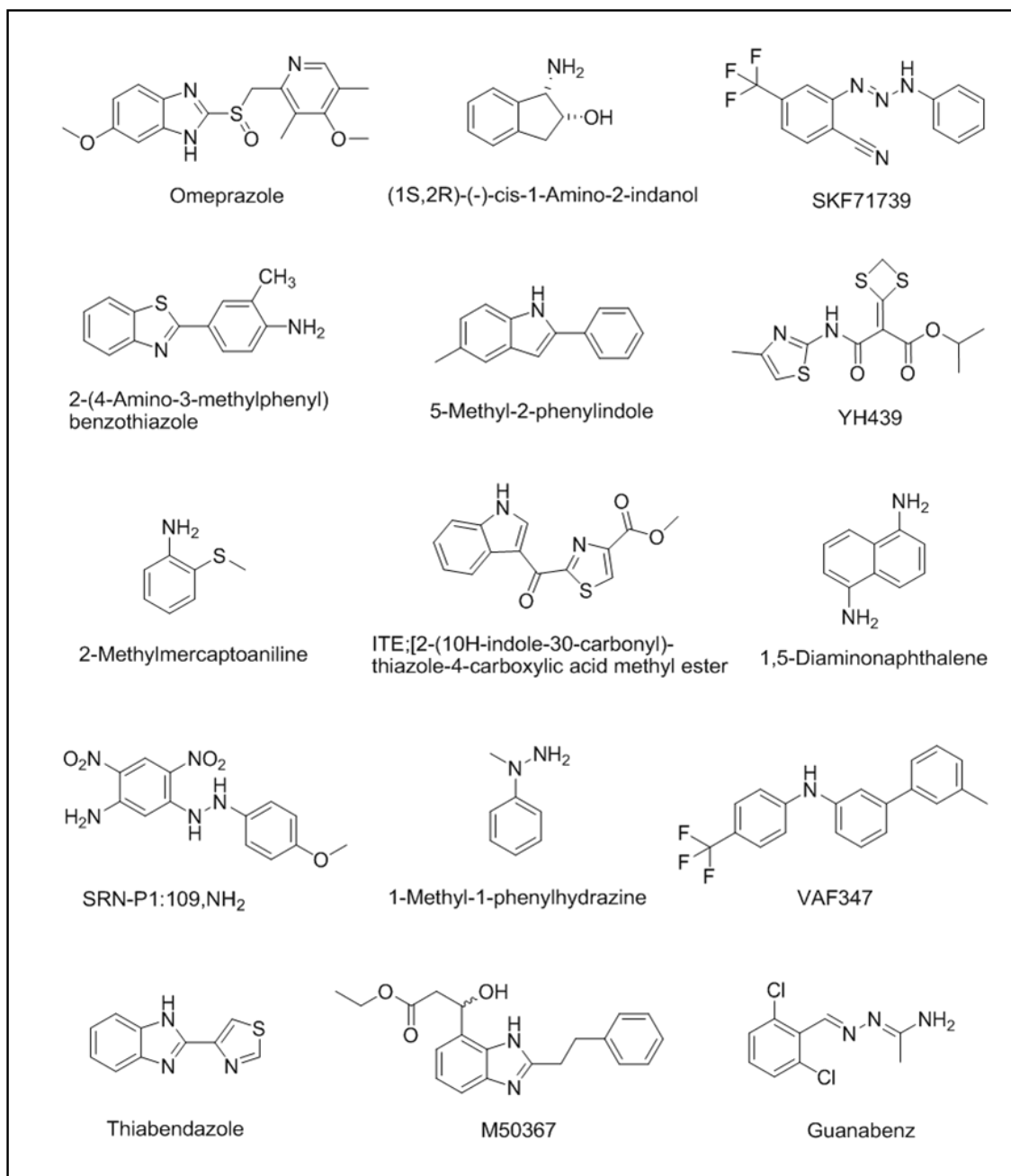


Figure 2.4 Non-classical ligands of AHR; omeprazole (66), (1S,2R)-(-)-cis-1-Amino-2-indanol (67), SKF71739 (68), 2-(4-Amino-3-methylphenyl)benzothiazole (69), 5-Methyl-2-phenylindole (65, 70), YH439 (71), 2-Methylmercaptoaniline (67), ITE;[2-(10H-indole-30-carbonyl)-thiazole-4-carboxylic acid methyl ester (72), 1,5-Diaminonaphthalene (73), SRN-P1:109,NH₂ (67), 1-Methyl-1-phenylhydrazine (67), VAF347 (74, 75), Thiabendazole (76,77), M50367 (78, 79) and Guanabenz (80).

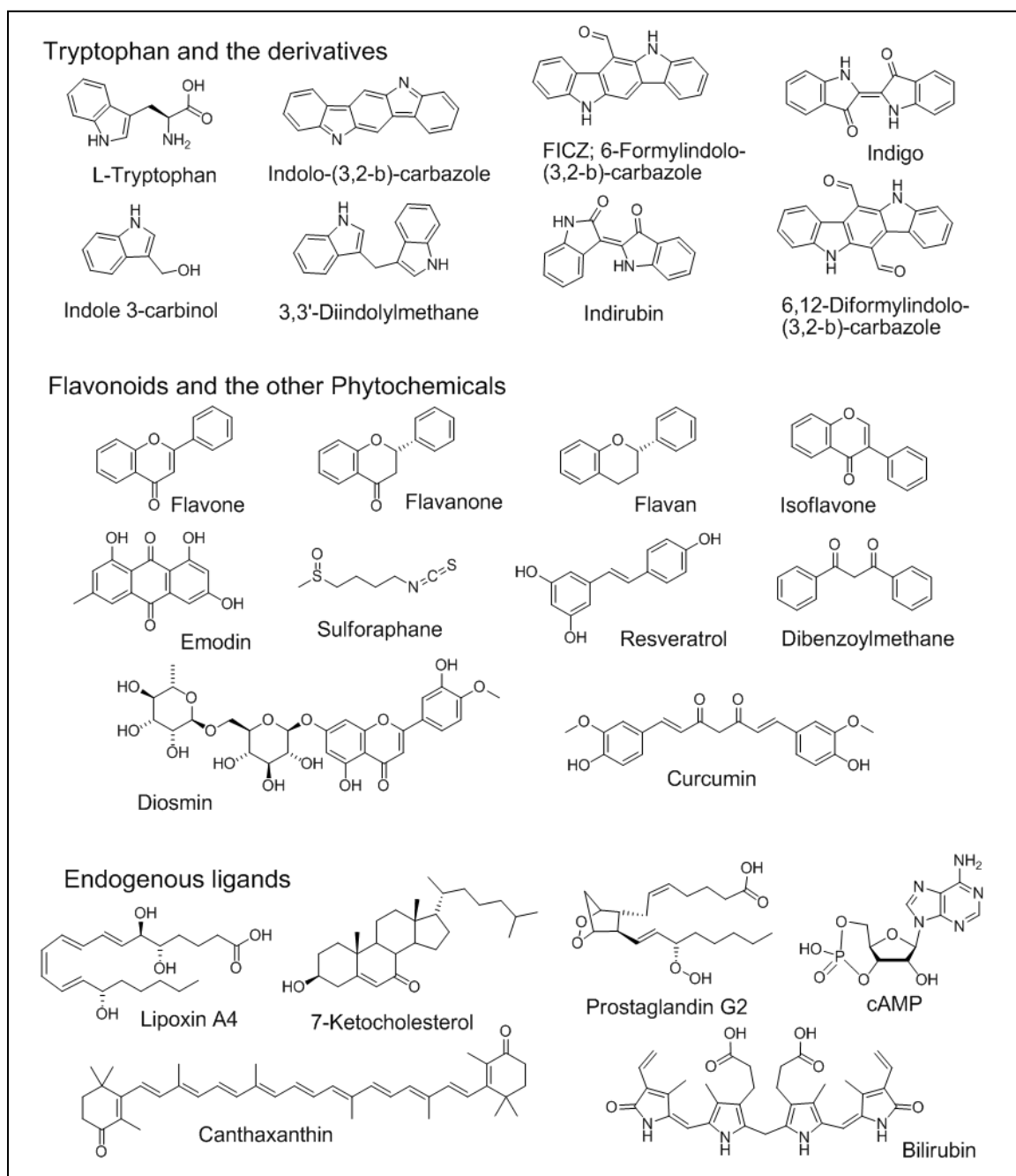


Figure 2.5 Naturally occurring ligands and endogenous ligands of AHR; L-tryptophan (81), indolo-(3,2-b)-carbazole (82), FICZ; 6-formylindolo-(3,2-b)-carbazole (83), indigo (84), indole 3-carbinol (85), 3,3'-diindolylmethane (85), indirubin (84), 6,12-diformyl indolo-(3,2-b)-carbazole (82), flavone(86, 87) , flavanone (88, 89), flavan (88, 90), isoflavone (91, 92), emodin (93), sulforaphane (94, 95), resveratrol (96, 97), dibenzoyl methane (98), diosmin (99), curcumin (100), lipoxin A4 (101), 7-ketocholesterol (102), prostaglandin G2 (103), cAMP (104), canthaxanthin (105, 106), bilirubin (107, 108).

Interestingly, several precursors are not potent in terms of agonistic activation of AHR, whereas simple modifications on structures can cause agonistic activities (65). Hence, it is suggested that the structure activity studies on these analogues of ligands and precursors will be helpful for the understanding on the structure activity relationship and for the rational design of synthetic ligands of AHR.

A number of studies revealed that while AHR is involved in many biological processes, the physiological role of the AHR, however, is not fully understood. More than anything else, endogenous ligands with high affinity have not been identified until the present time. Since the activation of AHR was observed in cultured cell in the absence of exogenous ligands, the endogenous ligands of AHR has been expected to be present (58). Thus far, a variety of endogenous ligands have been identified with weak agonistic activity compared to TCDD, suggesting the physiological role in cells. These ligands include indoles, arachidonic acid metabolites, carotinoids, cholesterol, and prostaglandin G (65). Taken together, it appears that the AHR plays a certain role in cells in the absence of exogenous ligands.

2.2.2 Antagonists

Despite of its usage as a molecular tool and potential therapeutic strategy, a pure AHR antagonist has not been developed, a number of flavonoids and their synthetic derivatives have been reported to exhibit AHR antagonistic activity. These include 7,8-naphthoflavone (α -naphthoflavone; ANF) (109), 3'-methoxyflavone (110), 3'-methoxy-4'-nitro-flavone (111), 4'-amino-3'-methoxy-flavone (112), 2'-amino-3'-methoxy-flavone (PD98059) (89), 4'-methoxyflavone (113) and 3',4'-dimethoxyflavone (112-114). Amongst these compounds, the 3',4'-dimethoxyflavone (DMF) is widely used as an AHR antagonist, since it inhibits AHR activation induced by TCDD in breast cancer cell line (113). However, most of synthetic derivatives exert protein tyrosine kinase inhibitory activity and cytotoxicity at a concentration higher than 10 μ M as well as partial agonistic activity (89, 110, 115). Recently, CH-223191 was identified as an AHR antagonist by screening a diversity-oriented random library (116). CH-223191 has not been reported to

induce AHR activation, implying that this compound may presumably be a pure antagonist. However, it is yet confirmed whether CH-223191 is truly a pure AHR antagonist in cells. In the present study, we used the CH-223191 scaffold to generate a library of CH-223191 analogues and screened for AHR antagonistic activity. The selected compounds were then used to develop PROTACs targeting AHR.

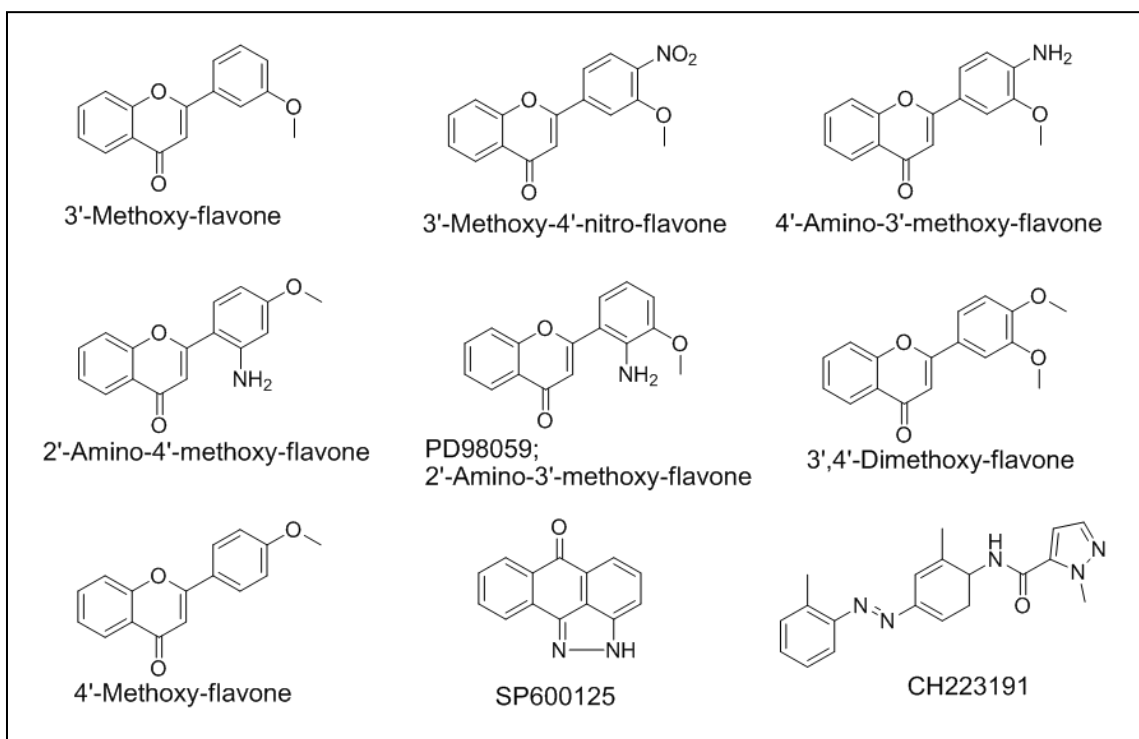


Figure 2.6 Antagonists of AHR; 3'-Methoxy-flavone, 3'-Methoxy-4'-nitro-flavone, 4'-Amino-3'-methoxy-flavone, 2'-Amino-4'-methoxy-flavone, PD98059; 2'-Amino-3'-methoxy-flavone, 3',4'-Dimethoxy-flavone, 4'-Methoxy-flavone, SP600125, CH223191

2.3 PROTAC technology

PROTAC (Proteolysis targeting chimeras) is a chimeric small molecule designed to induce the proteolysis of targeted protein by the intracellular ubiquitin-proteasome system (UPS). The PROTAC is comprised of a specific E3 ubiquitin-ligase recognition motif linked to a ligand that binds to a targeted protein. PROTAC recruits the targeted protein to the specific E3-ligase complex in proximity for multi- and poly- ubiquitination and subsequently induces the degradation of targeted protein by the 26S proteasome in an ATP-dependant manner (1). Unlike the conventional small molecules that inhibit protein function by direct or indirect interactions with the targeted protein, PROTACs inhibit protein function by the elimination of targeted protein rather than by simple inhibition, providing an alternative strategy for the modulation of protein function (4).

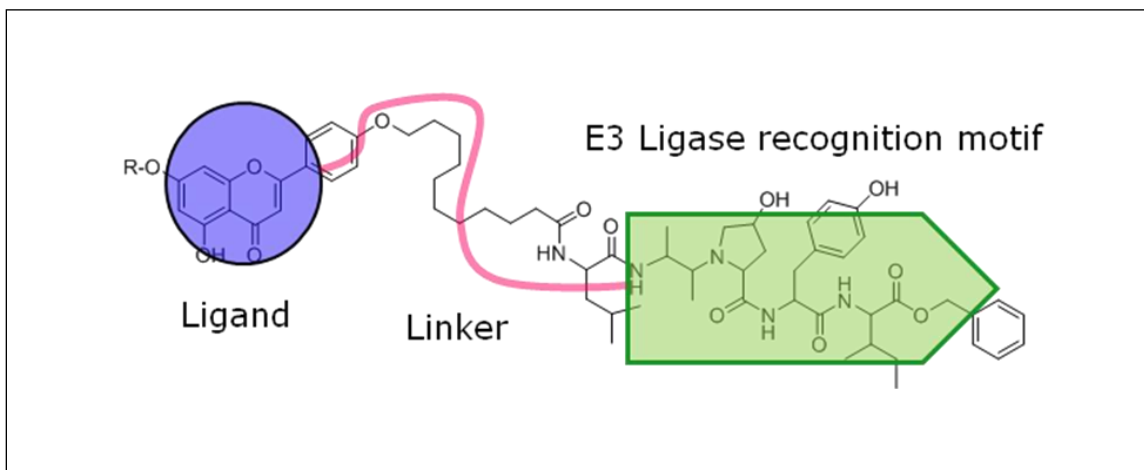


Figure 2.7 Structure of PROTAC

Thus far, several PROTACs have been developed, validating the PROTAC approach as a useful research tool. Target proteins of these PROTACs include estrogen receptor α (ER α), methionine amino peptidase 2 (MetAP2), and androgen receptor (AR) (1, 5, 117-120). However, the PROTAC technology has not been widely applied as a molecular probe despite its promising potential due to the lack of general design strategy and the limited number of protein-ligand pairs (4).

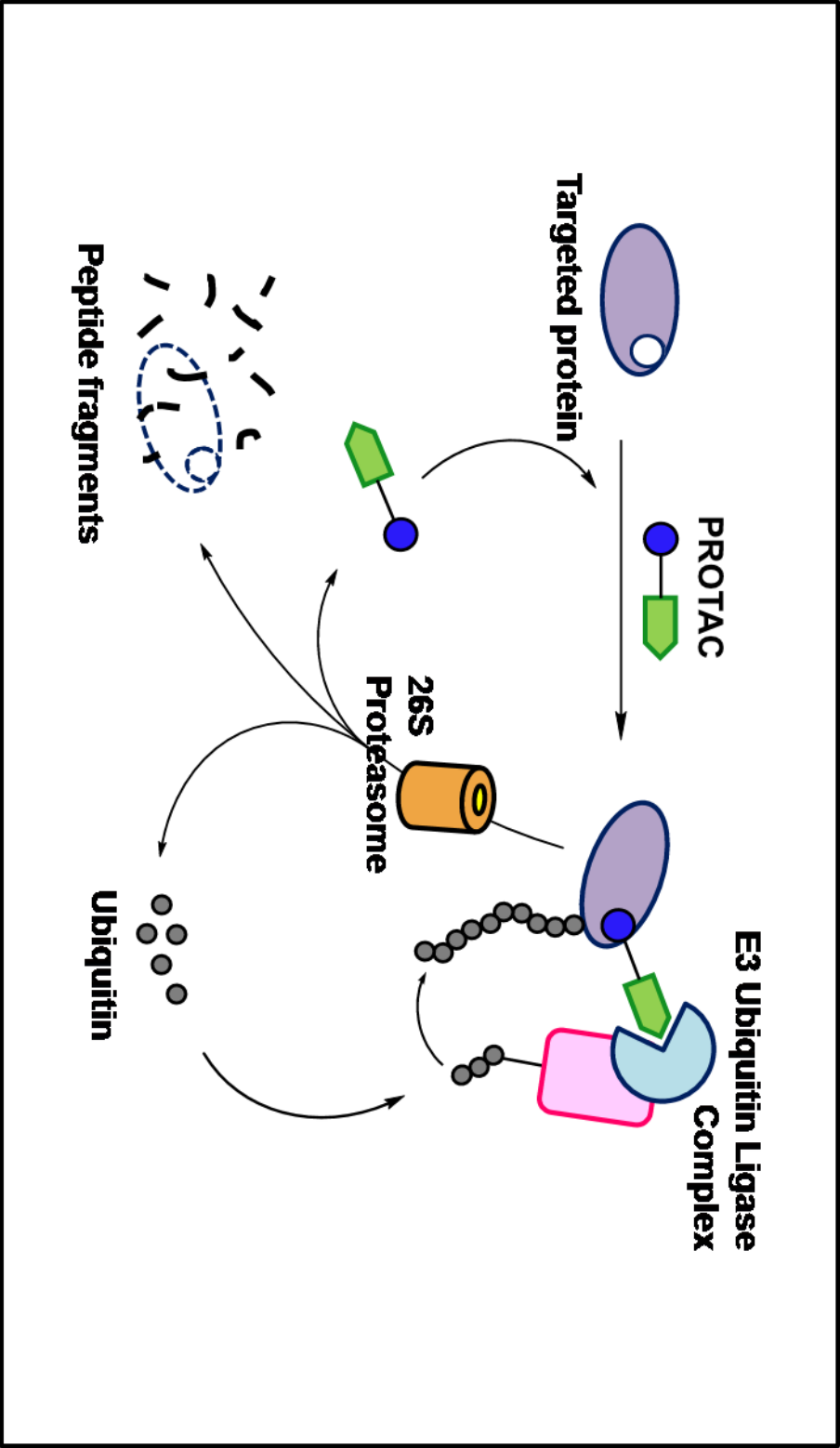


Figure 2.8 Mechanism of PROTAC

While the ligand for a target protein accounts for the specificity of the target, the E3 ligase recognition motif is responsible for ubiquitination. In the first generation PROTACs, a diphosphorylated peptide residue derived from I κ B was employed as an E3 ligase recognition residue (1).

Despite that the first generation PROTAC successfully induced the degradation of targeted protein, its delivery and stability in cells is a major concern due to its phosphopeptidyl nature. The second generation PROTACs used peptide fragments derived from HIF-1 α (3, 118). It should be noted that HIF-1 α under normoxic conditions is rapidly recruited to pVHL complex (E3 ligase complex) for ubiquitination and degradation (121, 122). The second generation PROTAC has been shown to successfully induce the degradation of the target protein (3, 118). The third generation PROTAC is equipped with the simplified version of recognition motif of HIF-1 α (4). The HIF-1 α peptide residue (degron peptide) is a pentapeptide of which the hydroxyproline is in the middle and the carboxylic acid is protected with benzyl group from the C-terminal proteases attack, whereas the HIF-1 α peptide of the second generation PROTAC is an octapeptide and its C-terminus is unprotected. The PROTACs containing the pentapeptide are relatively simple to synthesize compared to the former generation PROTACs and still capable of inducing the degradation of targets. Most importantly, these PROTACs are cell-permeable. The next generation PROTAC employing nutlin which is known to interact with mdm2, the E3 ligase of p53, has been developed, but its activity is, at most, comparable to the activity of PROTACs based on the HIF-1 α pentapeptide. Therefore, in the present study, the HIF-1 α pentapeptide was employed for the synthesis of AHR-targeting PROTAC.

2.4 The development of PROTAC as an antagonist of AHR signaling pathway

Considering the unique activity of PROTACs in inducing the degradation of its target, it is thought that the PROTAC technology may provide a novel chemical tool in dissecting complex signaling pathways. Thus, it is hypothesized that the PROTAC targeting AHR will provide a pure AHR antagonist. In addition, it is expected that the activity of PROTAC will be improved by linking an optimum AHR ligand to the E3 ligase recognition motif. Further, screening a small molecule library synthesized in this study may provide AHR ligands of the intrinsic antagonistic (or agonistic) activity, which may be a useful research tool for the study of AHR and a potent therapeutic agent as well.

In this study, the PROTAC targeting AHR was first developed using the natural product AHR antagonist apigenin. This provided the proof of concept that exogenous ligands can be exploited for the development of PROTAC targeting AHR. With this in mind, the development of PROTACs based on synthetic antagonists has been initiated, which aims to develop PROTACs with higher activity and specificity.

As it is designed to target only the protein which binds to the ligand part of the PROTAC, the availability of ligands defines the extent of PROTAC development. Thus, the systemic platform to identify the adequate ligand is desired to improve the antagonistic potency. In order to overcome the limits revealed in previous studies, we employed a positional scanning approach to identify AHR ligands that can be used to design PROTACs, using the scaffold of CH-223191. The selected compounds were then coupled to the HIF-1 α pentapeptide, completing the synthesis of PROTACs that target AHR for degradation.

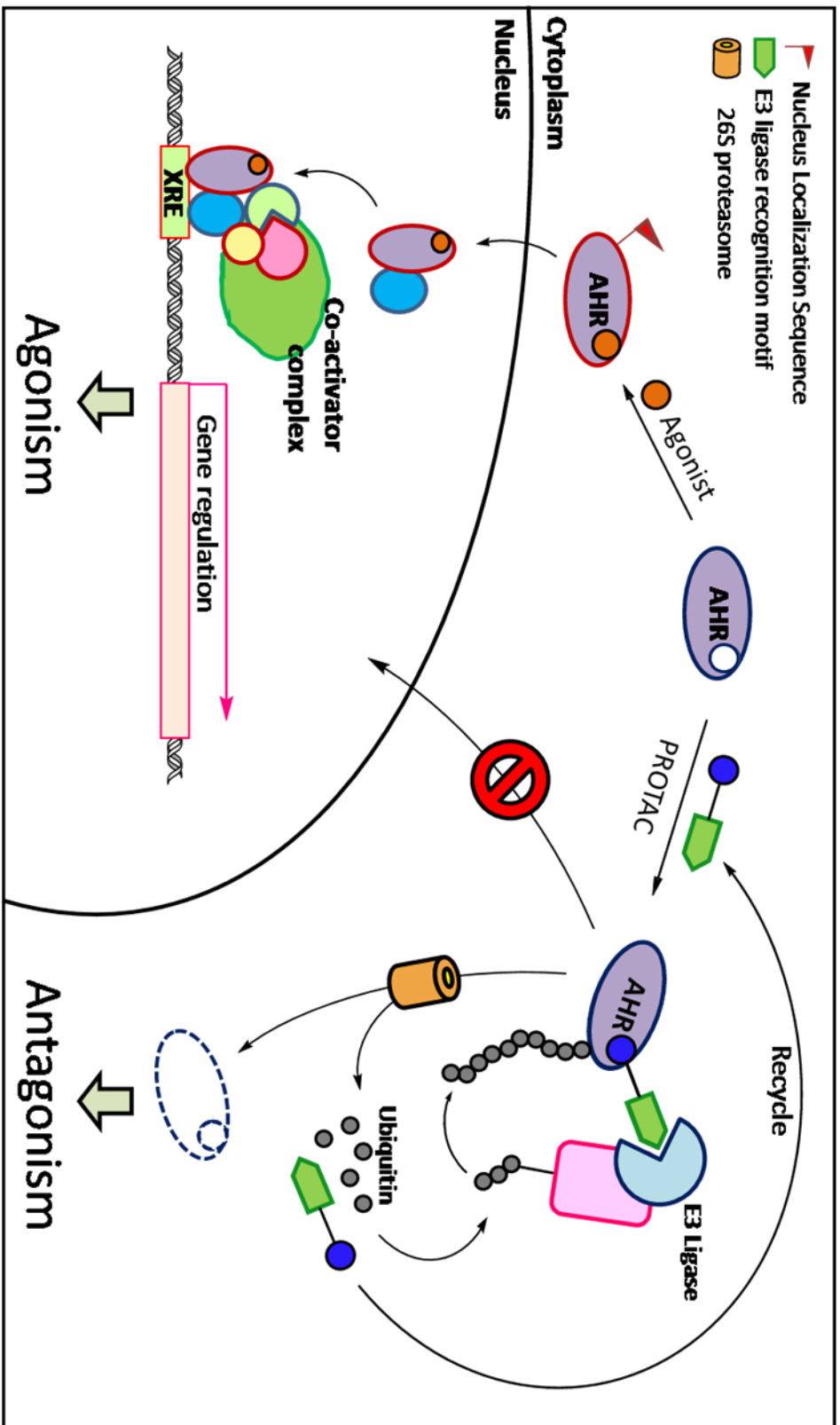


Figure 2.9 AHR antagonism induced by PROTAC

CHAPTER 3 PROTAC BASED ON NATURAL PRODUCT

3.1 Introduction

Since the efficacy of PROTAC technology has been demonstrated for a number of protein targets, it was hypothesized that PROTAC that targets the AHR selectively induces degradation of AHR. Although a number of AHR ligands are available, the use of those ligands for the synthesis of PROTAC is limited due to several factors such as difficulties of chemical manipulation and the loss of AHR binding affinity caused by derivatization. Recently, Zhang et al. reported that kaempferol and apigenin exhibited AHR antagonistic activity in breast cancer cells and liver carcinoma cells, respectively (93). Accordingly, a number of phytochemicals such as apigenin, emodin, kaempferol, Genistein, Chrysin and Quercetin have been selected for the test of their activity against AHR (Figure 3.1). Using a luciferase reporter assay, apigenin and kaempferol were found to be best antagonists among them (123). Furthermore, the structure of these compounds has an ideal functional group for the attachment of E3 ligase recognition motif without the loss of AHR antagonistic activity.

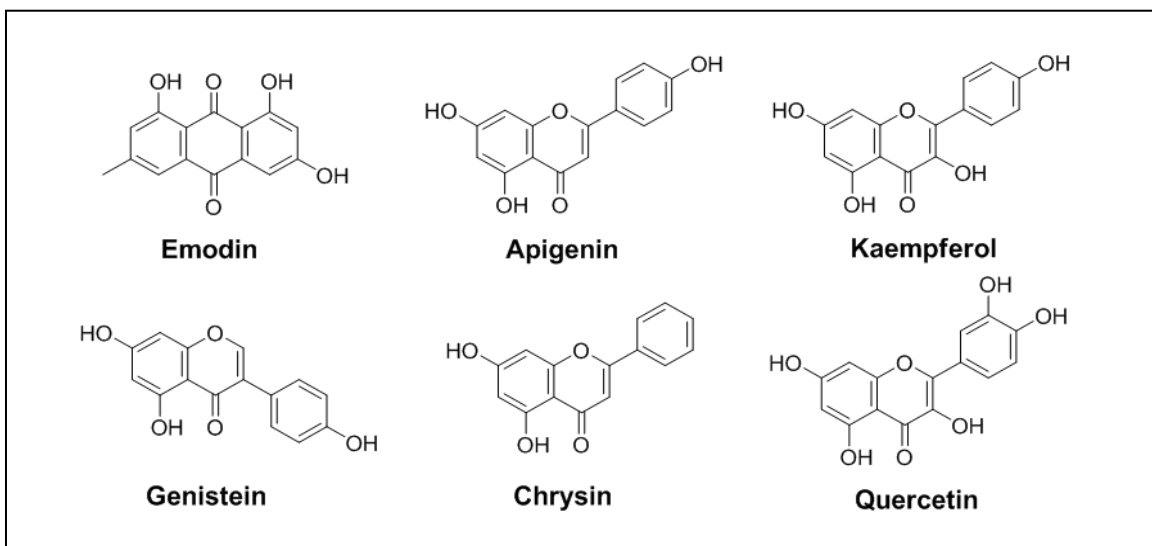


Figure 3.1 Phytochemicals interacting with AHR

3.2 Apigenin and PROTAC

Apigenin, which is found in apple, celery, tea, aromatic plants and honey, is identified as an AHR antagonist. Previous study revealed that apigenin (1) directly interacts with the AHR and inhibits AHR activation (*123*). Apigenin has been demonstrated to inhibit the proliferation of keratinocytes and prostate cancer cell (*124-126*). In addition, apigenin has shown to be effective for cancer prevention *in vitro* and *in vivo* (*91, 127*). Thus, it was decided to use apigenin in the synthesis of PROTAC that targets the AHR. After careful structure-activity-relationship study using acetylated apigenin, it was found that three hydroxyl groups in the rings can be derivatized without the loss of its activity (Figure 3.2).

3.2.1 Optimization of coupling position

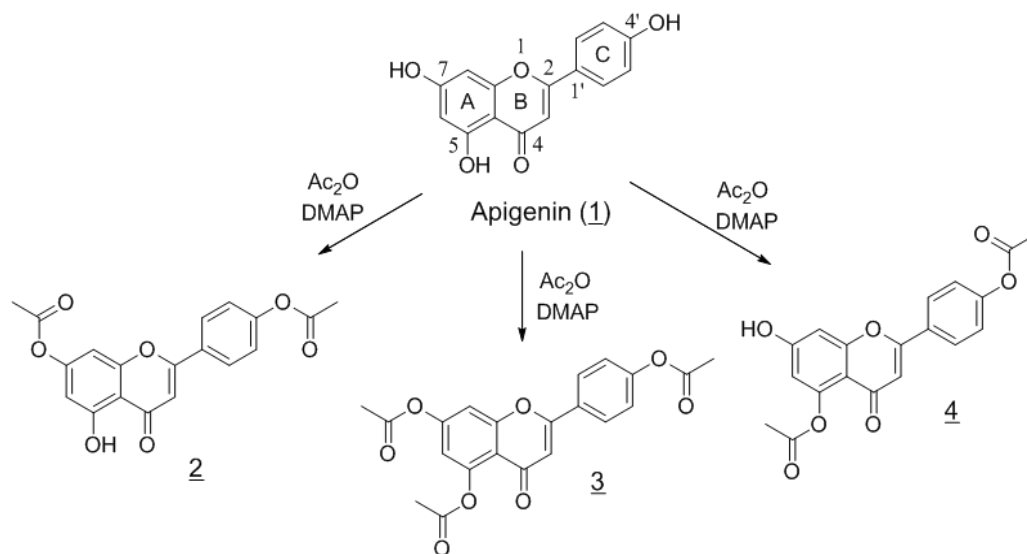


Figure 3.2 The synthesis of acetylated apigenins.

To investigate the role of hydroxyl groups in binding to AHR, the acetylated apigenins varying in position and number of acetyl group were prepared and subjected to

biological assessment. Apigenin was deprotonated by excess amount of potassium carbonate and treated with acetic anhydride to afford three acetylated apigenins in a one-pot manner (Figure 3.2). The resulting derivatives were tested the ability blocking AHR activation induced by TCDD. As shown in Figure 3.3, all of the acetylated apigenin derivatives retained the ability suppressing the transcriptional activation mediated by AHR, implying that none of these hydroxyl groups are critical for the interaction with AHR.

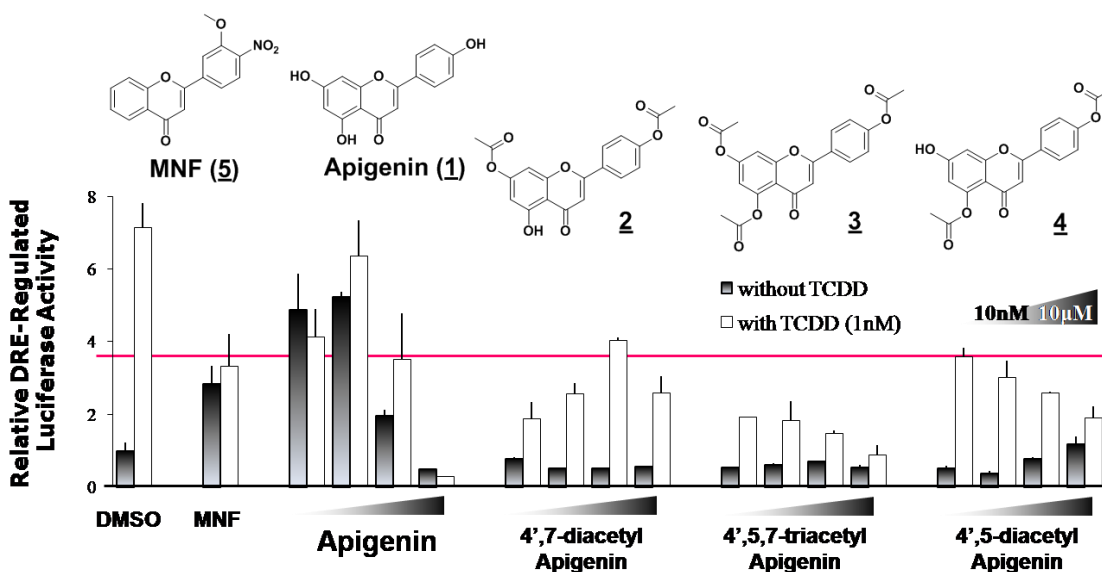


Figure 3.3 The effect of apigenin and acetylated derivatives on the activation of AHR. HepG2 cells transfected with human CYP1A1 promoter (HepG2-p450luc) was pre-treated with either DMSO alone or with the compounds (10^{-5} M to 10^{-8} M). After 1hr, TCDD (1 nM) was added. 4 hr after TCDD treatment the cells were harvested and luciferase activities were measured. MNF (3-methoxy-4-nitroflavone, 10 μ M) was used as a positive control. These assays were performed by a former student, Dinesh Puppala, Ph.D., under the direction of Hollie I. Swanson, Ph.D.

3.2.2 Synthesis of PROTACs based on apigenin

As the optimization study indicated that none of the three hydroxyl groups are important for the interaction with AHR, 4'-hydroxyl group was chosen for the coupling with E3 ubiquitin ligase recognition moiety. Accordingly, two different PROTACs were prepared and evaluated for the ability to induce the degradation of AHR (Figure 3.4). The PROTAC containing inactive mutant peptide in which the critical hydroxyproline is replaced with alanine was prepared and used as a negative control. The E3 ubiquitin ligase recognition moiety was separately prepared in a conventional method for peptide synthesis for the coupling with the linker-attached apigenin (Figure 3.5). The structures of the PROTACs are shown in Figure 3.6 A.

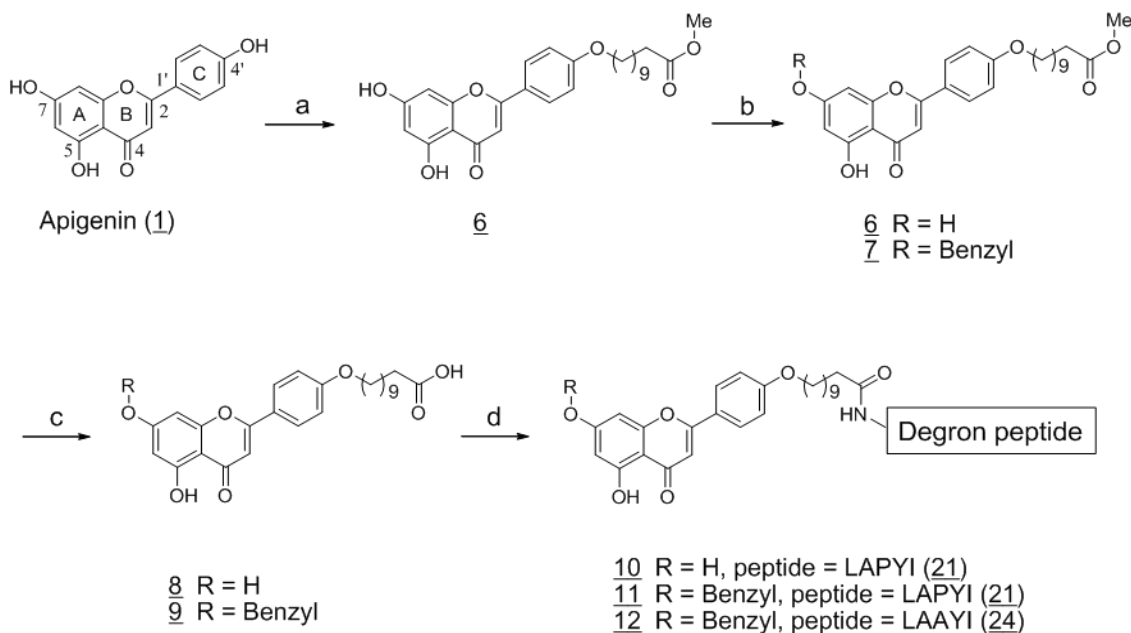
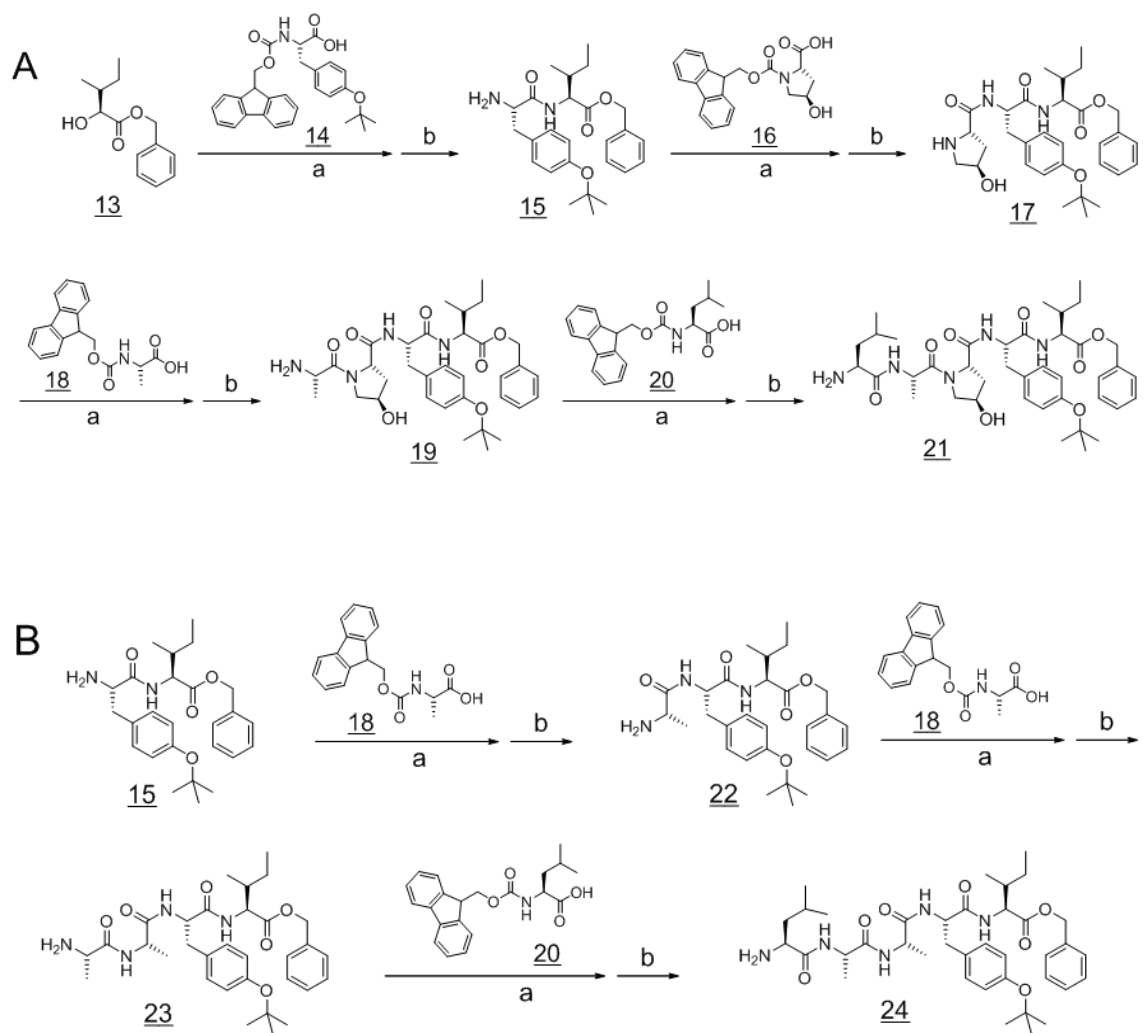


Figure 3.4 Synthetic schemes for the preparation of apigenin-based PROTACs.
a. Methyl-11-bromo undecanoate, K_2CO_3 ; b. Benzyl bromide (for compound 4 only); c. LiOH; d. 1. HBTU/ HOBt, Diisopropylethylamine, E3 ubiquitin ligase recognition peptide (21: $\text{H}_2\text{N}-\text{Leu}-\text{Ala}-\text{Pro}^{\text{OH}}-\text{Tyr}-\text{Ile}-\text{OBn}$). 2. TFA.



3.2.3 Biological assessment of PROTACs based on apigenin

The results shown in Figure 3.6 B indicated that the PROTACs successfully induced the degradation of AHR. PROTAC1 induced the complete degradation at a concentration of 100 μ M whereas the effective concentration range of PROTAC2 was less than 10 μ M, hence, implying that the potency of PROTAC2 would be higher than that of PROTAC1. Then, the effect of apigenin-based PROTACs on the expression of cytochrome p450 1A1 (CYP1A1) which is regulated by AHR was then investigated.

The results shown in Figure 3.6 B also indicated that both PROTACs inhibited the activation of AHR in terms of the up-regulation of CYP1A1 induced by TCDD. However, the CYP1A1 level in the presence of PROTAC1 was observed to be slightly higher than that of control whereas PROTAC2 did not induce the increase of CYP1A1 level, implying that PROTAC1 might be a weak agonist and PROTAC2 would be a more useful tool in order to induce the degradation of AHR without activating signaling pathway.

3.2.4 Confirmation of biological activity of PROTAC2 (4, 128)

To further examine the PROTAC-induced AHR degradation, GFP (green fluorescent protein)-fused AHR was over-expressed in HepG2 cells and the cells were treated with PROTAC2. The result showed that PROTACs induced degradation of GFP-fused AHR (Figure 3.7 C). Then, the role of proteasome in the degradation of the fusion protein was investigated by treatment of a natural product proteasome inhibitor epoxomicin. The proteasome inhibitor efficiently blocked the degradation of the fusion protein, implying that the PROTAC-induced degradation is proteasome-dependent. Since the PROTACs have been demonstrated to induce the degradation of AHR in human keratinocytes, HaCaT cells, it was questioned if the PROTACs are capable of inducing the degradation of AHR in the other cells. The result demonstrated that the PROTAC2 induced AHR degradation in mouse hepatocyte cells and human hepatocyte, HepG2 cells (Figure 3.7 B and C).

The PROTAC-induced degradation of AHR was further investigated in mouse hepatocyte. The AHR were demonstrated to be degraded in response to the treatment of PROTAC2 in a dose dependent manner (Figure 3.7 A). In addition, it was observed that the AHR activation induced by TCDD was blocked by PROTAC2, whereas the PROTAC2 did not induce the increase the CYP1A1 level, implying that PROTAC2 might be acting as a pure antagonist in the AHR signaling pathway.

To further examine PROTAC2-induced AHR degradation, enhanced green fluorescent protein (eGFP)-fused AHR was over-expressed in the CV-1 cells. The result showed that PROTAC2 efficiently induced degradation of eGFP-fused AHR in the cells (Figure 3.7 D). The degradation of eGFP-AHR was completely blocked by Epoxomicin, indicating that PROTAC2-induced eGFP-AHR degradation is proteasome-dependent. This result was verified by cy3-tagged anti-AHR IgG.

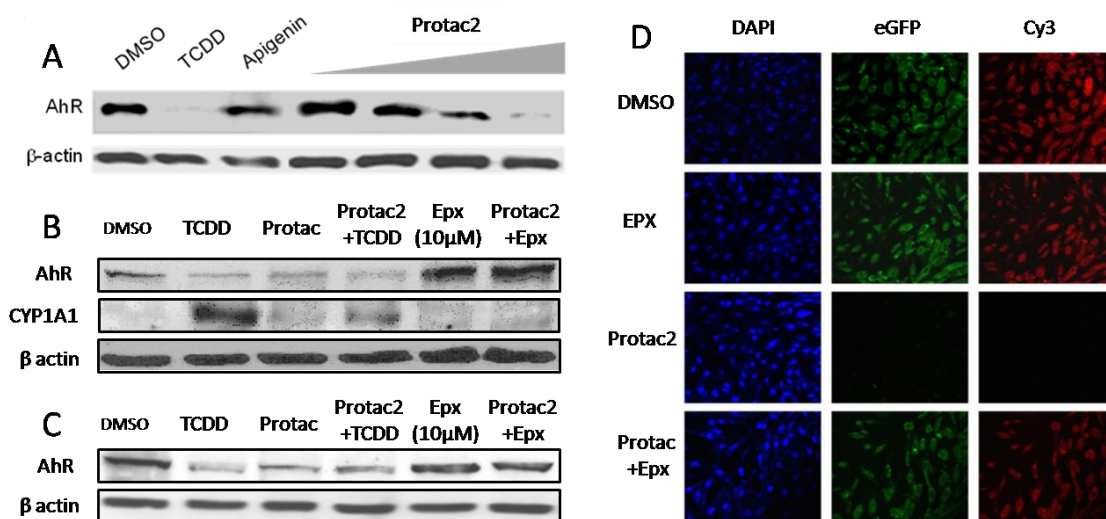


Figure 3.7 PROTAC2 induces degradation of AHR.

A) PROTAC-induced degradation of AHR in immortalized mouse hepatocytes. The cells were treated with DMSO (0.1 %), TCDD (1 nM), apigenin (10 μ M) or PROTAC2 (10, 25, 50 and 100 μ M) for 25 hr. After harvesting, the cell lysates were subjected to western blot analysis. B) and C) PROTAC-induced degradation of AHR in mouse hepatocyte (B) and human HepG2 (C). The cells were treated with DMSO (0.01 %), TCDD (1 nM), PROTAC2 (10 μ M) or epoxomicin (10 μ M) for 24 hr as indicated. After harvesting, the cell lysates were subjected to western blot analysis. D) PROTAC2 effectively degrades a eGFP-fused AHR in CV1 cells. After transfecting with eGFP-fused AHR, the cells were treated with DMSO control, a specific proteasome inhibitor epoxomicin alone (10 nM) or PROTAC2 (10 μ M) in the presence or absence of proteasome-specific inhibitor epoxomicin (10 nM). After 16 hr, the cells were visualized by fluorescent microscope. The western blot assays were performed by Eun-Young Choi, Ph. D. and a former student, Dinesh Puppala, Ph. D. under the direction of Hollie I. Swanson, Ph. D.. The confocal data were prepared by Wendy S Katz, Ph. D.

3.2.5 Characterization of PROTAC2

The antagonistic activity of PROTAC2 toward AHR prompted the further study of the PROTACs. To probe the stage where the signaling is blocked the effect PROTAC on the sequential events of each mechanistic steps following AHR ligand binding were investigated in. As PROTAC2-induced decrease of CYP1A1 protein level was shown in the presence of TCDD, the effect of PROTAC2 on the upstream stage, the transcription level of XRE-regulated gene was investigated. As a result, it was demonstrated that the TCDD-induced increase of mRNA level of CYP1A1 and CYP1B1 were blocked by PROTAC2 in dose-dependent manners (Figure 3.8 A). Next, the earlier stage of the signaling pathway, the binding of AHR/ARNT dimer to XRE on DNA as a transcriptional factor was investigated. As a result, the TCDD-induced DNA binding of AHR was demonstrated to be inhibited by PROTAC2 (Figure 3.8 B). These results indicate that PROTAC blocked the activation of AHR at earlier stages proceeding transcriptional activation.

As apigenin has been reported to exert the inhibitory activity toward proteasome, it was questioned whether or not the PROTAC2 also inhibits the proteasome activity (129). Further, since the studies on the PROTAC2 corroborated that the UPS plays a pivotal role in the AHR antagonism, the effect of PROTAC2 on the proteasomal activity required further investigation. The kinetic study demonstrated that the PROTAC based on apigenin did not inhibit the proteasomal activity whereas apigenin exerted a moderate inhibitory activity. The investigation on the IC_{50} value of three compounds, PROTAC2, apigenin and Epoxomicin revealed that the inhibitory activity of PROTAC2 is approximately 30 times and 20000 times weaker than that of apigenin and Epoxomicin, actually disapproving the PROTAC2 as an inhibitor of the proteasome. The Numerical data were shown in the figure 3.8 D.

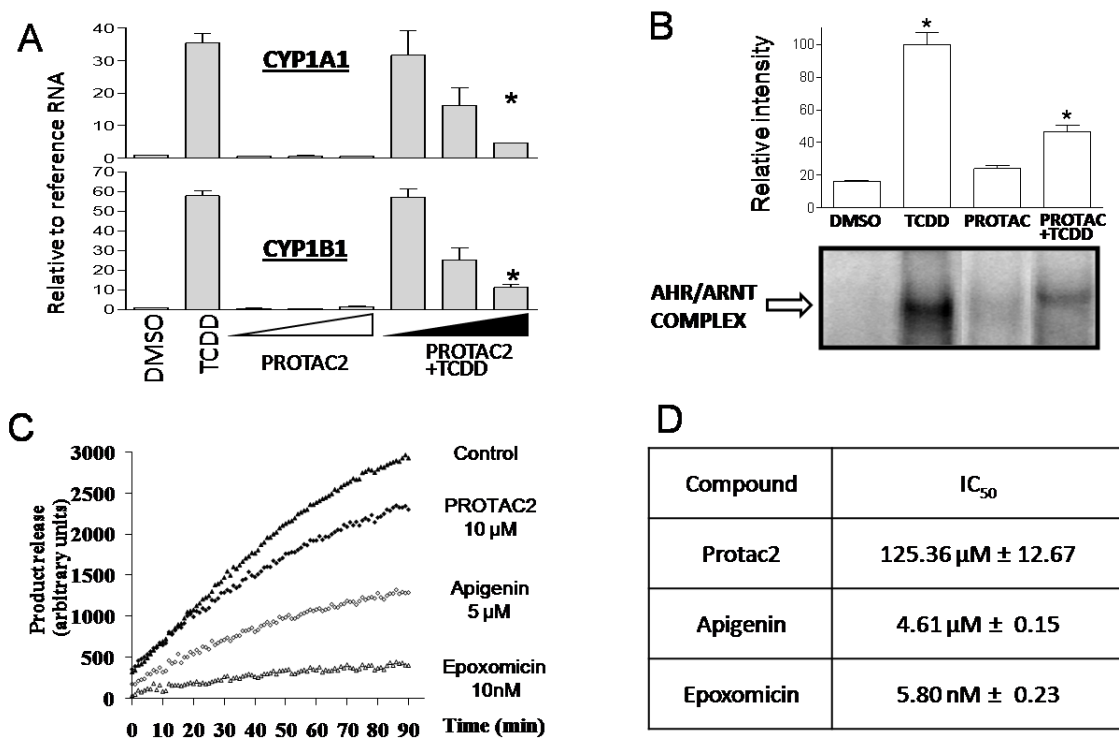


Figure 3.8 The characterization of PROTAC2.

A) The NHKs were treated with increasing concentrations of PROTAC2 (0.1 μ M to 10 μ M), harvested at the 16 hr time point and then subjected to RT real time PCR analysis. The data are representative of three independent experiments. B) HepG2 cells were cultured with either DMSO (0.01%) or TCDD (1 nM) for 1 hr in the absence (Lanes 1 and 2) or presence (Lanes 3 and 4) of a 7 hr pretreatment with PROTAC2 (10 μ M). The cells were harvested, nuclear extracts were prepared and EMSA's were performed using the ³²P labeled DRE as the radiolabeled probe. The experiments were quantified by phosphor imager analyses (Image quant software) and are expressed relative to the TCDD-treated samples. The data depict averages of three independent experiments + SE and were analyzed using ANOVA following by Bonferroni's Multiple Comparison Test. * implies significantly different from the TCDD treated sample (p value < 0.001). C) Effect of apigenin and apigenin-PROTAC on proteasomal activity. PROTAC2 (10 μ M), apigenin (5 μ M), and epoxomicin (10 nM) were combined with the fluorogenic peptide substrate and assay buffer in a 96-well plate and assayed as described under *Materials and Methods for biology*. The reactions were allowed to proceed for 90 min, and fluorescence data were evaluated in 1-min intervals. Fluorescence was quantified as arbitrary units, and progression curves were plotted for each reaction as a function of time. D) The corresponding IC₅₀ values for each treatment are indicated in the table. The PCR and EMSA assays were performed by Eun-Young Choi, Ph. D. and a former student, Dinesh Puppala, Ph.D. under the direction of Hollie I. Swanson, Ph. D.

3.3 Discussion

In this chapter, it was investigated whether the AHR can be targeted by the PROTAC approach. To test this, the natural product apigenin was used as an AHR ligand residue in the design of AHR-targeting PROTAC as a proof of concept experiment. Despite the fact that apigenin was a phytochemical identified as an antagonist of AHR, its use as an antagonist is limited in the AHR studies due to its partial agonistic activity at high concentrations (93). In addition, apigenin has been shown to display other biological activities, such as activation of the estrogen receptor (130).

However, it has been recently found that apigenin (**1**) directly interacts with the AHR and inhibits the ability of the AHR to activate genes (131). This phytochemical which is frequently found in apple, celery, tea, leafy aromatic plants, and honey, is a low estrogenic flavonoid phytochemical with anticancer properties (127). For example, apigenin has been shown to strongly inhibit the proliferation of keratinocytes and prostate cancer cells (124-126). More recently, apigenin has been evaluated for its beneficial effect on cancer prevention *in vitro* and *in vivo* (91, 132, 133). Taken together, these studies support the notion that apigenin may provide a promising avenue for the development of an AHR-based chemoprevention drug without serious adverse effect or toxicity. To this end, we envisioned that a PROTAC designed on the relationship between apigenin and AHR may provide the proof of principle, exhibiting AHR antagonistic activity.

The lack of understanding on the roles of hydroxyl groups on apigenin structure should be noted. Even though we tested the effects of acetyl protections of the hydroxyl groups, the result does not represent to entire roles of hydroxyl groups. We briefly extracted the idea that acylation on the hydroxyl group will be tolerated for AHR antagonistic activity from the data. However, the exact roles of the hydroxyl groups are yet to be elucidated. Actually, the overall activity of PROTAC1 appeared to be lower than PROTAC2 in spite that apigenin is simply coupled to the degron peptide as suggested. Although PROTAC2 fortunately induced a significant decrease in AHR level subsequently exhibiting antagonistic activity, we can't rule out the possibility that this

may be due to the additional benzyl moiety on 7-hydroxyl group rather than apigenin moiety.

As shown above, the apigenin-based PROTAC successfully induced degradation of the AHR in a dose-dependent manner as shown above. Consistent with the Western blot results, the transcriptional activation of AHR induced by TCDD was efficiently blocked by PROTAC2. Further, the detailed studies on PROTAC2 in the AHR signaling pathway characterized the PROTAC2 as an antagonist of AHR that lacked agonistic potency. In summary, the proof of concept experiment demonstrated that AHR can be successfully targeted by the PROTAC approach.

The low agonistic activity of ligand head of a PROTAC is desired, since the PROTAC based on an agonist is thought to be able to activate the AHR signaling pathway. Furthermore, the lack of toxicity or other adverse effect of ligand head is also required in order to reduce the negative influence when this ligand is released from PROTAC. In this context, dietary phytochemicals with low agonistic activity were thought to be suitable for the ligand part of PROTAC. However, one of our major concern was specificity and off-target effect. Since apigenin has also been reported to exhibit a wide range of various biological activities including its potency as an agonist in AHR signaling cascade (93), it has been suggested that it may target multiple proteins. Therefore, the possibility that the apigenin-based PROTAC may also suffer from off-target hits led to the development of AHR ligands that may exhibit higher specificity.

3.4 Materials and Methods

Material

PROTAC1, PROTAC2, and PROTAC3 were synthesized as described below. TCDD was a generous gift from Dr. Stephen H. Safe (Texas A&M University, College Station, TX). [³H]TCDD was obtained from ChemSyn Laboratories (Lenexa, KS). Unless otherwise mentioned, all other chemicals were purchased from Sigma-Aldrich (St. Louis, MO).

Cell Culture

Neonatal primary human keratinocytes (NHKs) were purchased from Cascade Biologics (Portland, OR). The cells were grown in Epilife medium with EDGS (Cascade Biologics) at 37°C and 5% CO₂. Murine (Hepa1c1c7) and human hepatoma (HepG2) cells were maintained in Dulbecco's modified Eagle's media with glucose and glutamine (Mediatech, Herndon, VA) supplemented with 10% fetal bovine serum (Invitrogen, Carlsbad, CA) at 37°C and 5% CO₂.

Luciferase assays

The HepG2-Luc cells were cultured in 96-well assay plates and pretreated with either DMSO alone or with the compounds at the indicated concentrations for 1 h. Subsequently, the cells were treated with TCDD (1 nM) for 4 h. The cells were then harvested and the CYP1A1 promoter activity was determined as a measure of luciferin generated using the Luciferase Assay System kit from Promega according to the manufacturer's protocol using TR 717 Microplate Luminometer from Applied Biosystem (Foster City, CA).

Electrophoretic Mobility Shift Assays

The impact of PROTAC2 on the AHR/ARNT DNA binding complex formed in cultured cells was determined by pretreating HepG2 cells with PROTAC2 for 7 h before the administration of either DMSO (0.1 %) or TCDD (1 nM). After an 1 h incubation, the cells were harvested, and nuclear extracts were prepared using the Nucbuster protein

extraction kit (Novagen, Madison, WI). Aliquots of the extracts (12 μ g) were incubated with salmon sperm DNA (1 μ g) and KCl (0.1 M final concentration) at room temperature for 15 min. The samples were then incubated for an additional 15 min at room temperature with the radiolabeled (³²P) consensus DRE sequences, (forward)TCGAGCTGGGGGCATTGCGTGACATTAC and (reverse) TCGA GGTATGTCACGCAATGCCCCCAGC, as described previously (131). After a 15-min incubation, the samples were separated using 4 % polyacrylamide nondenaturing electrophoretic gel and 0.5 \times Tris borate-EDTA (45 mM Tris base, 45 mM boric acid, and 1 mM EDTA, pH 8.0) as the running buffer.

Western Blot Analyses

NHKs were seeded into six-well plates. Once they reached approximately 70% confluence, they were treated with the indicated chemicals for varying time periods as described in the figure legends. The cells were harvested, and the total cellular extracts were prepared using radioimmunoprecipitation assay buffer (50 mM Tris, pH 7.5, 150 mM NaCl, 1 % Nonidet P-40, and 0.5 % sodium deoxycholate). The protein concentrations were estimated using BCA analysis (Pierce, Rockford, IL). Aliquots of the cellular extracts (approximately 100 μ g) were separated using SDS-polyacrylamide gel electrophoresis, and the proteins were transferred to nitrocellulose membranes. After a brief incubation in blocking buffer, the blots were probed using antibodies that recognized AHR (Abcam, Cambridge, MA), CYP1A1 (Santa Cruz Biotechnology, Santa Cruz, CA), and β -actin (Sigma-Aldrich).

Immunocytochemistry

CV-1 cells (monkey kidney cells) were plated in 6 well plates with coverslips. At 50 ~ 70 % confluency, the cells were transiently transfected with AHR-GFP plasmid using Lipofectamine 2000. After 32 hours, cells were treated with either DMSO (0.01 %), Epoxomicin (10 nM) or PROTACs2 (10 μ M) as described in the figure legends and the cells were incubated for an additional 16 hours. The cells were then washed twice with 1X PBS and were then fixed for 15 minutes in fresh formaldehyde. After washing with PBS, the cells were incubated overnight with blocking buffer (PBS Teleostin gelatin

0.1% Triton X-100). On the next day, the cells were washed with $1 \times$ PBS, incubated with normal blocking serum ($1 \times$ PBS and secondary antibody serum) for 20 minutes and finally, incubated with the primary GFP antibody (Abcam) for 60 minutes. The cells were then washed twice with $1 \times$ PBS and were then incubated with the secondary CY3 antibody (Cat. No 111-166-047 from Jackson Immunoresearch labs) for 60 minutes. The coverslips were then mounted on slides using mounting media containing DAPI stain (Prolong Gold antifade reagent Cat no. P 36931 from Invitrogen) and visualized using a $40 \times$ confocal microscope (Leica TCS SP5 inverted microscope)

RT Real-Time PCR

The cells were harvested at the time points described in the figure legends, and the RNA was extracted using TRIzol reagent (Invitrogen). For RT real-time PCR, the cDNA was prepared using the manufacturer's protocol for Omniscript RT kit (Qiagen, Valencia, CA) and random primers (Invitrogen). The cDNA was then analyzed using Brilliant SYBR Green QPCR Master Mix and Human QPCR Reference RNA (Stratagene). Oligonucleotide primers were synthesized by Integrated DNA Technologies, Inc. (Coralville, IA) and were specifically designed using Vector NTI 9.0.0 (InforMax; Invitrogen Life Science Software, Frederick, MD) to amplify regions spanning exon junctions. For CYP1A1, the primer sequences were the following: forward, 5'-CAAAACCTTTGAGAAGGGCCACATC-3'; and reverse, 5'-GACAGCTG GACATTGGCGTTCTC-3'. For CYP1B1, the primer sequences were the following: forward, 5'-GCTGCTCCTCCTCTTACCAGGTA-3'; and reverse, 5'-GCTGGTCACC CATAACAAGGCAGAC-3'.

Proteasome Inhibition Kinetics Assays

Apigenin, PROTAC2, or epoxomicin was mixed with a fluorogenic peptide substrate and assay buffer (20 mM Tris, pH 8.0, 0.5 mM EDTA, and 0.035 % SDS) in a 96-well plate. The chymotrypsin-like activity was assayed using the fluorogenic peptide substrates Suc-Leu-Leu-Val-Tyr-AMC (Sigma-Aldrich). Hydrolysis was initiated by the addition of human erythrocyte 20S proteasome (Biomol International, Plymouth Meeting, PA), and the reaction was monitored by fluorescence (360 nm excitation/460 nm

detection) using a Microplate Fluorescence Reader (FL600; Bio-Tek Instruments, Inc., Winooski, VT) using the software KC4 v.2.5 (Bio-Tek Instruments). The reactions were allowed to proceed for 90 min, and fluorescence was detected every 1 min. Fluorescence was quantified as arbitrary units, and progression curves were plotted for each reaction as a function of time. The range of concentrations tested was chosen such that several half-lives could be observed during the course of the analyses.

Statistical Analysis

The data were analyzed using analysis of variance (ANOVA) with Bonferroni's multiple comparison test as mentioned in the figure legends.

Synthesis of acetylated apigenin derivatives

To a solution of apigenin (20.0 mg, 0.0740 mmol) in DMF (1 ml) added acetic anhydride (34.0 mg, 0.333 mmol) and N,N-dimethylaminopyridine (0.5 mg, 0.0041 mmol). After stirring for 1 hour, the resulting mixture was concentrated under vacuum and subjected to flash column chromatography (CH₂Cl₂: MeOH = 99:1) yielding three acetylated apigenins as yellowish solids.

4',7-diacetyl-apigenin: ¹H NMR: δ = 7.92 (d, *J* = 7.5 Hz, 2H), 7.29 (d, *J* = 7.5 Hz, 2H), 6.84 (s, 1H), 6.65 (s, 1H), 6.59 (s, 1H), 2.37 (s, 6H) ppm. Mass calcd. for [M] 354.07, found (ES) [M] 354.

4',5,7-triacetyl-apigenin: ¹H NMR: δ = 7.87 (d, *J* = 7.5 Hz, 2H), 7.39 (s, 1H), 7.24 (d, *J* = 7.5 Hz, 2H), 6.83 (s, 1H), 6.61 (s, 1H), 2.44 (s, 3H), 2.36 (s, 6H) ppm. Mass calcd. for [M] 396.08, found (ES) [M] 396.

4',5-diacetyl-apigenin: ¹H NMR: δ = 7.90 (d, *J* = 7.5 Hz, 2H), 7.23 (d, *J* = 7.5 Hz, 2H), 6.83 (s, 1H), 6.58 (s, 2H), 2.42 (s, 3H), 2.37 (s, 3H) ppm. Mass calcd. for [M] 354.07, found (ES) [M] 354.

Synthesis of PROTACs

Synthesis of 6

To a solution of apigenin (100 mg, 0.3695 mmol) in DMF (2 ml) was added K_2CO_3 (70 mg, 0.2586 mmol) and methyl-11-Bromoundecanoate (103.2 mg, 0.3695 mmol). After stirring at room temperature for 15 h, the resulting mixture was concentrated under vacuum and subjected to flash column chromatography ($CH_2Cl_2/MeOH$, 95:5) yielding 6 (86.2 mg, 50 %) as a yellowish solid.

1H NMR: $\delta = 7.83$ (d, $J = 8.5$ Hz, 2H, 3'-H, 5'-H), 7.08 (d, $J = 8.5$ Hz, 2H, 2'-H, 6'-H), 6.57 (s, 1H, 3-H), 6.46 (s, 1H, 6-H), 6.34 (s, 1H, 8-H), 4.02 (t, $J = 6.1$ Hz, 2H, O- CH_2 -), 3.67 (s, 3H, O- CH_3), 2.31 (t, $J = 7.3$ Hz, 2H, - CH_2 -CO-), 1.81 (m, 2H, -O- CH_2 - CH_2), 1.63 (m, 2H, - CH_2 - CH_2 -CO-), 1.31 (s, 12H, - C_6H_{12} -) ppm.

Synthesis of 7

Compound 6 (25 mg, 0.0534 mmol) in DMF (1 ml) was treated with benzyl bromide (33 mg, 0.2134 mmol) and K_2CO_3 (26 mg, 0.1880 mmol) to produce 7 (25 mg, 84 %) at C7-OH position as a major product.

1H NMR: $\delta = 7.83$ (d, $J = 8.5$ Hz, 2H, 3'-H, 5'-H), 7.35 (m, 5H, -Ph), 7.08 (d, $J = 8.5$ Hz, 2H, 2'-H, 6'-H), 6.57 (s, 1H, 3-H), 6.46 (s, 1H, 6-H), 6.34 (s, 1H, 8-H), 4.02 (t, $J = 6.1$ Hz, 2H, O- CH_2 -), 3.67 (s, 3H, O- CH_3), 2.31 (t, $J = 7.3$ Hz, 2H, - CH_2 -CO-), 1.81 (m, 2H, -O- CH_2 - CH_2), 1.63 (m, 2H, - CH_2 - CH_2 -CO-), 1.31 (s, 12H, - C_6H_{12} -) ppm.

Synthesis of 8

To a solution of the 6 (25.0 mg, 0.0534 mmol) in THF/ H_2O , 3:1(1 ml) was added LiOH (6.4 mg, 0.2668 mmol). After stirring at room temperature for 15 h, the resulting mixture was poured into H_2O with cold 1N HCl and extracted with CH_2Cl_2 . The organic

layers were combined, washed with brine, dried over Na₂SO₄, filtered, concentrated and dried under vacuum to yield the free acid of 8 (19.0 mg, 78 %).

¹H NMR: δ = 7.83 (d, J = 8.5 Hz, 2H, 3'-*H*, 5'-*H*), 7.08 (d, J = 8.5 Hz, 2H, 2'-*H*, 6'-*H*), 6.57 (s, 1H, 3-*H*), 6.46 (s, 1H, 6-*H*), 6.34 (s, 1H, 8-*H*), 4.02 (t, J = 6.1 Hz, 2H, O-CH₂-), 2.31 (t, J = 7.3 Hz, 2H, -CH₂-CO-), 1.81 (m, 2H, -O-CH₂-CH₂), 1.63 (m, 2H, -CH₂-CH₂-CO-), 1.31 (s, 12H, -C₆H₁₂-) ppm.

Synthesis of 9

To a solution of 7 (25.0 mg, 0.0447 mmol) in THF/H₂O, 3:1(1 ml) was added LiOH (5.4 mg, 0.2237 mmol). After stirring at room temperature for 15 h, the resulting mixture was poured into H₂O with cold 1N HCl and extracted with CH₂Cl₂. The organic layers were combined, washed with brine, dried over Na₂SO₄, filtered, concentrated and dried under vacuum to yield the free acid 9 (20.0 mg, 81 %).

¹H NMR: δ = 7.83 (d, J = 8.5 Hz, 2H, 3'-*H*, 5'-*H*), 7.35 (m, 5H, -Ph), 7.08 (d, J = 8.5 Hz, 2H, 2'-*H*, 6'-*H*), 6.57 (s, 1H, 3-*H*), 6.46 (s, 1H, 6-*H*), 6.34 (s, 1H, 8-*H*), 4.02 (t, J = 6.1 Hz, 2H, O-CH₂-), 2.31 (t, J = 7.3 Hz, 2H, -CH₂-CO-), 1.81 (m, 2H, -O-CH₂-CH₂), 1.63 (m, 2H, -CH₂-CH₂-CO-), 1.31 (s, 12H, -C₆H₁₂-) ppm.

Synthesis of 10

To a solution of the resulting free acid 7 (10 mg, 0.0220 mmol) in DMF (1 ml) was added HBTU (10.0 mg, 0.0264 mmol), HOBt (4.0 mg, 0.0264 mmol), diisopropylethylamine (14.2 mg, 0.1100 mmol) and E3 ubiquitin ligase recognition peptide (H₂N-Leu-Ala-Pro^{OH}-Tyr^{*t*-butyl}-Ile-OBn ; 16.3 mg, 0.0221 mmol). After stirring at room temperature for 2 h, the resulting mixture was concentrated under vacuum and subjected to flash column chromatography (CH₂Cl₂/MeOH, 9:1) to yield the fully assembled product (10.1 mg, 39 %) as a yellowish solid.

^1H NMR: $\delta = 7.83$ (d, $J = 8.5$ Hz, 2H, 3'-H, 5'-H), 7.35 (m, 5H, -Ph), 7.08 (d, $J = 8.5$ Hz, 4H, 2'-H, 6'-H, 2- H_{Tyr} , 6- H_{Tyr}), 6.87 (d, $J = 8.5$ Hz, 2H, 3- H_{Tyr} , 5- H_{Tyr}), 6.59 (s, 1H, 3-H), 6.48 (s, 1H, 6-H), 6.36 (s, 1H, 8-H), 5.13 (s, 2H, -O- CH_2 -Ar), 4.42-4.63 (m, 5H, H^{α}_{Leu} , H^{α}_{Ala} , $H^{\alpha}_{\text{Pro}}^{\text{OH}}$, H^{α}_{Tyr} , H^{α}_{Ile}), 4.02 (t, $J = 6.1$ Hz, 2H, - CH_2 -CO-), 2.84-3.95 (m, 5H, $H^{\beta}_{\text{Pro}}^{\text{OH}}$, $H^{\gamma}_{\text{Pro}}^{\text{OH}}$, $H^{\delta}_{\text{Pro}}^{\text{OH}}$), 3.09 (m, 1H, H^{β}_{Tyr}), 2.89 (m, 1H, H^{β}_{Tyr}), 2.31 (t, $J = 7.3$ Hz, 2H, -O- CH_2 -), 1.93 (m, 2H, H^{β}_{Leu}), 1.80 (m, 2H, - CH_2 - CH_2 -CO-), 1.63 (m, 2H, -O- CH_2 - CH_2), 1.55 (m, 2H, H^{β}_{Ile} , H^{γ}_{Leu}), 1.45 (m, 1H, - CH'_2 - Ile), 1.31 (s, 12H, - C_6H_{12} -), 1.28 (s, 9H, O-*t*butyl), 1.25 (s, 3H, H^{β}_{Ala}), 1.17 (m, 1H, - CH'_2 - Ile), 0.83-1.00 (m, 12H, - CH'_3 Ile, H^{δ}_{Ile} , H^{δ}_{Leu}) ppm.

To a solution of the fully assembled product (10.1 mg, 0.0086 mmol) in CH_2Cl_2 (0.5 ml) was added trifluoroacetic acid (100 μl , 0.87 mmol) at room temperature for 15 min to deprotect *t*-butyl residue of tyrosine within the fully assembled compound. Subsequently, the concentrated mixture was dried under high vacuum to remove trifluoroacetic acid. The resulting crude product was subjected to flash column chromatography ($\text{CH}_2\text{Cl}_2/\text{MeOH}$, 9:1) to yield 10 (9.1 mg, 90 %) as a yellowish solid.

^1H NMR: $\delta = 7.83$ (d, $J = 8.5$ Hz, 2H, 3'-H, 5'-H), 7.35 (m, 5H, -Ph), 7.08 (d, $J = 8.5$ Hz, 4H, 2'-H, 6'-H, 2- H_{Tyr} , 6- H_{Tyr}), 6.87 (d, $J = 8.5$ Hz, 2H, 3- H_{Tyr} , 5- H_{Tyr}), 6.59 (s, 1H, 3-H), 6.48 (s, 1H, 6-H), 6.36 (s, 1H, 8-H), 5.13 (s, 2H, -O- CH_2 -Ar), 4.42-4.63 (m, 5H, H^{α}_{Leu} , H^{α}_{Ala} , $H^{\alpha}_{\text{Pro}}^{\text{OH}}$, H^{α}_{Tyr} , H^{α}_{Ile}), 4.02 (t, $J = 6.1$ Hz, 2H, - CH_2 -CO-), 2.84-3.95 (m, 5H, $H^{\beta}_{\text{Pro}}^{\text{OH}}$, $H^{\gamma}_{\text{Pro}}^{\text{OH}}$, $H^{\delta}_{\text{Pro}}^{\text{OH}}$), 3.09 (m, 1H, H^{β}_{Tyr}), 2.89 (m, 1H, H^{β}_{Tyr}), 2.31 (t, $J = 7.3$ Hz, 2H, -O- CH_2 -), 1.93 (m, 2H, H^{β}_{Leu}), 1.80 (m, 2H, - CH_2 - CH_2 -CO-), 1.63 (m, 2H, -O- CH_2 - CH_2), 1.55 (m, 2H, H^{β}_{Ile} , H^{γ}_{Leu}), 1.45 (m, 1H, - CH'_2 - Ile), 1.31 (s, 12H, - C_6H_{12} -), 1.25 (s, 3H, H^{β}_{Ala}), 1.17 (m, 1H, - CH'_2 - Ile), 0.83-1.00 (m, 12H, - CH'_3 Ile, H^{δ}_{Ile} , H^{δ}_{Leu}) ppm. MS (MALDI): $m/z = 1118$, calcd. for $\text{C}_{23}\text{H}_{42}\text{N}_2\text{O}_8\cdot\text{Na}$: $m/z = 1117.56$.

Synthesis of 11

To a solution of the resulting free acid 9 (10 mg, 0.0184 mmol) in DMF (1 ml) was added HBTU (10.4 mg, 0.0275 mmol), HOBt (4.2 mg, 0.0275 mmol), Diisopropylethylamine (14.2 mg, 0.1101 mmol) and E3 ubiquitin ligase recognition peptide ($\text{H}_2\text{N-Leu-Ala-Pro}^{\text{OH}}\text{-Tyr}^{\text{t-butyl}}\text{-Ile-OBn}$; 16.3 mg, 0.022 mmol). After stirring at room temperature for 2 h, the resulting mixture was concentrated under vacuum and subjected to flash column chromatography ($\text{CH}_2\text{Cl}_2/\text{MeOH}$, 9:1) to yield the fully assembled product (11.0 mg, 48 %) as a yellowish solid.

$^1\text{H NMR}$: $\delta = 7.83$ (d, $J = 8.5$ Hz, 2H, 3'-H, 5'-H), 7.35 (m, 10H, -Ph), 7.08 (d, $J = 8.5$ Hz, 4H, 2'-H, 6'-H, 2- H_{Tyr} , 6- H_{Tyr}), 6.87 (d, $J = 8.5$ Hz, 2H, 3- H_{Tyr} , 5- H_{Tyr}), 6.57 (s, 1H, 3-H), 6.46 (s, 1H, 6-H), 6.34 (s, 1H, 8-H), 5.13 (s, 4H, -O- CH_2 -Ar), 4.42-4.63 (m, 5H, H_{Leu}^{α} , H_{Ala}^{α} , $H_{\text{Pro}}^{\alpha \text{OH}}$, H_{Tyr}^{α} , H_{Ile}^{α}), 4.02 (t, $J = 6.1$ Hz, 2H, - CH_2 -CO-), 2.84-3.95 (m, 5H, $H_{\text{Pro}}^{\beta \text{OH}}$, $H_{\text{Pro}}^{\gamma \text{OH}}$, $H_{\text{Pro}}^{\delta \text{OH}}$), 3.09 (m, 1H, H_{Tyr}^{β}), 2.89 (m, 1H, H_{Tyr}^{β}), 2.31 (t, $J = 7.3$ Hz, 2H, -O- CH_2 -), 1.93 (m, 2H, H_{Leu}^{β}), 1.80 (m, 2H, - CH_2 - CH_2 -CO-), 1.63 (m, 2H, -O- CH_2 - CH_2), 1.55 (m, 2H, H_{Ile}^{β} , H_{Leu}^{γ}), 1.45 (m, 1H, - CH'_2 - Ile), 1.31 (s, 12H, - C_6H_{12} -), 1.28 (s, 9H, O-*t*-butyl), 1.25 (s, 3H, H_{Ala}^{β}), 1.17 (m, 1H, - CH'_2 - Ile), 0.83-1.00 (m, 12H, - CH'_3 Ile, H_{Ile}^{δ} , H_{Leu}^{δ}) ppm.

To a solution of the fully assembled product (11.0 mg, 0.0087 mmol) in CH_2Cl_2 (0.5 ml) was added trifluoroacetic acid (100 μl , 0.87 mmol) at room temperature for 15 min to deprotect *t*-butyl residue of tyrosine within the fully assembled compound. Subsequently, the concentrated mixture was dried under high vacuum to remove trifluoroacetic acid. The resulting crude product was subjected to flash column chromatography ($\text{CH}_2\text{Cl}_2/\text{MeOH}$, 9:1) to yield 11 (11.0 mg, 99 %) as a yellowish solid.

$^1\text{H NMR}$: $\delta = 7.83$ (d, $J = 8.5$ Hz, 2H, 3'-H, 5'-H), 7.35 (m, 10H, -Ph), 7.08 (d, $J = 8.5$ Hz, 4H, 2'-H, 6'-H, 2- H_{Tyr} , 6- H_{Tyr}), 6.87 (d, $J = 8.5$ Hz, 2H, 3- H_{Tyr} , 5- H_{Tyr}), 6.57 (s, 1H, 3-H), 6.46 (s, 1H, 6-H), 6.34 (s, 1H, 8-H), 5.13 (s, 4H, -O- CH_2 -Ar), 4.42-4.63 (m, 5H, H_{Leu}^{α} , H_{Ala}^{α} , $H_{\text{Pro}}^{\alpha \text{OH}}$, H_{Tyr}^{α} , H_{Ile}^{α}), 4.02 (t, $J = 6.1$ Hz, 2H, - CH_2 -CO-), 2.84-3.95 (m, 5H,

$H^{\beta}_{\text{Pro}}^{\text{OH}}$, $H^{\gamma}_{\text{Pro}}^{\text{OH}}$, $H^{\delta}_{\text{Pro}}^{\text{OH}}$), 3.09 (m, 1H, H^{β}_{Tyr}), 2.89 (m, 1H, H^{β}_{Tyr}), 2.31(t, $J = 7.3$ Hz, 2H, -O-CH₂-), 1.93 (m, 2H, H^{β}_{Leu}), 1.80 (m, 2H, -CH₂-CH₂-CO-), 1.63 (m, 2H, -O-CH₂-CH₂), 1.55 (m, 2H, H^{β}_{Ile} , H^{γ}_{Leu}), 1.45 (m, 1H, -CH^γ₂- Ile), 1.31 (s, 12H, -C₆H₁₂-), 1.25 (s, 3H, H^{β}_{Ala}), 1.17 (m, 1H, -CH^γ₂- Ile), 0.83-1.00 (m, 12H, -CH^γ₃ Ile, H^{δ}_{Ile} , H^{δ}_{Leu}) ppm. MS (MALDI): m/z = 1231, calcd. for C₂₃H₄₂N₂O₈·Na: m/z = 1230.60.

Synthesis of 12

To a solution of the resulting free acid 9 (10.0 mg, 0.0184 mmol) in DMF (1 ml) was added HBTU (10.4 mg, 0.0275 mmol), HOBt (4.2 mg, 0.0275 mmol), Diisopropylethylamine(14.2mg, 0.1101mmol) and E3 ubiquitin ligase recognition peptide (H₂N-Leu-Ala-Pro^{OH}-Tyr^{*t*-butyl}-Ile-OBn ; 15.3 mg, 0.0220 mmol). After stirring at room temperature for 2 h, the resulting mixture was concentrated under vacuum and subjected to flash column chromatography (CH₂Cl₂/MeOH, 9:1) to yield the fully assembled product (11.0 mg, 49 %) as a yellowish solid.

¹H NMR: δ = 7.83 (d, $J = 8.5$ Hz, 2H, 3'-H, 5'-H), 7.35 (m, 5H, -Ph), 7.08 (d, $J = 8.5$ Hz, 4H, 2'-H, 6'-H, 2-H_{Tyr}, 6-H_{Tyr}), 6.87 (d, $J = 8.5$ Hz, 2H, 3-H_{Tyr}, 5-H_{Tyr}), 6.59 (s, 1H, 3-H), 6.48 (s, 1H, 6-H), 6.36 (s, 1H, 8-H), 5.13 (s, 2H, -O-CH₂-Ar), 4.42-4.63 (m, 5H, H^{α}_{Leu} , 2 H^{α}_{Ala} , H^{α}_{Tyr} , H^{α}_{Ile}), 4.02 (t, $J = 6.1$ Hz, 2H, -CH₂-CO-), 3.09 (m, 1H, H^{β}_{Tyr}), 2.89 (m, 1H, H^{β}_{Tyr}), 2.31(t, $J = 7.3$ Hz, 2H, -O-CH₂-), 1.93 (m, 2H, H^{β}_{Leu}), 1.80 (m, 2H, -CH₂-CH₂-CO-), 1.63 (m, 2H, -O-CH₂-CH₂), 1.55 (m, 2H, H^{β}_{Ile} , H^{γ}_{Leu}), 1.45 (m, 1H, -CH^γ₂- Ile), 1.31 (s, 12H, -C₆H₁₂-), 1.28 (s, 9H, O-*t*butyl), 1.25 (s, 6H, H^{β}_{Ala}), 1.17 (m, 1H, -CH^γ₂- Ile), 0.83-1.00 (m, 12H, -CH^γ₃ Ile, H^{δ}_{Ile} , H^{δ}_{Leu}) ppm.

To a solution of the fully assembled product (11.0 mg, 0.0090 mmol) in CH₂Cl₂ (0.5 ml) was added trifluoroacetic acid (100 μl, 0.87 mmol) at room temperature for 15 min to deprotect *t*-butyl residue of tyrosine within the fully assembled compound. Subsequently, the concentrated mixture was dried under high vacuum to remove trifluoroacetic acid. The resulting crude product was subjected to flash column chromatography (CH₂Cl₂/MeOH, 9:1) to yield 12 (10.4 mg, 99 %) as a yellowish solid.

^1H NMR: $\delta = 7.83$ (d, $J = 8.5$ Hz, 2H, 3'- H , 5'- H), 7.35 (m, 5H, -Ph), 7.08 (d, $J = 8.5$ Hz, 4H, 2'- H , 6'- H , 2- H_{Tyr} , 6- H_{Tyr}), 6.87 (d, $J = 8.5$ Hz, 2H, 3- H_{Tyr} , 5- H_{Tyr}), 6.59 (s, 1H, 3- H), 6.48 (s, 1H, 6- H), 6.36 (s, 1H, 8- H), 5.13 (s, 2H, -O- CH_2 -Ar), 4.42-4.63 (m, 5H, H^{α}_{Leu} , 2 H^{α}_{Ala} , H^{α}_{Tyr} , H^{α}_{Ile}), 4.02 (t, $J = 6.1$ Hz, 2H, - CH_2 -CO-), 3.09 (m, 1H, H^{β}_{Tyr}), 2.89 (m, 1H, H^{β}_{Tyr}), 2.31 (t, $J = 7.3$ Hz, 2H, -O- CH_2 -), 1.93 (m, 2H, H^{β}_{Leu}), 1.80 (m, 2H, - CH_2 - CH_2 -CO-), 1.63 (m, 2H, -O- CH_2 - CH_2), 1.55 (m, 2H, H^{β}_{Ile} , H^{γ}_{Leu}), 1.45 (m, 1H, - $\text{CH}^{\gamma}_{2-\text{Ile}}$), 1.31 (s, 12H, - C_6H_{12} -), 1.25 (s, 6H, H^{β}_{Ala}), 1.17 (m, 1H, - $\text{CH}^{\gamma}_{2-\text{Ile}}$), 0.83-1.00 (m, 12H, - $\text{CH}^{\gamma}_{3-\text{Ile}}$, H^{δ}_{Ile} , H^{δ}_{Leu}) ppm. MS (MALDI): $m/z = 1169$, calcd. for $\text{C}_{23}\text{H}_{42}\text{N}_2\text{O}_8\cdot\text{Na}$: $m/z = 1168.60$.

CHAPTER 4 IDENTIFICATION OF NOVEL AHR LIGANDS

4.1 Introduction

Thus far, a large number of synthetic or naturally occurring small molecules of diverse structures were shown to interact with AHR. Several compounds such as, 3'-methoxy-4'-nitroflavone (MNF) and anthraquinones exhibited antagonistic activity and have been used to validate the AHR as a therapeutic target for chemoprevention (112, 134). Despite the promising activities of these compounds, their use as molecular probes is limited due to the lack of specificity and/or the partial potency as an agonist.

Recently, Kim and colleagues have reported a novel synthetic antagonist of AHR, 1-methyl-1H-pyrazole-5-carboxylic acid N-[2-methyl-4-[(2-methylphenyl)diazenyl]-phenyl]-amide (26) (116). They screened a large random library of synthetic molecules for AHR antagonistic activity (116). Since the concept of positional scanning of a given scaffold has been well-known in identifying the optimal compounds in the development of peptide-based ligands, it was thought to be plausible to apply this approach to non-peptide small molecules to identify optimum compounds. With this in mind, we identified a number of AHR ligands by positional scanning using 1-methyl 1H-pyrazole-5-carboxylic acid N-[2-methyl-4-[(2-methylphenyl)diazenyl]-phenyl]-amide as a scaffold.

Each aromatic ring system of the scaffold was modified stepwise with various structures affording a small chemical library. The resulting library was then screened for the ability to block the activation of AHR induced by TCDD using a luciferase reporter assay. N-[2-Methyl-4-[(2-methylphenyl)diazenyl]phenyl]-2-furan carboxamide (31) and N-[2-methyl-4-[(2-methylphenyl)diazenyl]phenyl]-2-pyridine carboxamide (36) were identified as antagonists and N-[2-methyl-4-[(2-ethylphenyl)diazenyl]phenyl]-2-pyridine carboxamide (47) was identified as an agonist. Interestingly, a diphenyldiazeno structure, 2-methyl-4-[(2-methylphenyl)diazenyl]-aniline (60), exerted antagonistic activity whereas the rest of the bipheyls did not show the antagonistic activity. The detailed structure-activity relationship studies revealed that three aromatic rings are critical for the

AHR antagonistic activity. The modification on middle ring structure did not change parent compound's activity, suggesting that the middle ring can be modified to attach affinity reagents or prepare PROTACs.

4.2 The construction of privileged library

Three aromatic rings of the parent compound are linked through diazenyl- and amide linkages (Figure 4.1). Since the condensation methods for both linkages are well established, three synthons were generated: 2-methylphenyl diazenylium, 2-methylphenylamino, and 1-methyl-1H-pyrazole-5-carbonyl fragments. The fragments were then converted into the corresponding synthetic equivalents, 2-methylphenyl diazenylium chloride, 2-methyl phenyl amine (*o*-toluidine), and 1-methyl-1H-pyrazole-5-carboxylic acid, respectively. Using modified Wang's (135) and Azumaya's method (136), diazenyl coupling and anilide condensation were sequentially carried out. Using similar strategies, compounds with various structures were synthesized (Figure 4.1).

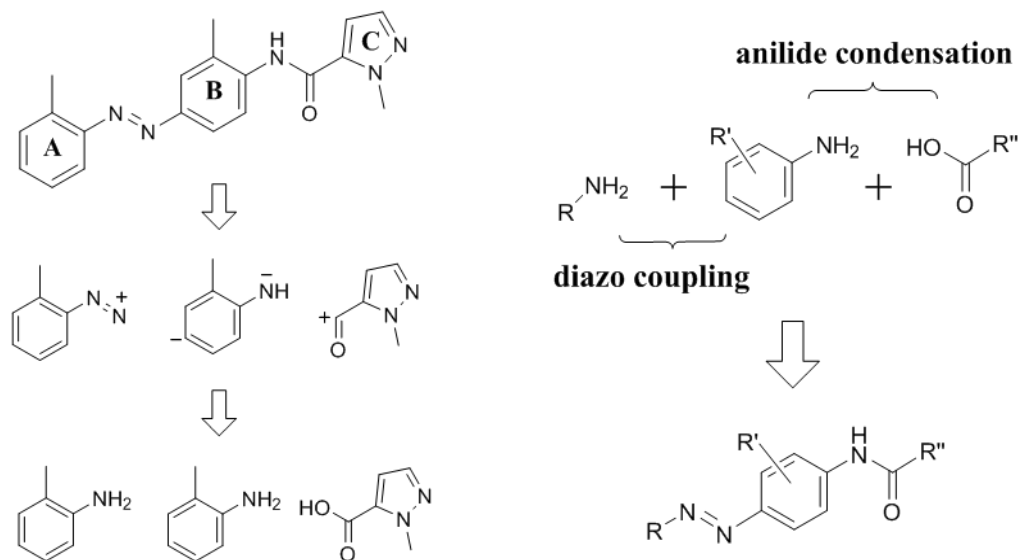


Figure 4.1 The structure of N-[2-methyl-4-[(2-methylphenyl)diazenyl]-phenyl]-1-Methyl-1H-pyridiazenylle-5-carboxamide and the synthetic approach for combinatorial chemistry.

4.2.1 C Ring optimization

The positional scanning strategy started with the C ring, while the structure of A- and B- rings was unchanged. The 1-methyl-1H-pyrazole of the parent compound was substituted with various residues: 1) 5-membered or 2) 6-membered aromatic rings varying in composition and position, 3) fully saturated cyclic hydrocarbons, 4) multinuclear aromatic rings and 5) bulky hydrocarbon (Figure 4.2).

Among 17 analogues prepared in these studies, compound 36 and 31 were comparable to the parent compound inhibiting AHR action. Interestingly, the compounds with fully saturated cyclic hydrocarbons (32, 33) did not inhibit AHR activity. The analogues containing N-methyl indole (35) or pyrene (42) structure exhibited agonistic activity whereas multi-ring structures, such as indole (34), naphthalene (38) or anthracene (41), did not show any agonistic activity (Figure 4.3).

The compound containing indole (34) moiety showed weak antagonistic activity whereas the analogue containing N-methyl indole (35) exhibited weak agonistic activity toward AHR, implying that the methyl group on this structure may influence the action of AHR. The contribution of a methyl group on the activity of was also observed in different ring systems such as pyrrole (27, 28) and naphthalene (38, 39), although the differences were not as significant as indole ring system. However, the contribution of methyl group was not observed in phenyl and tolyl pairing systems (29, 30). Differences in the activities of analogues containing bulky hydrocarbon, noradamantane (43) or bent aromatic ring, acenaphthene (40) were insignificant (Figure 4.3).

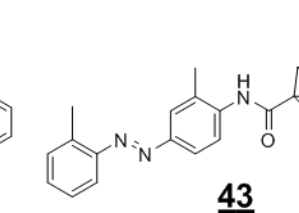
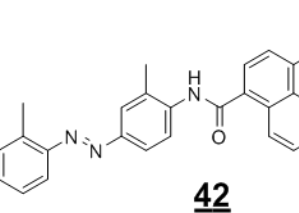
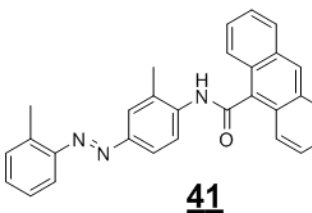
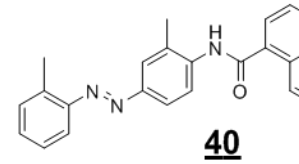
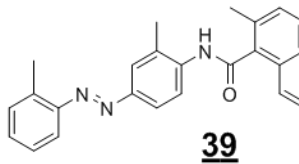
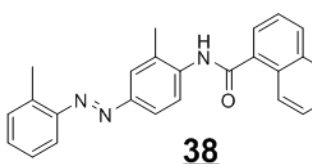
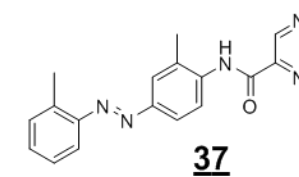
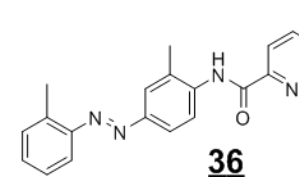
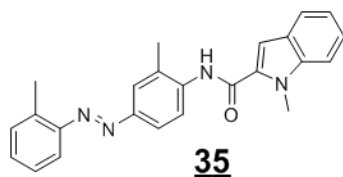
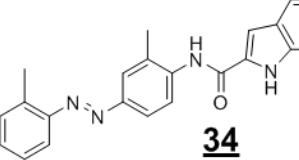
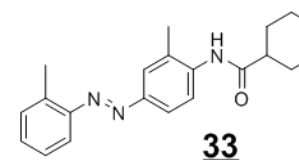
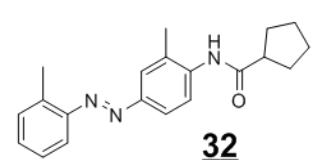
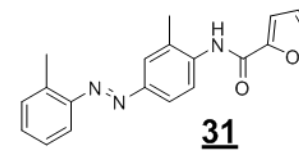
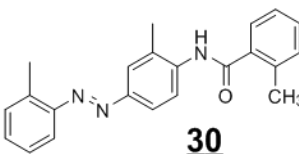
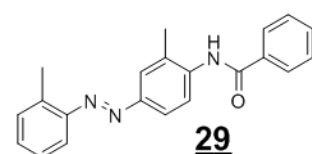
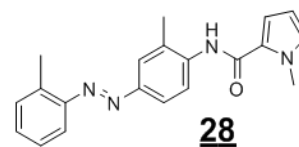
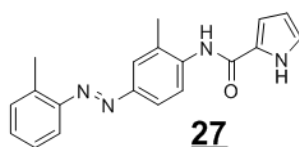
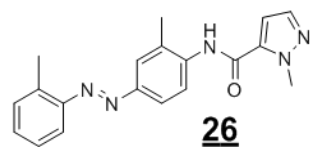
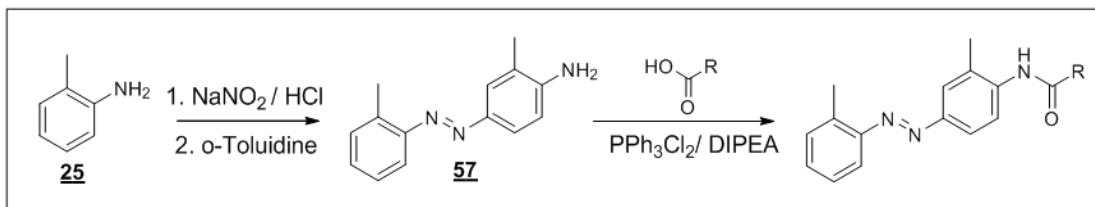


Figure 4.2 Synthetic scheme and the resulting library of C ring substituted analogues of 2-methyl-4-[(2-methylphenyl)diazenyl]phenyl carboxamides.

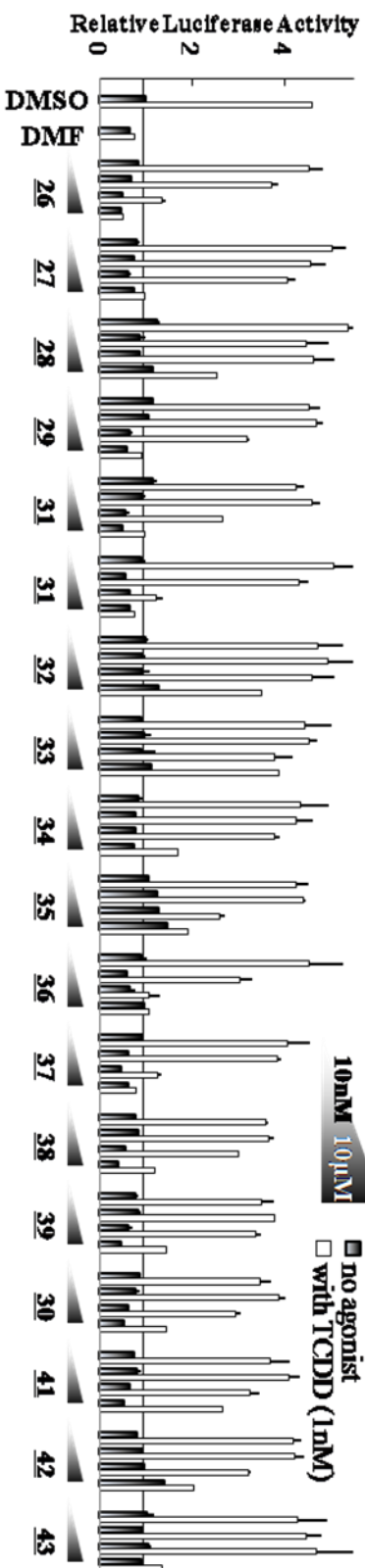


Figure 4.3 Biological activities of C ring substituted analogues. HepG2 cells were transfected with human CYP1A1 promoter coupled luciferase gene construct (HepG2-p450luc) and pre-treated either DMSO alone or with the compounds (10 nM to 10 µM). After 1hr, TCDD (1nM) was added. 4hr after TCDD treatment, the cells were harvested and luciferase activities were measured. These screening assays were performed by Eun-Young Choi, Ph.D. under the direction of Hollie I. Swanson Ph.D.

4.2.2 A ring optimization

Based on the result of C ring optimization, 2-picolinic group was selected for optimum C ring. Next, A ring was fine-tuned, attaching a methyl group at different positions of A ring. To investigate the impact of these changes, 3-methylphenyl and 4-methylphenyl groups were substituted with 2-methylphenyl of the parent group and tested the effects of these substitution using an AHR reporter assay (Figure 4.4).

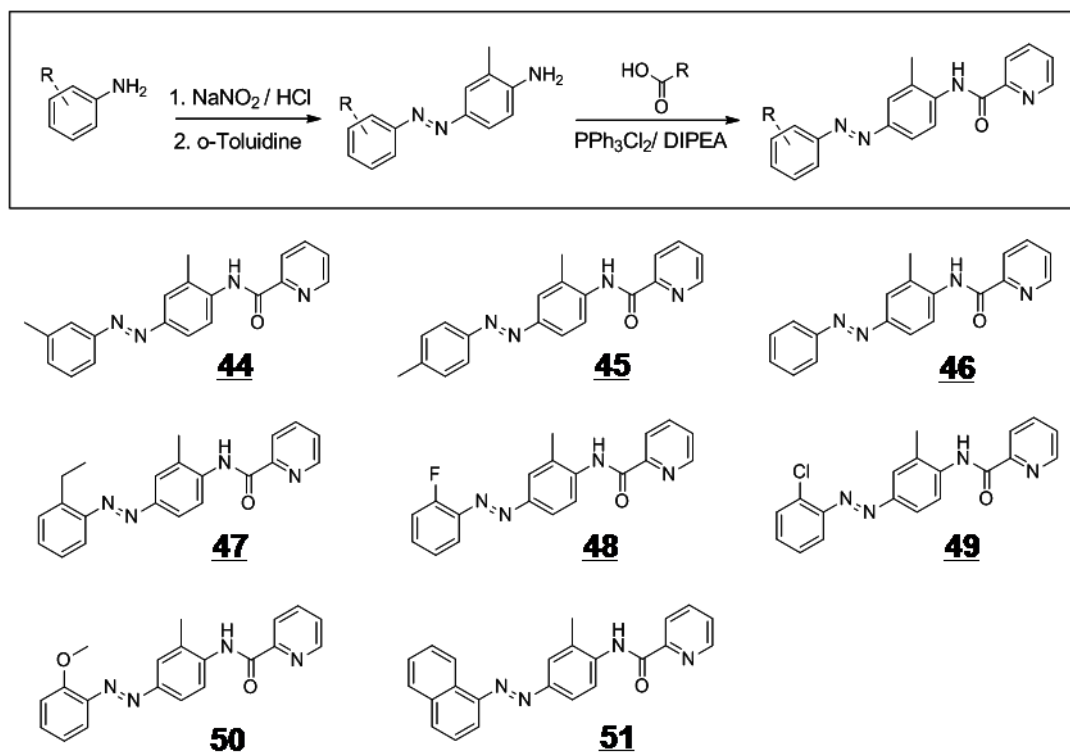


Figure 4.4 Synthetic scheme and the resulting library of C ring substituted analogues of 2-methyl-4-[(methylphenyl)diazenyl]phenyl picolinic carboxamides

In addition, 2-methylphenyl group was substituted with 1) benzene 2) halobenzene, 3) short branched phenyl structure 4) long branched structure and 5) large aromatic ring structure (Figure 4.4). The resulting compounds were evaluated for their ability to block AHR activation induced by TCDD. The location of methyl in the A ring caused significant changes in biological activity. For example, the antagonistic activity of

compound 44 was much lower than that of 36 (Figure 4.3). Further, the compound 45 did not show significant antagonistic activity even at the highest concentration, implying that the para substituent on the ring would interfere with the interaction between the ring and AHR. The removal of *ortho*-methyl (46) caused the loss of antagonistic activity displaying similar activities with 44 and the activity was restored by 2, 3-benzo substitution (51). Interestingly, when methyl group is substituted with 2-ethyl group, it displayed both agonistic and antagonistic activity. However, the replacement the methyl with 2-methoxy group (50) completely eliminated both activities. In summary, small substituents on *ortho* position appears to provide interactions with AHR. However, a para substitution seems to abolish the interaction (Figure 4.5).

The antagonistic activities of the compounds containing 2-fluorophenyl (48), 2-chlorophenyl (49) and 2-methoxyphenyl (50) structures were not comparable to the parent compound. As a whole, most compounds in the library did not exert higher activity than that of compound 36, except compound 51, which showed a comparable activity to that of compound 36. Compound 51 appears to be slightly more agonistic than 36 with 2-methylphenyl A ring group (Figure 4.5).

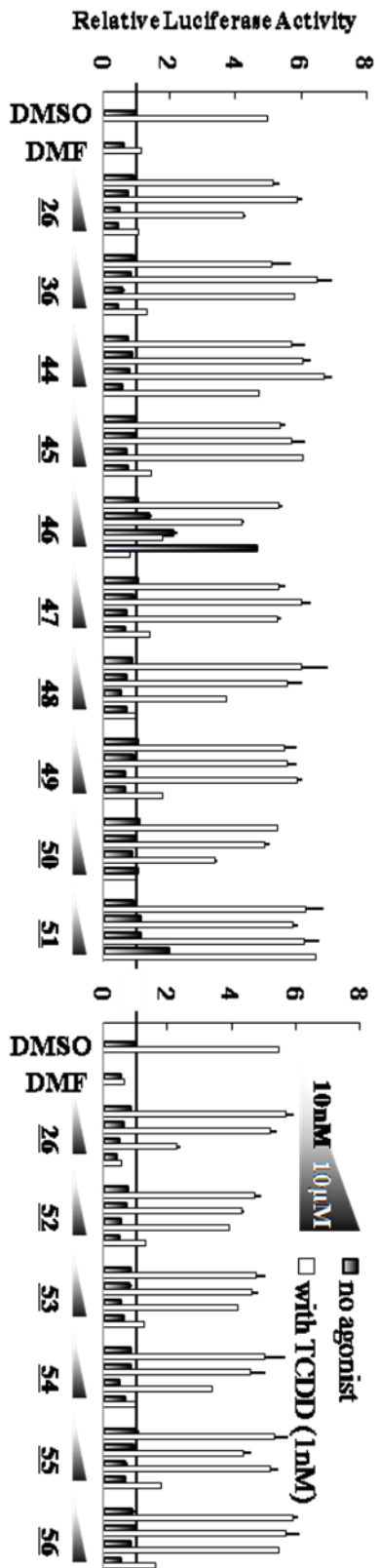


Figure 4.5 Biological activities of A ring or B ring substituted analogues. HepG2 cells were transfected with human CYP1A1 promoter coupled luciferase gene construct (HepG2-p450luc) and pre-treated either DMSO alone or with the compounds (10 nM to 10 µM). After 1hr, TCDD (1nM) was added. 4hr after TCDD treatment, the cells were harvested and luciferase activities were measured. These screening assays were performed by Eun-Young Choi, Ph.D. under the direction of Hollie I. Swanson Ph.D.

4.2.3 Ring B optimization and fine tuning

As A and C rings have been optimized with 2-methylphenyl and pyridine-2-carbonyl group, respectively, B ring was next investigated. To examine the role of 2-methyl group on B ring on the parent compound's activity, the 2-methyl group on **36** was moved to 3- position (**52**), removed (**53**), or replaced with an ethyl group (**54**) and evaluated for its impact on the AHR activity (Figure 4.6).

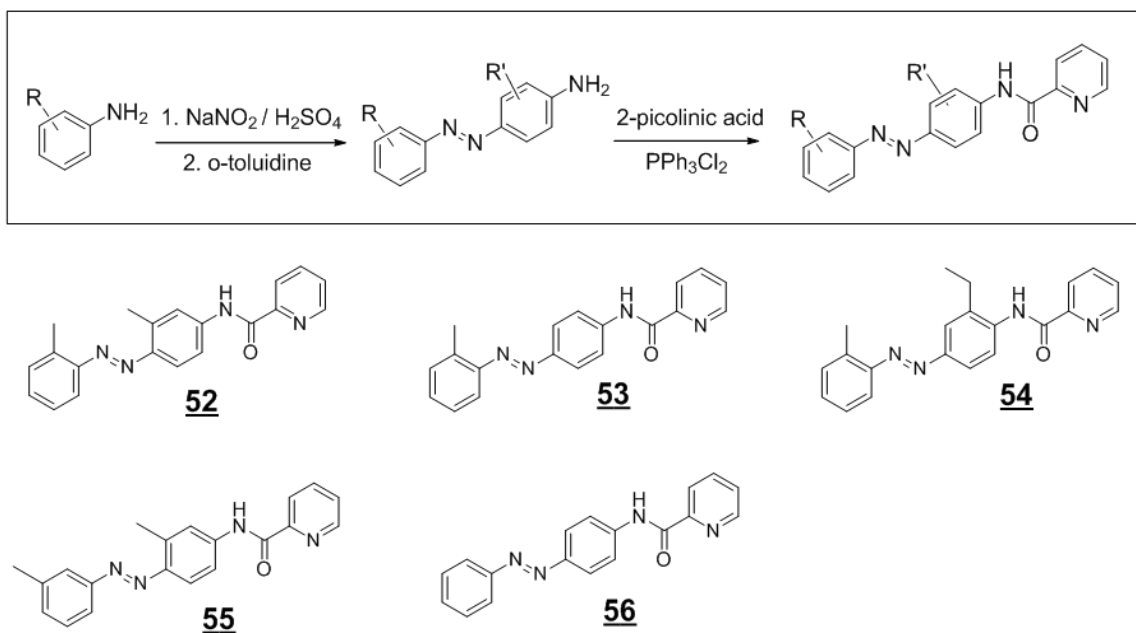


Figure 4.6 Synthetic scheme and the resulting library of diphenyldiazenyl picolinic carboxamides

All compounds prepared were not significant different from the parent compound (**36**). Based on these observations, 2-methylphenyl group is decided for the B ring. Further, the importance of methyl groups on A ring was confirmed by comparing the activities of compounds **53** and **56**. Compound (**56**) lacking methyl group on A ring completely lost its activity, supporting the importance of A ring methyl group (Figure 4.7).

4.2.4 Antagonistic evaluation of diphenyldiazenyl amines

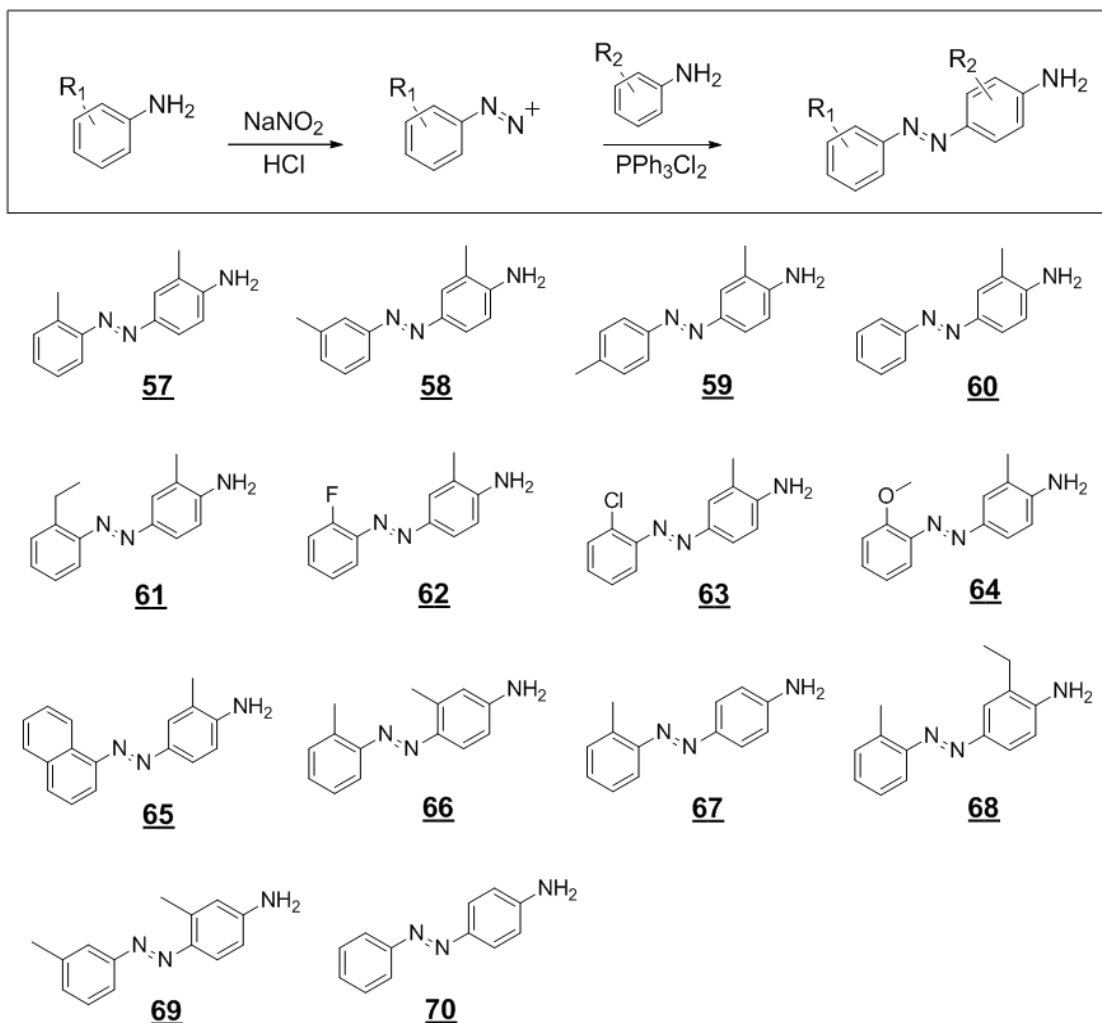


Figure 4.7 Synthetic scheme and the resulting library of diphenyldiazenyl amines

The diphenyldiazenyl amine structures were prepared as intermediates for the syntheses of carboxamides. These aromatic compounds were tested whether they have any activity against the AHR. Overall, the loss of AHR antagonistic activity was observed for all of these compounds except compound **59**. This indicates the important role of C ring in the action of the parent compound. Unlike other two ring compounds, **59** exhibited modest antagonistic activity. Furthermore, this compound synergistically increased AHR activation in concert with TCDD. On the other hand, several two ring compounds, such as **57**, **61**, **65** and **66**, exhibited AHR agonistic activities (Figure 4.7).

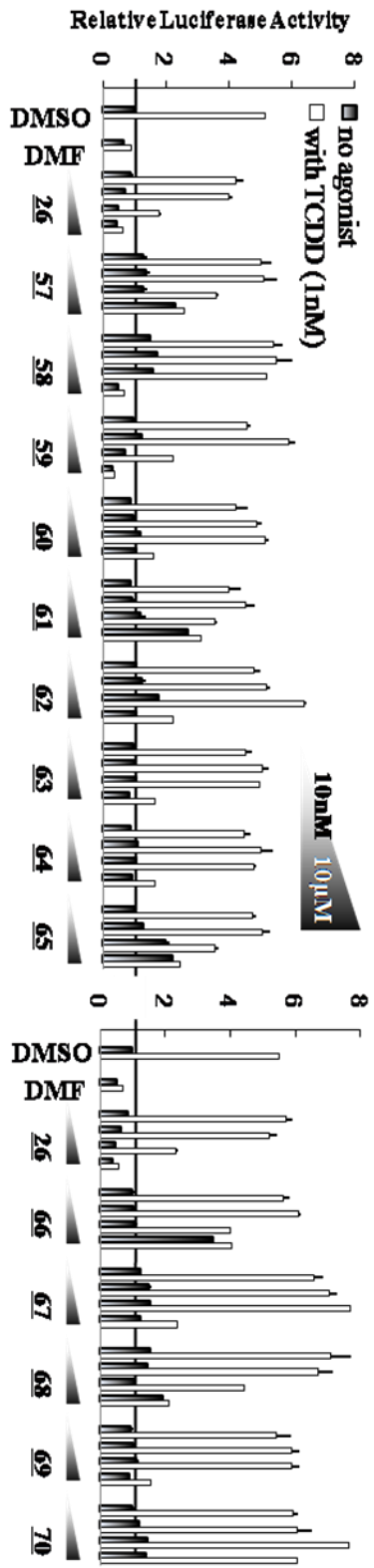


Figure 4.8 Biological activities of diphenyl diazenyl amine compounds. HepG2 cells were transfected with human CYP1A1 promoter coupled luciferase gene construct (HepG2-p450luc) and pre-treated either DMSO alone or with the compounds (10 nM to 10 µM). After 1hr, TCDD (1nM) was added. 4hr after TCDD treatment, the cells were harvested and luciferase activities were measured. These screening assays were performed by Eun-Young Choi, Ph.D. under the direction of Hollie I. Swanson Ph.D.

4.3 Discussion

To identify a novel AHR ligand, the positional scanning approach was used to optimize a parent compound CH-223191 in this chapter. Commencing with the substitution of 1-methyl-1H-pyrazole on C ring with various structures, C ring, A ring and B ring were optimized in order, identifying several compounds as antagonist or agonists. As the diphenyldiazenyl structure and an isosteric structure, stilbene, are frequently found in chemical agents exerting various biological activity suggesting the significance of this feature (97, 123, 137-142), the diphenyldiazenyl structure was conserved throughout the library due to the presumable role in the interaction with AHR.

The SAR studies reveal the optimal structure within the library generated herein. As shown above, heterocyclic ring structure, such as 1-methyl-1H-pyrazole (26), pyridine (36), furan (31) and pyrazine (37), appeared to be optimal in the C ring position for antagonistic activity while non aromatic structure (32, 33) attenuated both agonistic and antagonistic activities. To our surprise, the pyrrole and indole moiety, frequently found in endogenous ligands of AHR, did not increase the interaction with AHR. Beside, the pyrene and naphthalene structure, which are strong agonists, did not appear to increase the interaction with AHR, either.

The SAR on A and B ring revealed that methyl groups on ortho position on both rings are optimal for antagonistic activity (36, 44 and 45). Interestingly, it was found that the structural changes in methyl group on B ring were not important for interaction with AHR, whereas the concomitant shift on A ring of the same scaffold abolished the antagonistic activity. The role of B ring structure for AHR binding is yet to be elucidated. Interestingly, the partial structure of inactive compound (60) exhibited moderate antagonistic activity whereas diphenyldiazenyl amines lost the antagonistic activities observed in the corresponding three ring structures in general.

In conclusion, CH-223191 was optimized by positional scanning, identifying 36 as an optimized compound. The further biological activities of this compound are yet to be elucidated for better understanding on the ligand binding on AHR. This compound is subjected to the synthesis of a PROTAC that targets AHR.

4.4 Syntheses of compounds

Syntheses of aryl carboxamides of *o*-tolyl diazenyl-*o*-toluidine

N-[2-methyl-4-[(2-methylphenyl)diazenyl]phenyl]-1H-pyrrole-2-carboxamide (27)

To a solution of pyrrole-2-carboxylic acid (24.7 mg, 0.2219 mmol) in methylene chloride (CH₂Cl₂; 0.5 ml) was added dichlorotriphenylphosphorane (PPh₃Cl₂; 74.0 mg, 0.2219 mmol) and a drop of diisopropylethylamine. After stirring at room temperature for 30 min, the reaction mixture was added 57 (10.0 mg, 0.0444 mmol) and stirred for 1h. The resulting mixture was concentrated under vacuum and subjected to flash column chromatography (CH₂Cl₂) yielding 27 (3.8 mg, 29 %) as a yellowish solid.

¹H NMR: δ = 8.29 (d, *J* = 8.7 Hz, 1H), 7.88 (dd, *J* = 8.7, 2.1 Hz, 1H), 7.81 (s, 1H), 7.63 (s, 1H), 7.60 (d, *J* = 4.2 Hz, 2H), 7.34 (m, 2H), 7.04 (m, 1H), 6.74 (m, 1H), 6.33 (q, *J* = 3.9 Hz, 1H), 2.73 (s, 3H), 2.45 (s, 3H) ppm. Mass calcd. for [M] 318.15, found (ES) [M] 318.

1-Methyl-N-[2-methyl-4-[(2-methylphenyl)diazenyl]phenyl]-1-methyl-pyrrole-2-carboxamide (28)

To a solution of 1-methyl pyrrole-2-carboxylic acid (27.8 mg, 0.2219 mmol) in methylene chloride (CH₂Cl₂; 0.5 ml) was added dichlorotriphenylphosphorane (PPh₃Cl₂; 74.0 mg, 0.2219 mmol) and a drop of diisopropylethylamine. After stirring at room temperature for 30 min, the reaction mixture was added 57 (10.0 mg, 0.0444 mmol) and stirred for 1h. The resulting mixture was concentrated under vacuum and subjected to flash column chromatography (CH₂Cl₂) yielding 28 (1.0 mg, 7 %) as a yellowish solid.

¹H NMR: δ = 8.30 (d, *J* = 8.7 Hz, 1H), 7.88 (dd, *J*_a = 2.1 Hz, *J*_b = 8.7 Hz, 1H), 7.81 (s, 1H), 7.63 (d, *J* = 8.7 Hz, 2H), 7.36 (m, 2H), 6.85 (t, *J* = 1.8 Hz, 1H), 6.76 (dd, *J*_a = 1.5 Hz, *J*_b = 3.6 Hz, 1H), 6.20 (dd, *J*_a = 2.7 Hz, *J*_b = 3.9 Hz, 1H), 4.02 (s, 3H), 2.73 (s, 3H), 2.44 (s, 3H) ppm. Mass calcd. for [M] 332.16, found (ES) [M] 332.

N-[2-methyl-4-[(2-methylphenyl)diazenyl]phenyl]-benzamide (29)

To a solution of benzoic acid (27.1 mg, 0.2219 mmol) in methylene chloride (CH₂Cl₂; 0.5 ml) was added dichlorotriphenylphosphorane (PPh₃Cl₂; 74.0 mg, 0.2219 mmol) and a drop of diisopropylethylamine. After stirring at room temperature for 30 min, the reaction mixture was added 57 (10.0 mg, 0.0444 mmol) and stirred for 1h. The resulting mixture was concentrated under vacuum and subjected to flash column chromatography (CH₂Cl₂) yielding 29 (11.7 mg, 80 %) as a yellowish solid.

¹H NMR: δ = 8.35 (d, *J* = 8.7 Hz, 1H), 7.94 (t, *J* = 1.8 Hz, 1H), 7.92 (m, 1H), 7.90 (dd, *J*_a = 2.1 Hz, *J*_b = 8.7 Hz, 1H), 7.83 (s, 1H), 7.65 (dd, *J*_a = 7.5 Hz, *J*_b = 12.0 Hz, 2H), 7.59 (m, 2H), 7.37 (m, 2H), 7.31 (m, 1H), 2.73 (s, 3H), 2.44 (s, 3H) ppm. Mass calcd. for [M] 329.15, found (ES) [M] 329.

2-Methyl-N-[2-methyl-4-[(2-methylphenyl)diazenyl]phenyl]-benzamide (30)

To a solution of *o*-toluic acid (30.2 mg, 0.2219 mmol) in methylene chloride (CH₂Cl₂; 0.5 ml) was added dichlorotriphenylphosphorane (PPh₃Cl₂; 74.0 mg, 0.2219 mmol) and a drop of diisopropylethylamine. After stirring at room temperature for 30 min, the reaction mixture was added 57 (10.0 mg, 0.0444 mmol) and stirred for 1h. The resulting mixture was concentrated under vacuum and subjected to flash column chromatography (CH₂Cl₂) yielding 30 (14.5 mg, 95 %) as a yellowish solid.

¹H NMR: δ = 8.30 (dd, *J*_a = 1.5 Hz, *J*_b = 6.6 Hz, 1H), 7.88 (d, *J* = 9.0 Hz, 1H), 7.81 (d, *J* = 1.8 Hz, 1H), 7.63 (d, *J* = 7.8 Hz, 1H), 7.55 (d, *J* = 7.8 Hz, 1H), 7.44-7.23 (m, 6H), 2.72 (s, 3H), 2.56 (s, 3H), 2.44 (s, 3H) ppm. Mass calcd. for [M] 343.17, found (ES) [M] 343.

N-[2-methyl-4-[(2-methylphenyl)diazenyl]phenyl]-2-furancarboxamide (31)

To a solution of 2-furoic acid (24.9 mg, 0.2219 mmol) in methylene chloride (CH₂Cl₂; 0.5 ml) was added dichlorotriphenylphosphorane (PPh₃Cl₂; 74.0 mg, 0.2219

mmol) and a drop of diisopropylethylamine. After stirring at room temperature for 30 min, the reaction mixture was added 57 (10.0 mg, 0.0444 mmol) and stirred for 1h. The resulting mixture was concentrated under vacuum and subjected to flash column chromatography (CH₂Cl₂) yielding 31 (8.6 mg, 61 %) as a yellowish solid.

¹H NMR: δ = 7.87 (s, 1H), 7.78 (dd, $J_a = 2.4$ Hz, $J_b = 8.4$ Hz, 1H), 7.63 (d, $J = 7.8$ Hz, 1H), 7.48 (m, 1H), 7.42-7.26 (m, 2H), 7.05 (d, 1H), 6.47 (m, 2H), 6.34 (s, 1H), 2.72 (s, 3H), 2.41 (s, 12H) ppm. Mass calcd. for [M] 319.13, found (ES) [M] 319.

N-[2-methyl-4-[(2-methylphenyl)diazenyl]phenyl]-cyclopentanecarboxamide (32)

To a solution of cyclopentylcarboxylic acid (9.6 μL, 0.2219 mmol) in methylene chloride (CH₂Cl₂; 0.5 ml) was added dichlorotriphenylphosphorane (PPh₃Cl₂; 74.0 mg, 0.2219 mmol) and a drop of diisopropylethylamine. After stirring at room temperature for 30 min, the reaction mixture was added 57 (10.0 mg, 0.0444 mmol) and stirred for 1h. The resulting mixture was concentrated under vacuum and subjected to flash column chromatography (CH₂Cl₂) yielding 32 (14.0 mg, 98 %) as a yellowish solid.

¹H NMR: δ = 8.23 (d, $J = 8.4$, 1H), 7.84 (dd, $J_a = 2.1$ Hz, $J_b = 8.4$ Hz, 1H), 7.78 (d, $J = 1.8$ Hz, 1H), 7.63 (d, $J = 7.5$ Hz, 2H), 7.36-7.32 (m, 2H), 7.29-7.24 (m, 1H), 7.13 (m, 1H), 2.81 (quintet, $J = 8.1$ Hz, 1H), 2.73 (s, 3H), 2.37 (s, 3H), 2.00-1.61 (m, 8H) ppm. Mass calcd. for [M] 321.18, found (ES) [M] 321.

N-[2-methyl-4-[(2-methylphenyl)diazenyl]phenyl]-cyclohexanecarboxamide (33)

To a solution of cyclohexylcarboxylic acid (11 μL, 0.2219 mmol) in methylene chloride (CH₂Cl₂; 0.5 ml) was added dichlorotriphenylphosphorane (PPh₃Cl₂; 74.0 mg, 0.2219 mmol) and a drop of diisopropylethylamine. After stirring at room temperature for 30 min, the reaction mixture was added 57 (10.0 mg, 0.0444 mmol) and stirred for 1h. The resulting mixture was concentrated under vacuum and subjected to flash column chromatography (CH₂Cl₂) yielding 33 (12.9 mg, 87 %) as a yellowish solid.

^1H NMR: $\delta = 8.23$ (d, $J = 8.4$ Hz, 1H), 7.84 (dd, $J_a = 2.1$ Hz, $J_b = 8.4$ Hz, 1H), 7.81 (d, $J = 1.8$ Hz, 1H), 7.62 (d, $J = 7.5$ Hz, 2H), 7.36 - 7.33 (m, 2H), 7.26 - 7.18 (m, 1H), 7.14 (m, 1H), 2.72 (s, 3H), 2.38 (s, 3H), 2.35 - 1.26 (m, 10H) ppm. Mass calcd. for [M] 335.20, found (ES) [M] 335.

N-[2-methyl-4-[(2-methylphenyl)diazenyl]phenyl]-1H-indole-2-carboxamide (34)

To a solution of 1H-indole-2-carboxylic acid (35.8 mg, 0.2219 mmol) in methylene chloride (CH_2Cl_2 ; 0.5 ml) was added dichlorotriphenylphosphorane (PPh_3Cl_2 ; 74.0 mg, 0.2219 mmol) and a drop of diisopropylethylamine. After stirring at room temperature for 30 min, the reaction mixture was added 57 (10.0 mg, 0.0444 mmol) and stirred for 1h. The resulting mixture was concentrated under vacuum and subjected to flash column chromatography (CH_2Cl_2) yielding 34 (1.0 mg, 6 %) as a yellowish solid.

^1H NMR: $\delta = 8.36$ (d, $J = 8.7$ Hz, 1H), 7.89 (m, 3H), 7.74 (d, $J = 8.7$ Hz, 1H), 7.65 (d, $J = 7.8$ Hz, 1H), 7.51 (d, $J = 7.8$ Hz, 1H), 7.35 (m, 3H), 7.26 - 7.18 (m, 1H), 7.04 (s, 1H), 2.74 (s, 3H), 2.52 (s, 3H) ppm. Mass calcd. for [M] 368.16, found (ES) [M] 368.

1-Methyl-N-[2-methyl-4-[(2-methylphenyl)diazenyl]phenyl]-indole-2-carboxamide (35)

To a solution of 1-methylindole-2-carboxylic acid (38.9 mg, 0.2219 mmol) in methylene chloride (CH_2Cl_2 ; 0.5 ml) was added dichlorotriphenylphosphorane (PPh_3Cl_2 ; 74.0 mg, 0.2219 mmol) and a drop of diisopropylethylamine. After stirring at room temperature for 30 min, the reaction mixture was added 57 (10.0 mg, 0.0444 mmol) and stirred for 1h. The resulting mixture was concentrated under vacuum and subjected to flash column chromatography (CH_2Cl_2) yielding 35 (4.0 mg, 24 %) as a yellowish solid.

^1H NMR: $\delta = 8.37$ (d, $J = 8.7$ Hz, 1H), 7.94 - 7.88 (m, 2H), 7.85 (s, 1H), 7.73 (d, $J = 8.4$ Hz, 1H), 7.66 (d, $J = 8.4$ Hz, 1H), 7.45 - 7.40 (m, 2H), 7.36 (m, 2H), 7.29 - 7.19 (m, 1H),

7.14 (m, 1H), 4.14 (s, 3H), 2.75 (s, 3H), 2.49 (s, 3H) ppm. Mass calcd. for [M] 382.18, found (ES) [M] 382.

N-[2-methyl-4-[(2-methylphenyl)diazenyl]phenyl]-2-pyridinecarboxamide (36)

To a solution of 2-picolinic acid (27.3 mg, 0.2219 mmol) in methylene chloride (CH₂Cl₂; 0.5 ml) was added dichlorotriphenylphosphorane (PPh₃Cl₂; 74.0 mg, 0.2219 mmol) and a drop of diisopropylethylamine. After stirring at room temperature for 30 min, the reaction mixture was added 57 (10.0 mg, 0.0444 mmol) and stirred for 1h. The resulting mixture was concentrated under vacuum and subjected to flash column chromatography (CH₂Cl₂) yielding 36 (3.6 mg, 25 %) as a yellowish solid.

¹H NMR: δ = 8.67 (d, *J* = 4.5 Hz, 1H), 8.63 (d, *J* = 9.0 Hz, 1H), 8.36 (d, *J* = 8.1 Hz, 1H), 7.98-7.88 (dq, *J*_a = 1.6 Hz, *J*_b = 7.5 Hz, 2H), 7.84 (s, 1H), 7.64 (d, *J* = 8.4 Hz, 1H), 7.54 (m, 1H) 7.36 (m, 2H), 7.30 (m, 1H), 2.74 (s, 3H), 2.56 (s, 3H) ppm. Mass calcd. for [M] 330.15, found (ES) [M] 330.

N-[2-methyl-4-[(2-methylphenyl)diazenyl]phenyl]-pyrazinecarboxamide (37)

To a solution of pyrazinecarboxylic acid (27.6 mg, 0.2219 mmol) in methylene chloride (CH₂Cl₂; 0.5 ml) was added dichlorotriphenylphosphorane (PPh₃Cl₂; 74.0 mg, 0.2219 mmol) and a drop of diisopropylethylamine. After stirring at room temperature for 30 min, the reaction mixture was added 33 (10.0 mg, 0.0444 mmol) and stirred for 1h. The resulting mixture was concentrated under vacuum and subjected to flash column chromatography (CH₂Cl₂) yielding 37 (9.8 mg, 67 %) as a yellowish solid.

¹H NMR: δ = 9.56 (d, *J* = 1.5 Hz, 1H), 8.85 (d, *J* = 2.1 Hz, 1H), 8.63 (t, *J* = 2.1 Hz, 1H), 8.57 (d, *J* = 8.7 Hz, 1H), 7.91 (dd, *J*_a = 2.1 Hz, *J*_b = 8.7 Hz, 1H), 7.83 (d, *J* = 1.8 Hz, 1H), 7.61 (d, *J* = 7.5 Hz, 1H), 7.36 (m, 2H), 7.29 (m, 1H), 2.73 (s, 3H), 2.53 (s, 3H) ppm. Mass calcd. for [M] 331.14, found (ES) [M] 331.

N-[2-methyl-4-[(2-methylphenyl)diazenyl]phenyl]-1-naphthalenecarboxamide (38)

To a solution of 1-naphthoic acid (38.2 mg, 0.2219 mmol) in methylene chloride (CH₂Cl₂; 0.5 ml) was added dichlorotriphenylphosphorane (PPh₃Cl₂; 74.0 mg, 0.2219 mmol) and a drop of diisopropylethylamine. After stirring at room temperature for 30 min, the reaction mixture was added 57 (10.0 mg, 0.0444 mmol) and stirred for 1h. The resulting mixture was concentrated under vacuum and subjected to flash column chromatography (CH₂Cl₂) yielding 38 (10.5 mg, 63 %) as a yellowish solid.

¹H NMR: δ = 8.45 (d, *J* = 7.8 Hz, 2H), 8.02 (d, *J* = 9.0 Hz, 1H), 7.92 (m, 2H), 7.82 (m, 1H), 7.79 (s, 1H), 7.68-7.51 (m, 4H), 7.36 (m, 2H), 7.30 (m, 1H), 2.74 (s, 3H), 2.40 (s, 3H) ppm. Mass calcd. for [M] 379.17, found (ES) [M] 379.

2-Methyl-N-[2-methyl-4-[(2-methylphenyl)diazenyl]phenyl]-1-naphthalenecarboxamide (39)

To a solution of 2-methyl-1-naphthoic acid (41.3 mg, 0.2219 mmol) in methylene chloride (CH₂Cl₂; 0.5 ml) was added dichlorotriphenylphosphorane (PPh₃Cl₂; 74.0 mg, 0.2219 mmol) and a drop of diisopropylethylamine. After stirring at room temperature for 30 min, the reaction mixture was added 57 (10.0 mg, 0.0444 mmol) and stirred for 1h. The resulting mixture was concentrated under vacuum and subjected to flash column chromatography (CH₂Cl₂) yielding 39 (3.6 mg, 21 %) as a yellowish solid.

¹H NMR: δ = 8.27 (d, *J* = 8.7 Hz, 2H), 7.95 (s, 1H), 7.89 (dd, *J*_a = 0.9 Hz, *J*_b = 9.9 Hz, 1H), 7.80 (d, *J* = 6.6 Hz, 2H), 7.69-7.34 (m, 4H), 7.31 (m, 1H), 7.00 (m, 2H), 2.74 (s, 3H), 2.70 (s, 6H) ppm. Mass calcd. for [M] 393.18, found (ES) [M] 393.

N-[2-methyl-4-[(2-methylphenyl)diazenyl]phenyl]-5-Acenaphthenecarboxamide (40)

To a solution of 5-acenaphthene carboxylic acid (44.0 mg, 0.2219 mmol) in methylene chloride (CH₂Cl₂; 0.5 ml) was added dichlorotriphenylphosphorane (PPh₃Cl₂;

74.0 mg, 0.2219 mmol) and a drop of diisopropylethylamine. After stirring at room temperature for 30 min, the reaction mixture was added 57 (10.0 mg, 0.0444 mmol) and stirred for 1h. The resulting mixture was concentrated under vacuum and subjected to flash column chromatography (CH₂Cl₂) yielding 40 (6.0 mg, 33 %) as a yellowish solid.

¹H NMR: δ = 8.48 (d, *J* = 8.1 Hz, 1H), 8.27 (d, *J* = 8.7 Hz, 1H), 7.93 (m, 2H), 7.84 (s, 1H), 7.77 (s, 1H), 7.69 (m, 2H), 7.42 (d, *J* = 6.6 Hz, 1H), 7.37 (m, 2H), 7.31 (m, 1H), 3.47 (s, 4H), 2.75 (s, 3H), 2.43 (s, 3H) ppm. Mass calcd. for [M] 405.18, found (ES) [M] 405.

N-[2-methyl-4-[(2-methylphenyl)diazenyl]phenyl]-9-anthracenecarboxamide (41)

To a solution of 9-anthracenecarboxylic acid (49.3 mg, 0.2219 mmol) in methylene chloride (CH₂Cl₂; 0.5 ml) was added dichlorotriphenylphosphorane (PPh₃Cl₂; 74.0 mg, 0.2219 mmol) and a drop of diisopropylethylamine. After stirring at room temperature for 30 min, the reaction mixture was added 57 (10.0 mg, 0.0444 mmol) and stirred for 1h. The resulting mixture was concentrated under vacuum and subjected to flash column chromatography (CH₂Cl₂) yielding 41 (14.3 mg, 75 %) as a yellowish solid.

¹H NMR: δ = 8.65 (d, *J* = 9.0 Hz, 1H), 8.55 (s, 1H), 8.22 (d, *J* = 8.5 Hz, 2H), 8.07 (d, *J* = 9.0 Hz, 2H), 7.97, (d, *J* = 8.5 Hz, 1H), 7.81(s, 1H), 7.66 (m, 2H), 7.58-7.47 (m, 4H), 7.36 (m, 2H), 7.26 (m, 1H), 2.75 (s, 3H), 2.30 (s, 3H) ppm. Mass calcd. for [M] 429.18, found (ES) [M] 429.

N-[2-methyl-4-[(2-methylphenyl)diazenyl]phenyl]-1-pyrenecarboxamide (42)

To a solution of 1-pyrenecarboxylic acid (54.7 mg, 0.2219 mmol) in methylene chloride (CH₂Cl₂; 0.5 ml) was added dichlorotriphenylphosphorane (PPh₃Cl₂; 74.0 mg, 0.2219 mmol) and a drop of diisopropylethylamine. After stirring at room temperature for 30 min, the reaction mixture was added 57 (10.0 mg, 0.0444 mmol) and stirred for

1h. The resulting mixture was concentrated under vacuum and subjected to flash column chromatography (CH₂Cl₂) yielding 42 (12.4 mg, 62 %) as a yellowish solid.

¹H NMR: δ = 8.64 (d, *J* = 9.0 Hz, 1H), 8.32-8.27 (m, 2H), 8.23-8.10 (m, 5H), 8.08-8.01 (m, 2H), 7.85 (m, 1H), 7.79, (s, 1H), 7.57 (d, *J* = 8.0 Hz, 1H), 7.30-7.28 (m, 2H), 7.25-7.20 (m, 1H), 2.67 (s, 3H), 2.41 (s, 3H) ppm. Mass calcd. for [M] 453.18, found (ES) [M] 453.

N-[2-methyl-4-[(2-methylphenyl)diazenyl]phenyl]-noradamantane-3-carboxamide (43)

To a solution of 3-noradamantane carboxylic acid (36.9 mg, 0.2219 mmol) in methylene chloride (CH₂Cl₂; 0.5 ml) was added dichlorotriphenylphosphorane (PPh₃Cl₂; 74.0 mg, 0.2219 mmol) and a drop of diisopropylethylamine. After stirring at room temperature for 30 min, the reaction mixture was added 57 (10.0 mg, 0.0444 mmol) and stirred for 1h. The resulting mixture was concentrated under vacuum and subjected to flash column chromatography (CH₂Cl₂) yielding 43 (6.0 mg, 36 %) as a yellowish solid.

¹H NMR: δ = 8.33 (d, *J* = 8.7 Hz, 1H), 7.85 (dd, *J*_a = 0.9 Hz, *J*_b = 9.9 Hz, 1H), 7.77 (d, *J* = 6.6 Hz, 1H), 7.62 (d, *J* = 7.5 Hz, 1H), 7.37-7.33 (m, 2H), 7.26 (m, 1H), 2.86 (t, *J* = 6.3 Hz, 1H), 2.72 (s, 3H), 2.42 (s, 2H), 2.37 (s, 3H), 2.17 (dd, *J*_a = 2.7 Hz, *J*_b = 10.8 Hz, 2H), 1.97-1.89 (m, 4H), 1.75-1.63 (m, 4H) ppm. Mass calcd. for [M] 373.22, found (ES) [M] 373.

Synthesis of aminodiazenes (I)

p-(*o*-Tolyldiazenyl)-*o*-toluidine (57)

To a solution of hydrochloric acid (2 N, 5 ml) was added *o*-toluidine (1.0716 g, 10.0 mmol). The resulting ammonium solution salt was cooled to 0~5 °C and to this was gradually added NaNO₂ (0.828 g, 12.0 mmol) and stirred for 2 h. To the reaction mixture was added *o*-toluidine (1.0716 g, 10.0 mmol). The reaction mixture was then allowed to

come up to room temperature and stirred for 10 min. To the mixture was then added NaHCO₃ (aqueous solution, 1 M; until pH = 8~9). The precipitates were extracted with CH₂Cl₂, concentrated under vacuum and subjected to flash column chromatography (100 % CH₂Cl₂) yielding 57 (810 mg, 36 %) as a reddish solid.

¹H NMR: δ = 7.71 (d, *J* = 7.5 Hz, 2H), 7.57 (dd, *J*_a = 7.5 Hz, *J*_b = 1.0 Hz, 1H), 7.29 (m, 2H), 7.25 (m, 1H), 6.46 (dd, *J*_a = 8.0 Hz, *J*_b = 1.0 Hz, 1H), 2.68 (s, 3H), 2.24 (s, 3H) ppm. Mass calcd. for [M] 225.13, found (ES) [M] 225.

p-(*m*-tolylidiazanyl)-*o*-toluidine (58)

To a solution of hydrochloric acid was added *m*-toluidine (24.0 mg, 0.2239 mmol). The resulting ammonium solution salt was cooled to 0~5 °C and to this was gradually added NaNO₂ (20.00 mg, 0.2899 mmol) and stirred for 2 h. To the reaction mixture was added *o*-toluidine (20.0 mg, 0.1866 mmol). The reaction mixture was then allowed to come up to room temperature and stirred for 10 min. To the mixture was then added NaHCO₃ (aqueous solution, 1 M; until pH = 8~9). The precipitates were extracted with CH₂Cl₂, concentrated under vacuum and subjected to flash column chromatography (100 % CH₂Cl₂) yielding 58 (12.0 mg, 29 %) as a reddish solid.

¹H NMR: δ = 7.76 (d, *J* = 7.5 Hz, 2H), 7.71 (dd, *J*_a = 8.5 Hz, *J*_b = 1.0 Hz, 1H), 7.57 (dd, *J*_a = 8.0 Hz, *J*_b = 1.0 Hz, 1H), 7.32 (m, 2H), 7.26 (m, 1H), 6.88 (d, *J* = 8.5 Hz, 1H), 2.70 (s, 3H), 2.34 (s, 3H) ppm. Mass calcd. for [M] 225.13, found (ES) [M] 225.

p-(*p*-tolylidiazanyl)-*o*-toluidine (59)

To a solution of hydrochloric acid was added *p*-toluidine (20.0 mg, 0.1866 mmol). The resulting ammonium solution salt was cooled to 0~5 °C and to this was gradually added NaNO₂ (20.00 mg, 0.2899 mmol) and stirred for 2 h. To the reaction mixture was added *o*-toluidine (20.0 mg, 0.1866 mmol). The reaction mixture was then allowed to come up to room temperature and stirred for 10 min. To the mixture was then added

NaHCO₃ (aqueous solution, 1 M; until pH = 8~9). The precipitates were extracted with CH₂Cl₂, concentrated under vacuum and subjected to flash column chromatography (100 % CH₂Cl₂) yielding 59 (12.0 mg, 29 %) as a reddish solid.

¹H NMR: δ = 7.79 (d, *J* = 8.0 Hz, 2H), 7.73 (m, 2H), 7.31 (d, *J* = 8.0 Hz, 2H), 6.76 (d, *J* = 8.5 Hz, 1H), 2.44 (s, 3H), 2.25 (s, 3H) ppm. Mass calcd. for [M] 225.13, found (ES) [M] 225.

p-(phenyldiazenyl)-*o*-toluidine (60)

To a solution of hydrochloric acid was added aniline (17.4 mg, 0.1866 mmol). The resulting ammonium solution salt was cooled to 0~5 °C and to this was gradually added NaNO₂ (20.00 mg, 0.2899 mmol) and stirred for 2 h. To the reaction mixture was added *o*-toluidine (20.0 mg, 0.1866 mmol). The reaction mixture was then allowed to come up to room temperature and stirred for 10 min. To the mixture was then added NaHCO₃ (aqueous solution, 1 M; until pH = 8~9). The precipitates were extracted with CH₂Cl₂, concentrated under vacuum and subjected to flash column chromatography (100 % CH₂Cl₂) yielding 60 (12.4 mg, 32 %) as a reddish solid.

¹H NMR: δ = 7.89 (dd, *J*_a = 8.5 Hz, *J*_b = 0.5 Hz, 2H), 7.75 (m, 2H), 7.52 (m, 2H), 7.44 (m, 1H), 6.76 (m, 1H), 2.26 (s, 3H) ppm. Mass calcd. for [M] 211.11, found (ES) [M] 211.

p-(*o*-ethylphenyldiazenyl)-*o*-toluidine (61)

To a solution of hydrochloric acid was added 2-ethylaniline (22.6 mg, 0.1866 mmol). The resulting ammonium solution salt was cooled to 0~5 °C and to this was gradually added NaNO₂ (20.00 mg, 0.2899 mmol) and stirred for 2 h. To the reaction mixture was added *o*-toluidine (20.0 mg, 0.1866 mmol). The reaction mixture was then allowed to come up to room temperature and stirred for 10 min. To the mixture was then added NaHCO₃ (aqueous solution, 1 M; until pH = 8~9). The precipitates were extracted

with CH₂Cl₂, concentrated under vacuum and subjected to flash column chromatography (100 % CH₂Cl₂) yielding 61 (4.7 mg, 11 %) as a reddish solid.

¹H NMR: δ = 7.80 (d, *J* = 2.5 Hz, 1H), 7.73 (m, 1H), 7.60 (m, 1H), 7.37 (m, 2H), 7.28 (m, 1H), 2.75 (m, 2H), 2.70 (s, 3H), 1.37 (s, 3H) ppm. Mass calcd. for [M] 239.14, found (ES) [M] 239.

p-(*o*-fluorophenyldiazenyl)-*o*-toluidine (62)

To a solution of hydrochloric acid was added *o*-fluoroaniline (20.7 mg, 0.1866 mmol). The resulting ammonium solution salt was cooled to 0~5 °C and to this was gradually added NaNO₂ (20.00 mg, 0.2899 mmol) and stirred for 2 h. To the reaction mixture was added *o*-toluidine (20.0 mg, 0.1866 mmol). The reaction mixture was then allowed to come up to room temperature and stirred for 10 min. To the mixture was then added NaHCO₃ (aqueous solution, 1 M; until pH = 8~9). The precipitates were extracted with CH₂Cl₂, concentrated under vacuum and subjected to flash column chromatography (100 % CH₂Cl₂) yielding 62 (27.0 mg, 63 %) as a reddish solid.

¹H NMR: δ = 7.67 (s, 2H), 7.65 (m, 1H), 7.27 (m, 1H), 7.17 (m, 2H), 6.65 (d, *J* = 8.5 Hz, 1H), 6.76 (d, *J* = 8.5 Hz, 1H), 2.14 (s, 3H) ppm. Mass calcd. for [M] 229.10, found (ES) [M] 229.

p-(*o*-chlorophenyldiazenyl)-*o*-toluidine (63)

To a solution of hydrochloric acid was added *o*-chloroaniline (23.8 mg, 0.1866 mmol). The resulting ammonium solution salt was cooled to 0~5 °C and to this was gradually added NaNO₂ (20.00 mg, 0.2899 mmol) and stirred for 2 h. To the reaction mixture was added *o*-toluidine (20.0 mg, 0.1866 mmol). The reaction mixture was then allowed to come up to room temperature and stirred for 10 min. To the mixture was then added NaHCO₃ (aqueous solution, 1 M; until pH = 8~9). The precipitates were extracted

with CH₂Cl₂, concentrated under vacuum and subjected to flash column chromatography (100 % CH₂Cl₂) yielding 63 (20.0 mg, 44 %) as a reddish solid.

¹H NMR: δ = 7.75 (d, J = 7.5 Hz, 2H), 7.65 (d, J = 9.5 Hz, 1H), 7.51(d, J = 9.0 Hz, 1H), 7.30 (m, 2H), 6.71 (d, J = 8.5 Hz, 1H), 2.21 (s, 3H) ppm. Mass calcd. for [M] 245.07, found (ES) [M] 245.

p-(*o*-methoxyphenyldiazenyl)-*o*-toluidine (64)

To a solution of hydrochloric acid was added *o*-anisidine (24.0 mg, 0.1866 mmol). The resulting ammonium solution salt was cooled to 0~5 °C and to this was gradually added NaNO₂ (20.00 mg, 0.2899 mmol) and stirred for 2 h. To the reaction mixture was added *o*-toluidine (20.0 mg, 0.1866 mmol). The reaction mixture was then allowed to come up to room temperature and stirred for 10 min. To the mixture was then added NaHCO₃ (aqueous solution, 1 M; until pH = 8~9). The precipitates were extracted with CH₂Cl₂, concentrated under vacuum and subjected to flash column chromatography (100 % CH₂Cl₂) yielding 64 (12.2 mg, 27.1%) as a reddish solid.

¹H NMR: δ = 7.70 (d, J = 7.5 Hz, 2H), 7.62 (dd, J_a = 8.0 Hz, J_b = 1.5 Hz, 1H), 7.35 (m, 1H), 7.05 (d, J = 8.5 Hz, 1H), 7.00 (m, 1H), 6.71 (d, J = 8.0 Hz, 1H), 4.00 (s, 3H), 2.22 (s, 3H) ppm. Mass calcd. for [M] 241.12, found (ES) [M] 241.

p-(1-naphthyldiazenyl)-*o*-toluidine (65)

To a solution of hydrochloric acid was added 1-naphthylamine (26.7 mg, 0.1866 mmol). The resulting ammonium solution salt was cooled to 0~5 °C and to this was gradually added NaNO₂ (20.00 mg, 0.2899 mmol) and stirred for 2 h. To the reaction mixture was added *o*-toluidine (20.0 mg, 0.1866 mmol). The reaction mixture was then allowed to come up to room temperature and stirred for 10 min. To the mixture was then added NaHCO₃ (aqueous solution, 1 M; until pH = 8~9). The precipitates were extracted

with CH₂Cl₂, concentrated under vacuum and subjected to flash column chromatography (100 % CH₂Cl₂) yielding 65 (4.0 mg, 8.2%) as a reddish solid.

¹H NMR: δ = 7.91 (d, *J* = 8.0 Hz, 2H), 7.85 (m, 2H), 7.75 (dd, *J*_a = 8.0 Hz, *J*_b = 2.0 Hz, 1H), 7.62 (m, 1H), 7.57 (m, 3H), 6.79 (d, *J* = 8.5 Hz, 1H), 2.29 (s, 3H) ppm. Mass calcd. for [M] 261.13, found (ES) [M] 261.

Synthesis of picolinic carboxamides of aminodiazenes (I)

N-[2-methyl-4-[(3-methylphenyl)diazenyl]phenyl]-2-pyridine carboxamide (44)

To a solution of 2-picolinic acid (16.4 mg, 0.1332 mmol) in methylene chloride (CH₂Cl₂; 0.5 ml) was added dichlorotriphenylphosphorane (PPh₃Cl₂; 44.4 mg, 0.2219 mmol) and a drop of diisopropylethylamine. After stirring at room temperature for 30 min, the reaction mixture was added 58 (6.0 mg, 0.0266 mmol) and stirred for 1h. The resulting mixture was concentrated under vacuum and subjected to flash column chromatography (100 % CH₂Cl₂) yielding 44 (2.6 mg, 30 %) as a yellowish solid.

¹H NMR: δ = 8.66 (m, 2H), 8.35 (d, *J* = 7.5 Hz, 1H), 7.97 (m, 2H), 7.93 (m, 1H), 7.83 (s, 1H), 7.72 (s, 2H), 7.54 (m, 1H), 7.43 (m, 1H), 7.29 (m, 1H) 2.55 (s, 3H), 2.47 (s, 3H) ppm. Mass calcd. for [M] 330.15, found (ES) [M] 330.

N-[2-methyl-4-[(4-methylphenyl)diazenyl]phenyl]-2-pyridine carboxamide (45)

To a solution of 2-picolinic acid (16.4 mg, 0.1332 mmol) in methylene chloride (CH₂Cl₂; 0.5 ml) was added dichlorotriphenylphosphorane (PPh₃Cl₂; 44.4 mg, 0.1332 mmol) and a drop of diisopropylethylamine. After stirring at room temperature for 30 min, the reaction mixture was added 59 (6.0 mg, 0.0266 mmol) and stirred for 1h. The resulting mixture was concentrated under vacuum and subjected to flash column chromatography (100 % CH₂Cl₂) yielding 45 (6.0 mg, 68 %) as a yellowish solid.

^1H NMR: δ = 8.65 (d, J = 10.0 Hz, 1H), 8.62 (d, J = 8.5 Hz, 1H), 8.34 (m, 1H), 7.95 (m, 1H), 7.88 (m, 1H), 7.83 (m, 3H), 7.52 (m, 1H), 7.32 (d, J = 8.5 Hz, 2H), 2.54 (s, 3H), 2.44 (s, 3H) ppm. Mass calcd. for [M] 330.15, found (ES) [M] 330.

N-(2-methyl-4-phenyldiazenyl-phenyl)-2-pyridine carboxamide (46)

To a solution of 2-picolinic acid (18.1 mg, 0.1467 mmol) in methylene chloride (CH_2Cl_2 ; 0.5 ml) was added dichlorotriphenylphosphorane (PPh_3Cl_2 ; 48.9 mg, 0.1467 mmol) and a drop of diisopropylethylamine. After stirring at room temperature for 30 min, the reaction mixture was added 60 (6.2 mg, 0.0293 mmol) and stirred for 1h. The resulting mixture was concentrated under vacuum and subjected to flash column chromatography (100 % CH_2Cl_2) yielding 46 (4.6 mg, 50 %) as a yellowish solid.

^1H NMR: δ = 8.66 (d, J = 4.5 Hz, 1H), 8.63 (d, J = 8.5 Hz, 1H), 8.35 (m, 1H), 7.96 (m, 1H), 7.92 (m, 4H), 7.84 (m, 1H), 7.54 (m, 2H), 7.48 (m, 1H), 2.55 (s, 3H) ppm. Mass calcd. for [M] 316.13, found (ES) [M] 316.

N-[2-methyl-4-[(2-ethylphenyl)diazenyl]phenyl]-2-pyridine carboxamide (47)

To a solution of 2-picolinic acid (6.4 mg, 0.0522 mmol) in methylene chloride (CH_2Cl_2 ; 0.5 ml) was added dichlorotriphenylphosphorane (PPh_3Cl_2 ; 17.4 mg, 0.0522 mmol) and a drop of diisopropylethylamine. After stirring at room temperature for 30 min, the reaction mixture was added 61 (2.5 mg, 0.0104 mmol) and stirred for 1h. The resulting mixture was concentrated under vacuum and subjected to flash column chromatography (100 % CH_2Cl_2) yielding 47 (3.5 mg, 97 %) as a yellowish solid.

^1H NMR: δ = 8.89 (d, J = 4.5 Hz, 1H), 8.32 (d, J = 8.0 Hz, 1H), 7.97 (m, 2H), 7.85 (m, 1H), 7.63 (m, 2H), 7.37-7.31 (m, 3H), 7.29 (m, 1H), 2.76 (m, 5H), 1.32 (s, 3H) ppm. Mass calcd. for [M + H] 345.17, found (ES) [M + H] 345.

N-[2-methyl-4-[(2-fluorophenyl)diazenyl]phenyl]-2-pyridine carboxamide (48)

To a solution of 2-picolinic acid (24.2 mg, 0.1963 mmol) in methylene chloride (CH₂Cl₂; 0.5 ml) was added dichlorotriphenylphosphorane (PPh₃Cl₂; 65.4 mg, 0.1963 mmol) and a drop of diisopropylethylamine. After stirring at room temperature for 30 min, the reaction mixture was added 62 (9.0 mg, 0.0393 mmol) and stirred for 1h. The resulting mixture was concentrated under vacuum and subjected to flash column chromatography (100 % CH₂Cl₂) yielding 48 (7.9 mg, 60 %) as a yellowish solid.

¹H NMR: δ = 8.66 (m, 2H), 8.34 (d, *J* = 7.5 Hz, 1H), 7.96-7.90 (m, 2H), 7.86 (s, 1H), 7.78 (m, 1H), 7.53 (m, 1H), 7.44 (m, 1H), 7.28 (m, 2H), 2.54 (s, 3H) ppm. Mass calcd. for [M] 334.12, found (ES) [M] 334.

N-[2-methyl-4-[(2-chlorophenyl)diazenyl]phenyl]-2-pyridine carboxamide (49)

To a solution of 2-picolinic acid (25.0 mg, 0.2035 mmol) in methylene chloride (CH₂Cl₂; 0.5 ml) was added dichlorotriphenylphosphorane (PPh₃Cl₂; 67.8 mg, 0.2035 mmol) and a drop of diisopropylethylamine. After stirring at room temperature for 30 min, the reaction mixture was added 63 (10.0 mg, 0.0407 mmol) and stirred for 1h. The resulting mixture was concentrated under vacuum and subjected to flash column chromatography (100 % CH₂Cl₂) yielding 49 (10.0 mg, 70 %) as a yellowish solid.

¹H NMR: δ = 8.66 (m, 2H), 8.34 (m, 1H), 7.96 (m, 2H), 7.87 (s, 1H), 7.71 (d, *J* = 8.0 Hz, 1H), 7.56 (m, 2H), 7.39 (m, 2H), 2.55 (s, 3H) ppm. Mass calcd. for [M] 350.09, found (ES) [M] 350.

N-[2-methyl-4-[(2-methoxyphenyl)diazenyl]phenyl]-2-pyridine carboxamide (50)

To a solution of 2-picolinic acid (15.6 mg, 0.1264 mmol) in methylene chloride (CH₂Cl₂; 0.5 ml) was added dichlorotriphenylphosphorane (PPh₃Cl₂; 42.1 mg, 0.1264 mmol) and a drop of diisopropylethylamine. After stirring at room temperature for 30 min, the reaction mixture was added 64 (6.1 mg, 0.0253 mmol) and stirred for 1h. The

resulting mixture was concentrated under vacuum and subjected to flash column chromatography (100 % CH₂Cl₂) yielding 50 (3.2 mg, 37 %) as a yellowish solid.

¹H NMR: δ = 8.66 (d, *J* = 4.5 Hz, 1H), 8.63 (d, *J* = 9.0 Hz, 1H), 8.34 (d, *J* = 7.5 Hz, 1H), 7.96 (m, 2H), 7.83 (s, 1H), 7.69 (d, *J* = 8.0 Hz, 1H), 7.53 (m, 1H), 7.45 (m, 1H), 7.11 (d, *J* = 8.5 Hz, 1H), 7.05 (m, 1H), 4.04 (s, 3H), 2.54 (s, 3H) ppm. Mass calcd. for [M] 346.14, found (ES) [M] 346.

N-[2-methyl-4-(1-naphthyldiazenyl)phenyl]-2-pyridine carboxamide (51)

To a solution of 2-picolinic acid (4.7 mg, 0.0383 mmol) in methylene chloride (CH₂Cl₂; 0.5 ml) was added dichlorotriphenylphosphorane (PPh₃Cl₂; 12.8 mg, 0.0383 mmol) and a drop of diisopropylethylamine. After stirring at room temperature for 30 min, the reaction mixture was added 65 (2.0 mg, 0.0077 mmol) and stirred for 1h. The resulting mixture was concentrated under vacuum and subjected to flash column chromatography (100 % CH₂Cl₂) yielding 51 (1.0 mg, 36 %) as a yellowish solid.

¹H NMR: δ = 8.96 (d, *J* = 8.5 Hz, 1H), 8.68 (m, 2H), 8.36 (d, *J* = 7.5 Hz, 1H), 8.04 (d, *J* = 8.5 Hz, 1H), 7.99-7.93 (m, 5H), 7.83 (m, 1H), 7.68 (m, 1H), 7.61 (m, 2H), 7.54 (m, 1H), 2.56 (s, 3H) ppm. Mass calcd. for [M] 366.15, found (ES) [M] 366.

Synthesis of aminodiazenes (II)

p-(*o*-tolylidiazanyl)-*m*-toluidine (66)

To a solution of hydrochloric acid was added *o*-toluidine (20.0 mg, 0.1866 mmol). The resulting ammonium solution salt was cooled to 0~5 °C and to this was gradually added NaNO₂ (20.00 mg, 0.2899 mmol) and stirred for 2 h. To the reaction mixture was added *m*-toluidine (20.0 mg, 0.1866 mmol). The reaction mixture was then allowed to come up to room temperature and stirred for 10 min. To the mixture was then added NaHCO₃ (aqueous solution, 1 M; until pH = 8~9). The precipitates were extracted with

CH₂Cl₂, concentrated under vacuum and subjected to flash column chromatography (100 % CH₂Cl₂) yielding 66 (10.0 mg, 24 %) as a reddish solid.

¹H NMR: δ = 7.66 (d, *J* = 9.0 Hz, 1H), 7.59 (dd, *J*_a = 8.0 Hz, *J*_b = 1.0 Hz, 1H), 7.30 (m, 2H), 7.25 (m, 1H), 6.59 (d, *J* = 2.5 Hz, 1H), 6.54 (dd, *J*_a = 9.0 Hz, *J*_b = 2.5 Hz, 1H), 2.69 (s, 3H), 2.67 (s, 3H) ppm. Mass calcd. for [M] 225.13, found (ES) [M] 225.

p-(*o*-tolylidiazanyl)-aniline (67)

To a solution of hydrochloric acid was added *o*-toluidine (19.6 mg, 0.1825 mmol). The resulting ammonium solution salt was cooled to 0~5 °C and to this was gradually added NaNO₂ (18.89 mg, 0.2738 mmol) and stirred for 2 h. To the reaction mixture was added aniline (17.0 mg, 0.1828 mmol). The reaction mixture was then allowed to come up to room temperature and stirred for 10 min. To the mixture was then added NaHCO₃ (aqueous solution, 1 M; until pH = 8~9). The precipitates were extracted with CH₂Cl₂, concentrated under vacuum and subjected to flash column chromatography (100 % CH₂Cl₂) yielding 67 (5.0 mg, 13 %) as a reddish solid.

¹H NMR: δ = 7.85 (m, 3H), 7.72 (m, 1H), 7.50-7.47 (m, 2H), 7.41-7.38 (m, 1H), 6.76 (m, 2H), 2.25 (s, 3H) ppm. Mass calcd. for [M] 211.11, found (ES) [M] 211.

p-(*o*-tolylidiazanyl)-*o*-ethylaniline (68)

To a solution of hydrochloric acid was added *o*-toluidine (20.3 mg, 0.1898 mmol). The resulting ammonium solution salt was cooled to 0~5 °C and to this was gradually added NaNO₂ (19.64 mg, 0.2847 mmol) and stirred for 2 h. To the reaction mixture was added 2-ethylaniline (23.0 mg, 0.1898 mmol). The reaction mixture was then allowed to come up to room temperature and stirred for 10 min. To the mixture was then added NaHCO₃ (aqueous solution, 1 M; until pH = 8~9). The precipitates were extracted with CH₂Cl₂, concentrated under vacuum and subjected to flash column chromatography (100 % CH₂Cl₂) yielding 68 (7.0 mg, 15 %) as a reddish solid.

^1H NMR: $\delta = 7.76$ (s, 1H), 7.71-7.68 (m, 1H), 7.59 (m, 1H), 7.33 (m, 1H), 7.30 (m, 1H), 7.26 (m, 1H), 6.76 (m, 1H), 3.15 (q, $J = 7.5$ Hz, 2H), 2.68(s, 3H), 1.29 (t, $J = 7.5$ Hz, 3H) ppm. Mass calcd. for [M] 239.14, found (ES) [M] 239.

p-(phenyldiazenyl)-aniline (69)

To a solution of hydrochloric acid was added aniline (17.0 mg, 0.1828 mmol). The resulting ammonium solution salt was cooled to 0~5 °C and to this was gradually added NaNO₂ (18.92 mg, 0.2742 mmol) and stirred for 2 h. To the reaction mixture was added aniline (17.0 mg, 0.1828 mmol). The reaction mixture was then allowed to come up to room temperature and stirred for 10 min. To the mixture was then added NaHCO₃ (aqueous solution, 1 M; until pH = 8~9). The precipitates were extracted with CH₂Cl₂, concentrated under vacuum and subjected to flash column chromatography (100 % CH₂Cl₂) yielding 69 (20.0 mg, 56 %) as a reddish solid.

^1H NMR: $\delta = 7.85$ -7.80 (m, 4H), 7.50 (m, 2H), 7.42 (m, 1H), 6.75(m, 2H) ppm. Mass calcd. for [M] 197.10, found (ES) [M] 197.

p-(*m*-tolylidiazanyl)-*m*-toluidine (70)

To a solution of hydrochloric acid was added *m*-toluidine (20.0 mg, 0.1866 mmol). The resulting ammonium solution salt was cooled to 0~5 °C and to this was gradually added NaNO₂ (20.00 mg, 0.2899 mmol) and stirred for 2 h. To the reaction mixture was added *m*-toluidine (20.0 mg, 0.1866 mmol). The reaction mixture was then allowed to come up to room temperature and stirred for 10 min. To the mixture was then added NaHCO₃ (aqueous solution, 1 M; until pH = 8~9). The precipitates were extracted with CH₂Cl₂, concentrated under vacuum and subjected to flash column chromatography (100 % CH₂Cl₂) yielding 70 (6.3 mg, 15 %) as a reddish solid.

^1H NMR: δ = 7.66 (m, 3H), 7.37 (m, 1H), 7.22 (m, 1H), 6.59 (m, 1H), 6.55 (m, 1H), 2.67 (s, 3H), 2.44 (s, 3H) ppm. Mass calcd. for [M] 225.13, found (ES) [M] 225.

Synthesis of picolinic carboxamides of aminodiazenes (II)

N-[3-methyl-4-[(2-methylphenyl)diazenyl]phenyl]-2-pyridine carboxamide (52)

To a solution of 2-picolinic acid (9.0 mg, 0.0732 mmol) in methylene chloride (CH_2Cl_2 ; 0.5 ml) was added dichlorotriphenylphosphorane (PPh_3Cl_2 ; 24.40 mg, 0.0732 mmol) and a drop of *N,N*-diisopropylethylamine. After stirring at room temperature for 30 min, the reaction mixture was added 66 (3.3 mg, 0.0146 mmol) and stirred for 1h. The resulting mixture was concentrated under vacuum and subjected to flash column chromatography (100 % CH_2Cl_2) yielding 52 (3.2 mg, 66 %) as a yellowish solid.

^1H NMR: δ = 8.65 (d, J = 4.0 Hz, 1H), 8.33 (d, J = 8.0 Hz, 1H), 7.95 (t, J = 4.0 Hz, 1H), 7.89 (s, 1H), 7.76 (d, J = 9.0 Hz, 1H), 7.66 (m, 2H), 7.52 (m, 1H), 7.34 (s, 2H), 7.29 (m, 1H), 2.79 (s, 3H), 2.75 (s, 3H) ppm. Mass calcd. for [M] 330.15, found (ES) [M] 330.

N-[4-(2-methylphenyldiazenyl)phenyl]-2-pyridine carboxamide (53)

To a solution of 2-picolinic acid (4.7 mg, 0.0379 mmol) in methylene chloride (CH_2Cl_2 ; 0.5 ml) was added dichlorotriphenylphosphorane (PPh_3Cl_2 ; 11.84 mg, 0.0355 mmol) and a drop of diisopropylethylamine. After stirring at room temperature for 30 min, the reaction mixture was added 67 (1.6 mg, 0.0076 mmol) and stirred for 1h. The resulting mixture was concentrated under vacuum and subjected to flash column chromatography (100 % CH_2Cl_2) yielding 53 (0.9 mg, 36 %) as a yellowish solid.

^1H NMR: δ = 8.67 (m, 1H), 8.64 (d, J = 9.0 Hz, 1H), 8.35 (m, 1H), 7.97 (t, J = 2.0 Hz, 1H), 7.92 (m, 3H), 7.84 (d, J = 1.0 Hz, 1H), 7.54 (m, 3H), 7.48 (m, 1H), 2.55 (s, 3H) ppm. Mass calcd. for [M] 316.13, found (ES) [M] 316.

N-[2-ethyl-4-[(2-methylphenyl)diazenyl]phenyl]-2-pyridine carboxamide (54)

To a solution of 2-picolinic acid (5.9 mg, 0.0481 mmol) in methylene chloride (CH₂Cl₂; 0.5 ml) was added dichlorotriphenylphosphorane (PPh₃Cl₂; 11.83 mg, 0.0355 mmol) and a drop of diisopropylethylamine. After stirring at room temperature for 30 min, the reaction mixture was added 68 (2.3 mg, 0.0096 mmol) and stirred for 1h. The resulting mixture was concentrated under vacuum and subjected to flash column chromatography (100 % CH₂Cl₂) yielding 54 (2.8 mg, 88 %) as a yellowish solid.

¹H NMR: δ = 8.67 (d, *J* = 4.0 Hz, 1H), 8.62 (d, *J* = 8.5 Hz, 1H), 8.35 (d, *J* = 8.0 Hz, 1H), 7.96 (t, *J* = 7.5 Hz, 1H), 7.91 (m, 2H), 7.87 (m, 1H), 7.53 (m, 1H), 7.39-7.33 (m, 2H), 7.30-7.25 (m, 1H), 2.92 (q, *J* = 7.5 Hz, 2H), 2.73 (s, 3H), 1.43 (t, *J* = 7.5 Hz, 3) ppm. Mass calcd. for [M] 344.16, found (ES) [M] 344.

N-(4-phenyldiazenylphenyl)-2-pyridine carboxamide (55)

To a solution of 2-picolinic acid (20.9 mg, 0.1698 mmol) in methylene chloride (CH₂Cl₂; 0.5 ml) was added dichlorotriphenylphosphorane (PPh₃Cl₂; 49.55 mg, 0.1487 mmol) and a drop of diisopropylethylamine. After stirring at room temperature for 30 min, the reaction mixture was added 69 (6.7 mg, 0.0340 mmol) and stirred for 1h. The resulting mixture was concentrated under vacuum and subjected to flash column chromatography (100 % CH₂Cl₂) yielding 55 (6.1 mg, 57 %) as a yellowish solid.

¹H NMR: δ = 8.64 (d, *J* = 5.5 Hz, 1H), 8.33 (d, *J* = 8.0 Hz, 1H), 8.01-7.90 (m, 7H), 7.51 (m, 3H), 7.46 (m, 1H) ppm. Mass calcd. for [M] 302.12, found (ES) [M] 302.

N-[3-methyl-4-[(3-methylphenyl)diazenyl]phenyl]-2-pyridine carboxamide (56)

To a solution of 2-picolinic acid (5.7 mg, 0.0522 mmol) in methylene chloride (CH₂Cl₂; 0.5 ml) was added dichlorotriphenylphosphorane (PPh₃Cl₂; 15.53 mg, 0.0466 mmol) and a drop of diisopropylethylamine. After stirring at room temperature for 30

min, the reaction mixture was added 70 (2.1 mg, 0.0093 mmol) and stirred for 1h. The resulting mixture was concentrated under vacuum and subjected to flash column chromatography (100 % CH₂Cl₂) yielding 56 (2.8 mg, 87 %) as a yellowish solid.

¹H NMR: δ = 8.64 (d, *J* = 4.0 Hz, 1H), 8.33 (d, *J* = 8.0 Hz, 1H), 7.95 (t, *J* = 5.5 Hz, 1H), 7.90 (s, 1H), 7.74 (m, 3H), 7.65 (d, *J* = 9.0 Hz, 1H), 7.52 (m, 1H), 7.41 (m, 1H), 7.28 (m, 1H), 2.78 (s, 3H), 2.47 (s, 3H) ppm. Mass calcd. for [M] 330.15, found (ES) [M] 330.

CHAPTER 5 PROTAC BASED ON THE SYNTHETIC LIGAND

5.1 Introduction

Based on the positional scanning studies, N-[2-methyl-4-[(2-methylphenyl) diazenyl]phenyl]-2-pyridine carboxamide (**36**) was chosen as an optimal ligand to be used for the development of PROTAC. Since compound **35** does not have an appropriate handle (functional group) to link to the E3 ligase recognition motif, the structure was derivatized to introduce a 'handle'. In this chapter, the effort for the functionalization of the compound **36** and the synthesis of PROTAC based on the synthetic structure is described. The biological activities of PROTACs are evaluated herein as well.

5.2 Synthesis and biological evaluation of PROTAC4

First, it was designed to introduce a carboxylic acid functional group at the methyl group of A-ring. The carboxylic acid residue was expected to be useful for coupling with an amine-containing linker, which then can be linked to the E3 ligase recognition motif.

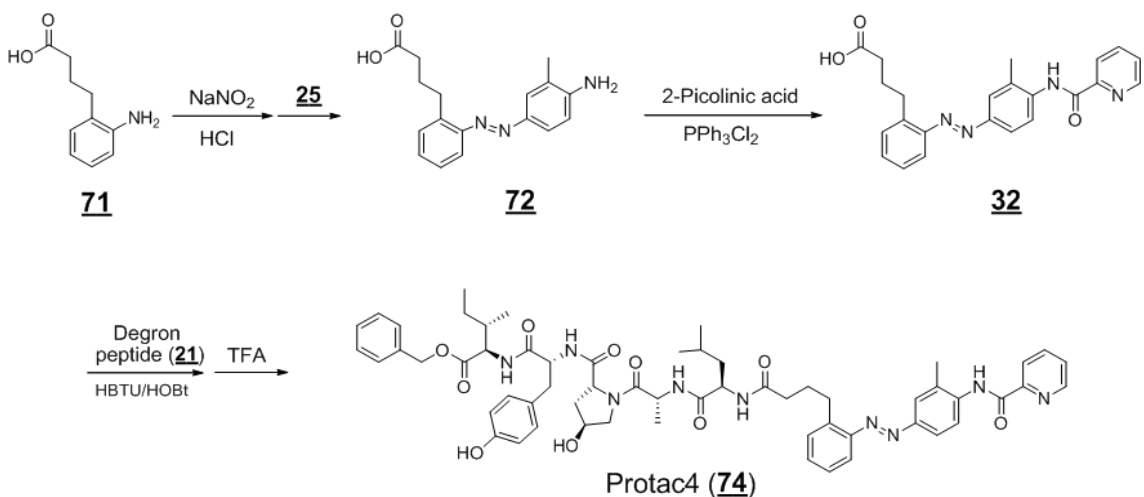


Figure 5.1 Synthesis of PROTAC4

To this end, 2-Aminophenylbutyric acid was activated by diazotization and then coupled to a 2-methylaniline via an electrophilic addition yielding 72. The third ring moiety was coupled to the resulted aniline to provide 73 as proposed. The resulting carboxylic acid was used to couple with the peptide moiety to give a fully assembled PROTAC. The treatment of fully assembled PROTAC with neat TFA yielded PROTAC4 (74).

The PROTAC4 was tested for AHR antagonistic activity using a luciferase reporter assay. Although PROTAC4 did not exhibit good AHR antagonistic activity (Figure 5.2 A), PROTAC4 was further tested whether it induces the degradation of AHR. Contrary to the reporter assay result PROTAC4 apparently displayed modest antagonistic activity targeting AHR in terms of the transcription of downstream gene. Specifically, the effect of PROTAC4 on the mRNA level of XRE-regulated gene, CYP1A1, was investigated. The result indicated that the treatment of PROTAC4 attenuated TCDD-induced up-regulation of CYP1A1 transcription (Figure 5.2 B). For another XRE-regulated gene, CYP1B1, PROTAC4 diminished the TCDD-induced up-regulation of CYP1B1 transcription (Figure 5.2 C). These results indicate that PROTAC4, to a certain extent, suppresses the transcription of downstream genes such as CYP1A1 and CYP1B1, though the result from the luciferase assay did not confirm the antagonistic activity of PROTAC4. The possibility that this effect is due to the decreased level of AHR was ruled out as the treatment of PROTAC4 did not change AHR transcription in the presence or absence of TCDD (Figure 5.2 D and E).

In conclusion,, the effect of PROTAC4 appears to be limited to the suppression of the TCDD-induced up-regulation of XRE-regulated luciferase. In addition, PROTAC4 modestly attenuated the TCDD-induced transcription of downstream genes. Taken all together, it appears that PROTAC4 is a weak antagonist of AHR signaling pathway without agonistic potency.

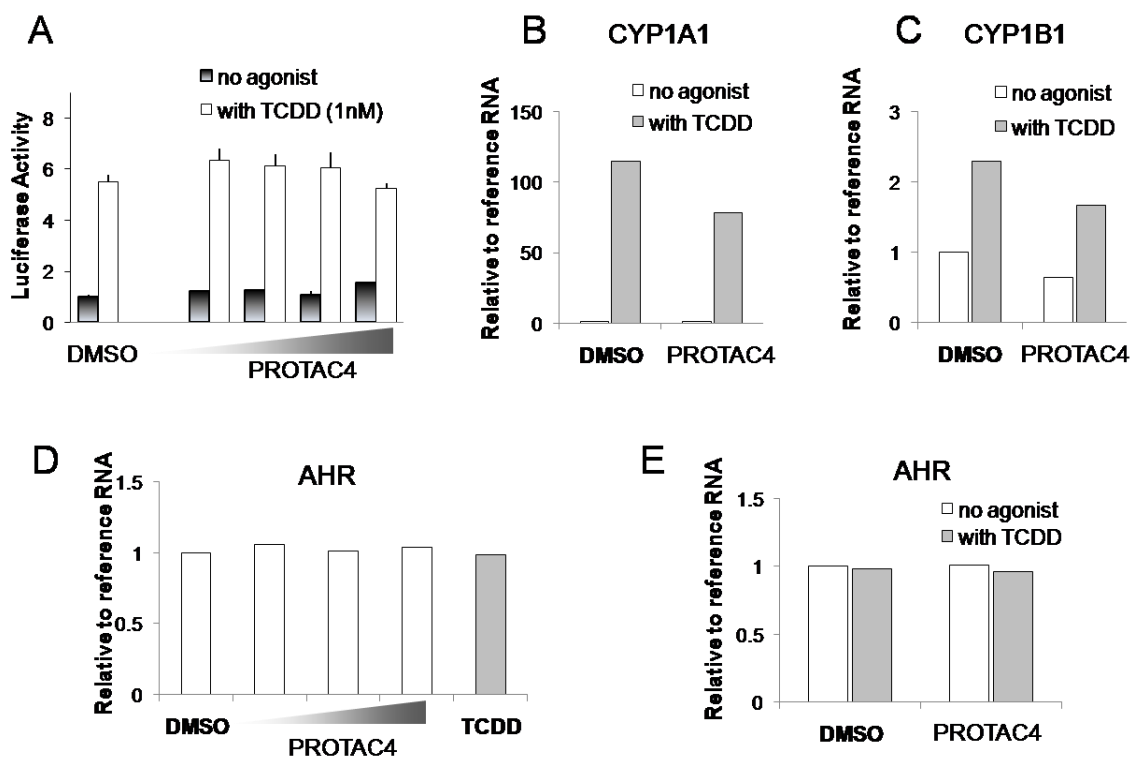


Figure 5.2 The Biological activity of PROTAC4

A) PROTAC4 did not block TCDD-induced luciferase activity. HepG2 cells were transfected with human CYP1A1 promoter coupled luciferase gene construct (HepG2-p450luc) and pre-treated either DMSO alone or with the compounds (10 nM to 10 μ M). After 1hr, TCDD (1nM) was added. 4hr after TCDD, the cells were harvested, activities were measured. B) PROTAC4 blocked the TCDD-induced transcription of CYP 1A1 gene. The NHK cells were treated with PROTAC4 (50 μ M), harvested at the 16 hr time point and then subjected to RT real time PCR analysis. C) PROTAC4 blocked the TCDD-induced transcription of CYP1B1 gene. The NHK cells were treated with PROTAC4 (50 μ M), harvested at the 16 hr time point and then subjected to RT real time PCR analysis. D) PROTAC4 did not look affecting on the mRNA level of AHR at any given concentration. The NHK cells were treated with increasing concentrations of PROTAC4 (5 μ M, 10 μ M and 50 μ M), harvested at the 16 hr time point and then subjected to RT real time PCR analysis. E) Neither PROTAC4 nor TCDD appear to affect on the mRNA level of AHR. The NHK cells were treated with PROTAC4 (10 μ M), harvested at the 16 hr time point and then subjected to RT real time PCR analysis. These assays were performed by Eun-Young Choi, Ph.D. under the direction of Hollie I. Swanson Ph.D. This data are not statistically analyzed

5.3 C ring-linked PROTACs

Despite the apparent inhibitory activity of PROTAC4 on the transcription of natural XRE-regulated genes, the XRE-regulated luciferase activity was not diminished by PROTAC4. Thus, it was thought to be ideal to prepare optimum PROTACs, Given the difficulties of preparing the intermediates of PROTAC4, the introduction of a functional group at other position was examined to prepare optimum PROTAC with varying linker lengths.

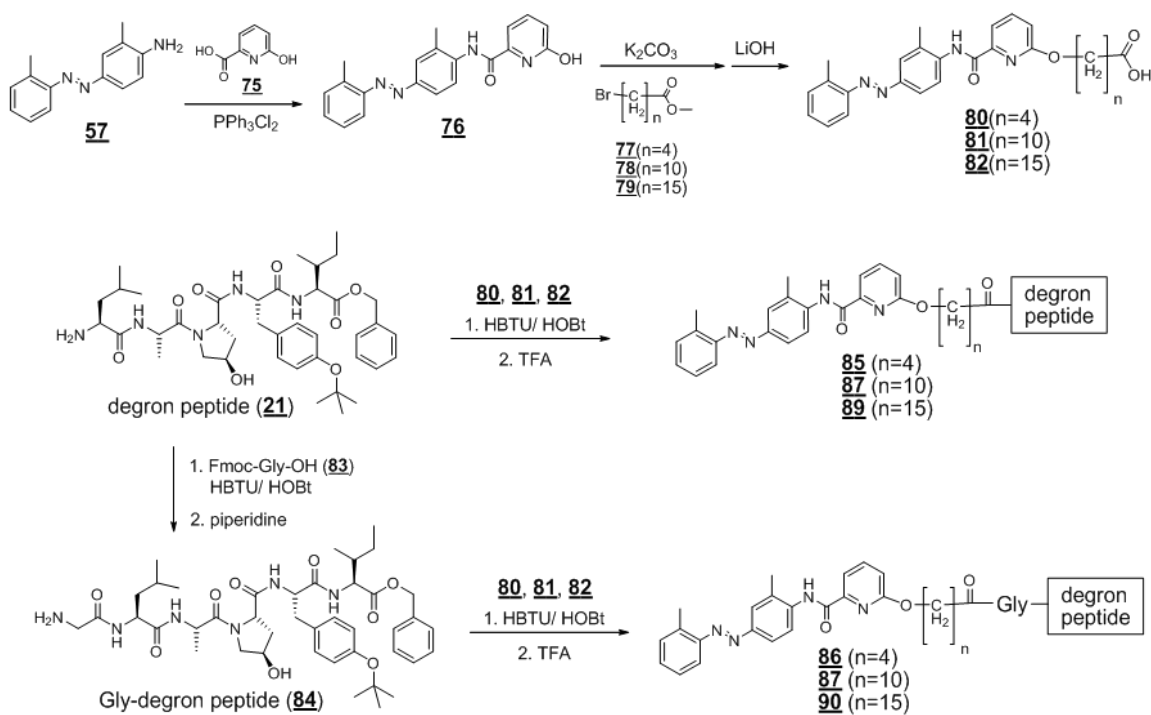


Figure 5.3 Synthetic scheme of C ring linked PROTACs

Thus, compound **35** was further derivatized to give a three-ring compound with a hydroxyl group on C-ring. It is important to note that a critical residue, 5-hydroxyl-2-picolinic acid, is readily available. To optimize the length of spacer that connects E3 ligase to AHR, the hydroxyl group of **75** was derivatized using linker residue such as methyl-bromopentanoate (**77**), methyl-bromoundecanoate (**78**), and methyl-bromohexadecanoate (**79**). These resulting esters were then hydrolyzed under basic

condition unleashing the carboxylic group. The carboxylic acids were coupled to E3 ligase recognition motif (21) or glycine-attached E3 ligase recognition motif (degron peptide; 84) yielding fully assembled PROTACs. The resulting PROTACs were then treated with neat TFA to remove t-butyl group from tyrosine residue of HIF-1 α pentapeptide yielding PROTACs (85~90) with varying lengths of spacer (Figure 5.3). The structures of C ring-linked PROTACs were described in Figure 5.4. The PROTACs coupled through 5-hydroxyl group on the C ring was tested for their activity.

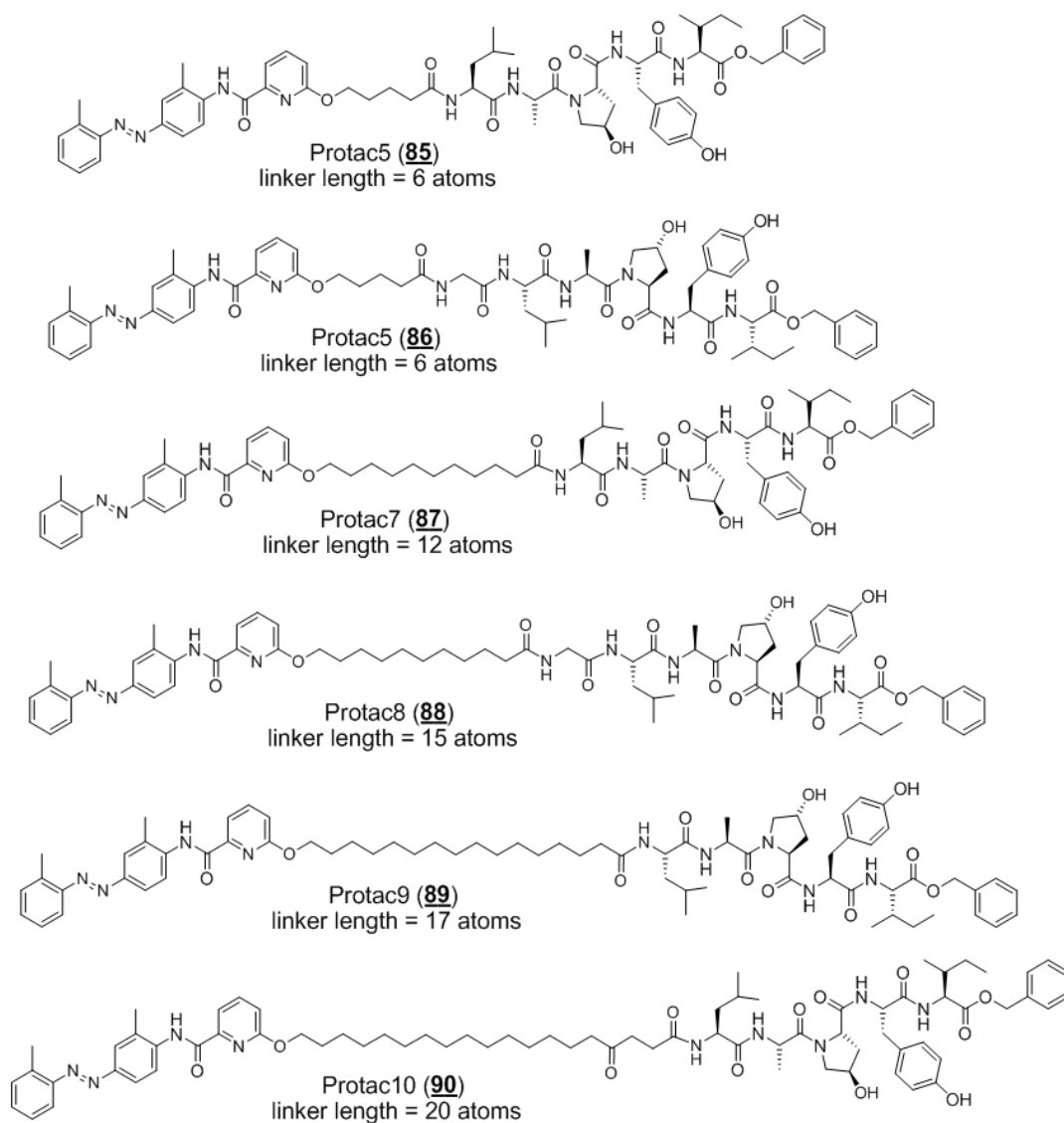


Figure 5.4 C Ring linked PROTACs with various spacer lengths.

The activity of PROTACs was evaluated using the TCDD-induced luciferase activity in cultured cells. The PROTACs coupled through 5-hydroxyl group on the C ring did not exhibit the ability to block TCDD-induced activation of AHR. The differences among the activity of PROTACs were hardly observed (Data not shown). Hence, it appears that C ring has no tolerance for derivatization.

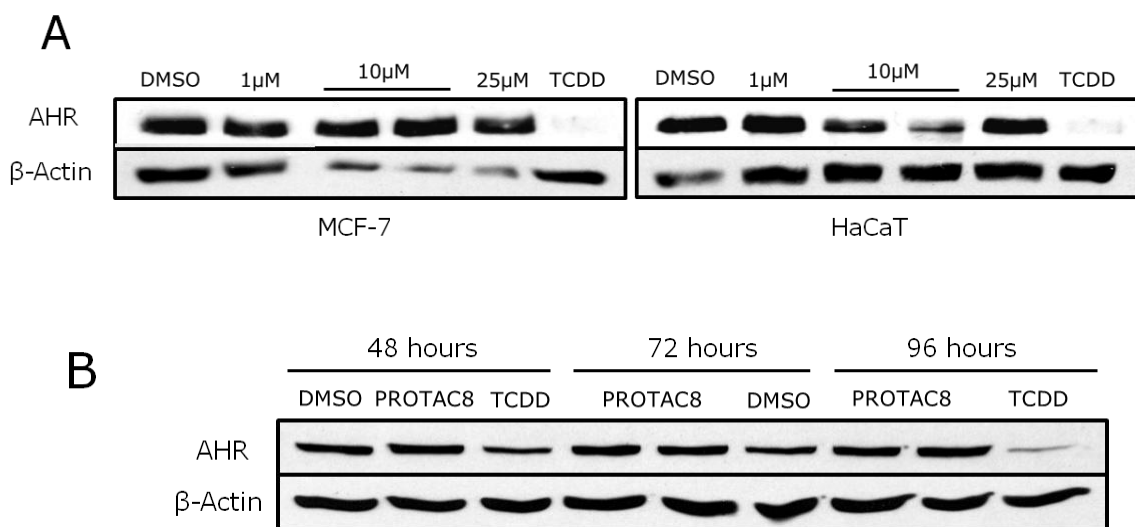


Figure 5.5 The effect of PROTAC8 on the cellular level of AHR.

A) DMSO (0.01 %), TCDD (1 nM) or PROTAC8 (1 μ M, 10 μ M and 25 μ M) were treated to MCF-7 cells or HaCaT cells for 72 hours. After harvesting, the cell lysates were subjected to western blot analysis. B) The HaCaT cells were treated with DMSO (0.01 %), TCDD (1 nM) and PROTAC8 (10 μ M) for the period indicated. After harvesting, the cell lysates were subjected to western blot analysis. These western blot assays were performed by Eun-Young Choi, Ph.D. under the direction of Hollie I. Swanson Ph.D.

Next, we questioned whether the PROTACs are able to induce the degradation of AHR. Based on the previous studies investigating the correlation between linker length and PROTAC activity, PROTAC8 which has 15 atoms linker was selected to further examine its ability to induce the degradation of AHR. However, PROTAC8 did not induce AHR degradation even after a 3-day incubation (Figure 5.4 A). To rule out the possibility that the 72 hours time point was not optimum for the degradation of AHR, the effect of PROTAC8 was investigated at different time points but no AHR degradation could be observed.

5.4 Discussion

The PROTAC4 based on the synthetic ligand was successfully prepared through coupling the compound 36 to E3 ligase recognition motif through A ring and subjected to assessment of biological activity. In the meantime, the intermediate, which has carboxylic acid handle on the 2-methyl position, was proposed to be further derivatized for the preparation of other PROTACs with longer linkers. However, the zwitter-ionic intermediate caused several problems in the purification and synthetic strategy resulting in extremely low overall productivity. The protection of the carboxylic acid moiety was largely limited, since the electrophilic addition coupling between A and B rings was designed to be performed in acidic condition (pH < 1). Moreover, the next coupling reaction with picolinic acid was affected by the presence of an active carboxylic acid at the end of the handle causing a substantial side reaction and a low yield.

Therefore, the ligand structure was proposed to be functionalized on C ring for linker coupling for the next series of PROTACs were prepared of different linker length. With the benefit of a readily available building block, 5-hydroxy-2-picolinic acid, the ligand structure of 36 was functionalized on C ring with hydroxyl group. Subsequently, the C ring coupled PROTACs with various lengths of linker were successfully prepared and subjected to biological evaluations in order to figure out the optimal linker length for PROTACs targeting AHR.

The results from the biological assessments informed that all the C-ring-coupled PROTACs with varying linker length are inactive either to block the TCDD-induced activation of AHR or to induce the degradation of AHR at the given concentrations and time points. These PROTACs are undergoing further investigation of the presumed effect of PROTAC8. However, it is possible that chemical modification of C ring may cause the loss of interaction with AHR. Hence, it is suggested to shift onto the further functionalization on the other position leading to the development of different types of PROTACs.

5.5 Syntheses of PROTACs

p-[*o*-(3-carboxylpropylphenyl)diazenyl]-*o*-toluidine (72)

To an aqueous solution of hydrochloric acid (2 N, 0.25 ml) was added 2-aminophenylbutyric acid, hydrochloride (20 mg, 92.73 μ mol). The resulting solution of amine salt was cooled to 0~5 °C and to this was gradually added NaNO₂ (41.65 mg, 0.6 mmol) and stirred for 2 h. To the reaction mixture was added *o*-toluidine (0.99 mg, 92.73 μ mol). The reaction mixture was then allowed to come up to room temperature and stirred for 10 min. To the mixture was then added NaHCO₃ (aqueous solution, 1 M; until pH = 8~9). The precipitates were extracted with CH₂Cl₂, concentrated under vacuum and subjected to flash column chromatography (100 % CH₂Cl₂). The resulting product was further purified by prep-HPLC (waters 600) yielding 72 (2.1 mg, 7.6 %) as a reddish solid.

¹H NMR: δ = 7.71 (d, J = 7.5 Hz, 2H), 7.57 (dd, J_a = 7.5 Hz, J_b = 1.0 Hz, 1H), 7.29 (m, 2H), 7.25 (m, 1H), 6.46 (dd, J_a = 8.0 Hz, J_b = 1.0 Hz, 1H), 2.68 (s, 3H), 2.24 (s, 3H) ppm.

N-[2-methyl-4-[(2-(3-carboxylpropyl)-phenyl)diazenyl]phenyl]-2-pyridinecarboxamide (73)

To a solution of 2-picolinic acid (3.3 mg, 0.0269 mmol) in methylene chloride (CH₂Cl₂; 0.5 ml) was added dichlorotriphenylphosphorane (PPh₃Cl₂; 8.0 mg, 0.0269 mmol) and a drop of DIPEA. After stirring at room temperature for 30 min, the reaction mixture was added 72 (2.1 mg, 0.0071 mmol) and stirred for 1h. The resulting mixture was concentrated under vacuum and subjected to flash column chromatography (100 % CH₂Cl₂) yielding 73 (1.2 mg, 46 %) as a yellowish solid.

¹H NMR: δ = 8.67 (d, J = 4.5 Hz, 1H), 8.63 (d, J = 9.0 Hz, 1H), 8.36 (d, J = 8.1 Hz, 1H), 7.98-7.88 (m, 2H), 7.84 (s, 1H), 7.64 (d, J = 8.4 Hz, 1H), 7.54 (m, 1H) 7.36 (m, 2H), 7.30 (m, 1H), 3.16 (m, 2H), 2.80 (s, 2H), 2.26 (s, 3H), 2.04 (m, 2H) ppm. Mass calcd. for [M] 402.17, found (ES) [M] 402.

PROTAC4 (74)

To a solution of 73 (1.2 mg, 0.0030 mmol) in methylene chloride (CH₂Cl₂; 0.5 ml) was added HBTU (3.4 mg, 0.0090 mmol), HOBt (1.4 mg, 0.0090 mmol), DIPEA (3.2 mg, 0.0250 mmol) and E3 ubiquitin ligase recognition peptide (H₂N-Leu-Ala-Pro^{OH}-Tyr^{*t*-butyl}-Ile-OBn ; 6.6 mg, 0.0090 mmol). After stirring at room temperature for 2 h, the resulting mixture was concentrated under vacuum and subjected to flash column chromatography (CH₂Cl₂:MeOH = 9:1) to yield a fully assembled product (1.8 mg, 53 %) as a yellowish solid.

¹H NMR: δ = 8.67 (bs, 1H), 8.51 (bs, 1H), 8.31 (bs, 1H), 7.94 (m, 1H), 7.82 (m, 2H), 7.63 (m, 1H), 7.53 (m, 1H), 7.40-7.27 (m, 8H), 7.02 (m, 2H), 6.81 (m, 2H), 5.17-5.12 (m, 2H), 4.60 (m, 2H), 4.42 (m, 4H), 3.52 (m, 1H), 3.35 (m, 1H), 3.17 (m, 2H), 3.05 (m, 1H), 2.95 (m, 1H), 2.81 (s, 4H), 2.53 (s, 4H), 2.35 (m, 5H), 2.06 (m, 2H), 1.09 (m, 2H), 1.68-1.45 (m, 3H), 1.25 (m, 1H), 1.13 (m, 2H), 0.96-0.72 (m, 1H) ppm.

To a solution of the fully assembled product (1.8 mg, 0.0016 mmol) in CH₂Cl₂ (0.2 ml) was added trifluoroacetic acid (100 μl, 0.87 mmol) at room temperature for 15 min to deprotect *t*-butyl residue of tyrosine within the fully assembled compound. Subsequently, the concentrated mixture was dried under high vacuum to remove trifluoroacetic acid. The resulting crude product was subjected to flash column chromatography (CH₂Cl₂/MeOH, 9:1) to yield 74 (1.7 mg, 90 %) as a yellowish solid.

¹H NMR: δ = 8.67 (bs, 1H), 8.51 (bs, 1H), 8.31 (bs, 1H), 7.94 (m, 1H), 7.82 (m, 2H), 7.63 (m, 1H), 7.53 (m, 1H), 7.40-7.27 (m, 8H), 7.02 (m, 2H), 6.81 (m, 2H), 5.17-5.12 (m, 2H), 4.60 (m, 2H), 4.42 (m, 4H), 3.52 (m, 1H), 3.35 (m, 1H), 3.17 (m, 2H), 3.05 (m, 1H), 2.95 (m, 1H), 2.81 (s, 4H), 2.53 (s, 4H), 2.35 (m, 5H), 2.06 (m, 2H), 1.09 (m, 2H), 1.68-1.45 (m, 3H), 1.25 (m, 10H), 1.13 (m, 2H), 0.96-0.72 (m, 1H) ppm.

Mass calcd. for [M] 1065.53, found (MALDI) [M] 1066.

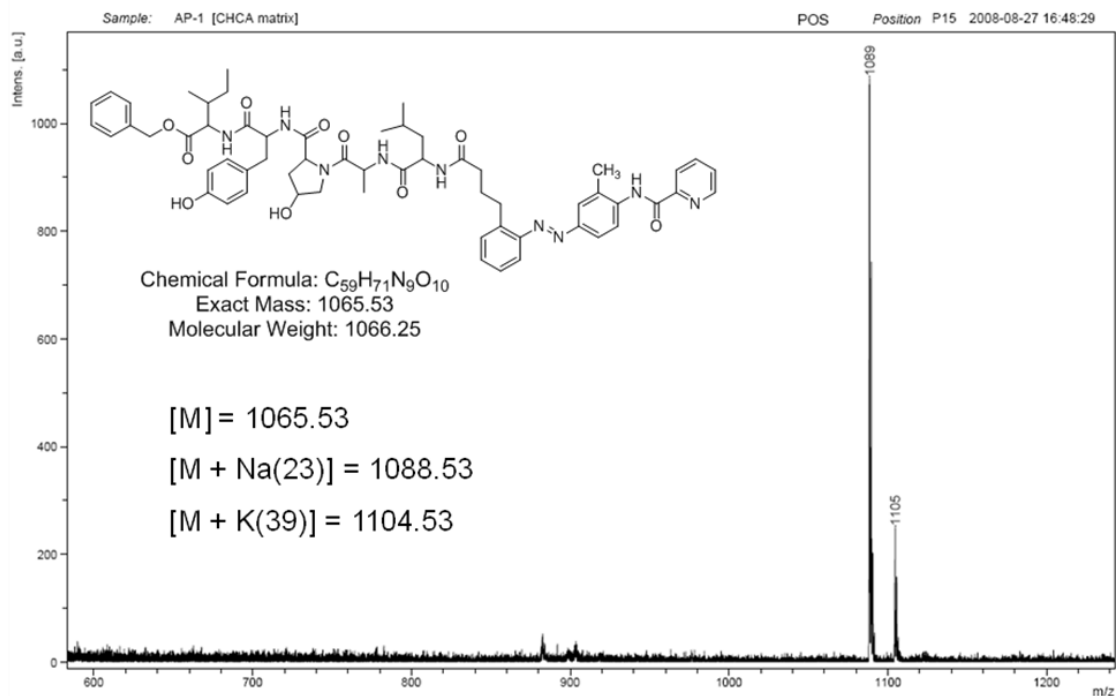


Figure 5.6 Mass spectrum for PROTAC4

N-[2-methyl-4-[(2-methylphenyl)azo]phenyl]-6-hydroxypyridine-2-carboxamide (76)

To a solution of 6-hydroxypyridine-2-carboxylic acid (75, 30.9 mg, 0.2219 mmol) in methylene chloride (CH_2Cl_2 ; 1 ml) was added dichlorotriphenylphosphorane (PPh_3Cl_2 ; 74.0 mg, 0.2219 mmol) and a drop of diisopropylethylamine. After stirring at room temperature for 30 min, the reaction mixture was added 57 (10.0 mg, 0.0444 mmol) and stirred for 1h. The resulting mixture was concentrated under vacuum and subjected to flash column chromatography (CH_2Cl_2). The resulting product was further purified by prep-HPLC (waters 600) yielding 76 (14.2 mg, 92 %) as a yellowish solid.

1H NMR: $\delta = 8.67$ (d, $J = 4.5$ Hz, 1H), 8.63 (d, $J = 9.0$ Hz, 1H), 8.36 (d, $J = 8.1$ Hz, 1H), 7.98-7.88 (dq, $J_a = 1.6$ Hz, $J_b = 7.5$ Hz, 2H), 7.84 (s, 1H), 7.64 (d, $J = 8.4$ Hz, 1H), 7.54 (m, 1H) 7.36 (m, 2H), 7.30 (m, 1H), 2.74 (s, 3H), 2.56 (s, 3H) ppm. Mass calcd. for [M] 346.14, found (ES) [M] 346.

Synthesis of 80

To a solution of 76 (4.0 mg, 0.0116 mmol) in methylene chloride (CH₂Cl₂; 1 ml) was added K₂CO₃ (7.0 mg, 0.0259 mmol) and methyl-5-bromovalerate (77, 4.6 mg, 0.0232 mmol). After stirring at room temperature for 15 h, the resulting mixture was concentrated under vacuum and subjected to flash column chromatography (CH₂Cl₂/MeOH, 95:5) yielding an methyl ester (4.8 mg, 84 %) as a yellowish solid.

¹H NMR: δ = 8.57 (d, *J* = 8.5 Hz, 1H), 7.86 (m, 2H), 7.75 (m, 2H), 7.56 (d, *J* = 8.0 Hz, 1H), 7.27 (s, 2H), 7.20 (s, 1H), 6.90 (d, *J* = 8.5 Hz, 1H), 4.42 (t, *J* = 6.0 Hz, 2H), 3.69 (s, 3H), 2.73 (s, 3H), 2.52 (s, 3H) 2.44 (t, *J* = 7.0 Hz, 2H), 1.91-1.89 (m, 4H) ppm. Mass calcd. for [M] 460.21, found (ES) [M] 460.

To a solution of the ester in THF/H₂O, 3:1(1 ml) was added LiOH (5.4mg, 0.2237mmol). After stirring at room temperature for 15 h, the resulting mixture was poured into H₂O with cold 1N HCl and extracted with CH₂Cl₂. The organic layers were combined, washed with brine, dried over Na₂SO₄, filtered, concentrated and dried under vacuum to yield 80 (4.6 mg, 99 %) as a yellowish solid.

Synthesis of 84

To a solution of E3 ligase recognition motif (21, 20.0 mg, 0.0271 mmol) was added HBTU (15.4 mg, 0.0407 mmol), HOBt (6.2 mg, 0.0407 mmol), diisopropylethylamine (14.2 mg, 0.1100 mmol) and Fmoc-Gly-OH (83, 9.1 mg, 0.03252). After stirring at room temperature for 2 h, the resulting mixture was concentrated under reduced pressure and subjected to flash column chromatography (CH₂Cl₂/MeOH, 95:5). The resulting compound was treated with a 20% solution of piperidine in DMF (0.7 ml, v/v) to deprotect fluorenylmethyloxycarbonyl group on amine group. After 15 min the resulting mixture was concentrated under vacuum and subjected

to flash column chromatography (CH₂Cl₂/MeOH, 95:5) yielding 84 (20.0 mg, 93 %) as a white solid.

Synthesis of 81

To a solution of 76 (4.0 mg, 0.0116 mmol) in methylene chloride (CH₂Cl₂; 1 ml) was added K₂CO₃ (7.0 mg, 0.0259 mmol) and methyl-11-bromoundecanoate (78, 6.4 mg, 0.0232 mmol). After stirring at room temperature for 15 h, the resulting mixture was concentrated under vacuum and subjected to flash column chromatography (CH₂Cl₂/MeOH, 95:5) yielding an methyl ester (5.5 mg, 87 %) as a yellowish solid.

¹H NMR: δ = 8.66 (d, *J* = 8.5 Hz, 1H), 7.91 (m, 2H), 7.82 (m, 2H), 7.63 (d, *J* = 8.0 Hz, 1H), 7.34 (s, 2H), 7.27 (s, 1H), 6.96 (d, *J* = 8.5 Hz, 1H), 4.38 (t, *J* = 6.0 Hz, 2H), 3.76 (s, 3H), 2.73 (s, 3H), 2.52 (s, 3H), 2.33 (m, 3H), 1.87 (m, 2H), 1.63(m 3H), 1.48 (m, 2H), 1.38-1.25 (m, 8H) ppm. Mass calcd. for [M] 544.30, found (ES) [M] 544.

To a solution of the ester in THF/H₂O, 3:1(1 ml) was added LiOH (5.4mg, 0.2237mmol). After stirring at room temperature for 15 h, the resulting mixture was poured into H₂O with cold 1N HCl and extracted with CH₂Cl₂. The organic layers were combined, washed with brine, dried over Na₂SO₄, filtered, concentrated and dried under vacuum to yield 81 (5.3 mg, 98 %) as a yellowish solid.

Synthesis of 82

To a solution of 76 (4.0 mg, 0.0116 mmol) in methylene chloride (CH₂Cl₂; 1 ml) was added K₂CO₃ (6.8 mg, 0.0259 mmol) and methyl-16-bromohexadecanoate (79, 4.1 mg, 0.0232 mmol). After stirring at room temperature for 15 h, the resulting mixture was concentrated under vacuum and subjected to flash column chromatography (CH₂Cl₂/MeOH, 95:5) yielding an methyl ester (6.8 mg, 95 %) as a yellowish solid.

^1H NMR: δ = 8.66 (d, J = 8.5 Hz, 1H), 7.91 (m, 2H), 7.82 (m, 2H), 7.63 (d, J = 8.0 Hz, 1H), 7.34 (s, 2H), 7.27 (s, 1H), 6.96 (d, J = 8.5 Hz, 1H), 4.38 (t, J = 6.0 Hz, 2H), 3.76 (s, 3H), 2.73 (s, 3H), 2.52 (s, 3H), 2.33 (m, 3H), 1.87 (m, 2H), 1.63 (m, 3H), 1.48 (m, 2H), 1.38-1.25 (m, 18H) ppm. Mass calcd. for [M] 614.38, found (ES) [M] 614.

To a solution of the ester in THF/H₂O, 3:1(1 ml) was added LiOH (5.4mg, 0.2237mmol). After stirring at room temperature for 15 h, the resulting mixture was poured into H₂O with cold 1N HCl and extracted with CH₂Cl₂. The organic layers were combined, washed with brine, dried over Na₂SO₄, filtered, concentrated and dried under vacuum to yield 82 (6.6 mg, 98 %) as a yellowish solid.

PROTAC5 (85)

To a solution of 80 (1.0 mg, 0.0022 mmol) in methylene chloride (CH₂Cl₂; 0.5 ml) was added HBTU (1.3 mg, 0.0033 mmol), HOBt (0.5 mg, 0.0033 mmol), DIPEA (1.4 mg, 0.0110 mmol) and E3 ligase recognition motif (2.4 mg, 0.0033 mmol). After stirring at room temperature for 2 h, the resulting mixture was concentrated under vacuum and subjected to flash column chromatography (CH₂Cl₂:MeOH = 9:1) to yield a fully assembled product (2.1 mg, 82 %) as a yellowish solid.

^1H NMR: δ = 8.57 (d, J = 8.5 Hz, 1H), 7.86 (m, 2H), 7.75 (m, 2H), 7.56 (d, J = 8.0 Hz, 1H), 7.35 (m, 5H), 7.27 (s, 2H), 7.20 (s, 1H), 7.08 (d, J = 8.5 Hz, 2H), 6.90 (m, 3H), 5.13 (s, 2H), 4.63-4.42 (m, 7H), 3.09 (m, 1H), 2.89 (m, 1H), 2.73 (s, 3H), 2.52 (s, 3H) 2.33 (m, 2H), 1.93 (m, 2H), 1.91-1.89 (m, 4H) 1.55 (m, 2H), 1.45 (m, 1H), 1.28 (s, 9H), 1.25 (s, 6H), 1.16 (m, 1H), 1.05-0.83 (m, 12H) ppm.

To a solution of the fully assembled product (2.1 mg, 0.0018 mmol) in CH₂Cl₂ (0.2 ml) was added trifluoroacetic acid (100 μ l, 0.87 mmol) at room temperature for 15 min to deprotect *t*-butyl residue of tyrosine within the fully assembled compound. Subsequently, the concentrated mixture was dried under high vacuum to remove

trifluoroacetic acid. The resulting crude product was subjected to flash column chromatography ($\text{CH}_2\text{Cl}_2/\text{MeOH}$, 9:1) to yield **85** (2.0 mg, 100 %) as a yellowish solid.

^1H NMR: δ = 8.57 (d, J = 8.5 Hz, 1H), 7.86 (m, 2H), 7.75 (m, 2H), 7.56 (d, J = 8.0 Hz, 1H), 7.35 (m, 5H), 7.27 (s, 2H), 7.20 (s, 1H), 7.08 (d, J = 8.5 Hz, 2H), 6.90 (m, 3H), 5.13 (s, 2H), 4.63-4.42 (m, 7H), 3.09 (m, 1H), 2.89 (m, 1H), 2.73 (s, 3H), 2.52 (s, 3H) 2.33 (m, 2H), 1.93 (m, 2H), 1.91-1.89 (m, 4H) 1.55 (m, 2H), 1.45 (m, 1H), 1.25 (s, 6H), 1.18 (m, 1H), 1.00-0.84 (m, 12H) ppm.

Mass calcd. for [M] 1109.56, found (MALDI) [M] 1110.

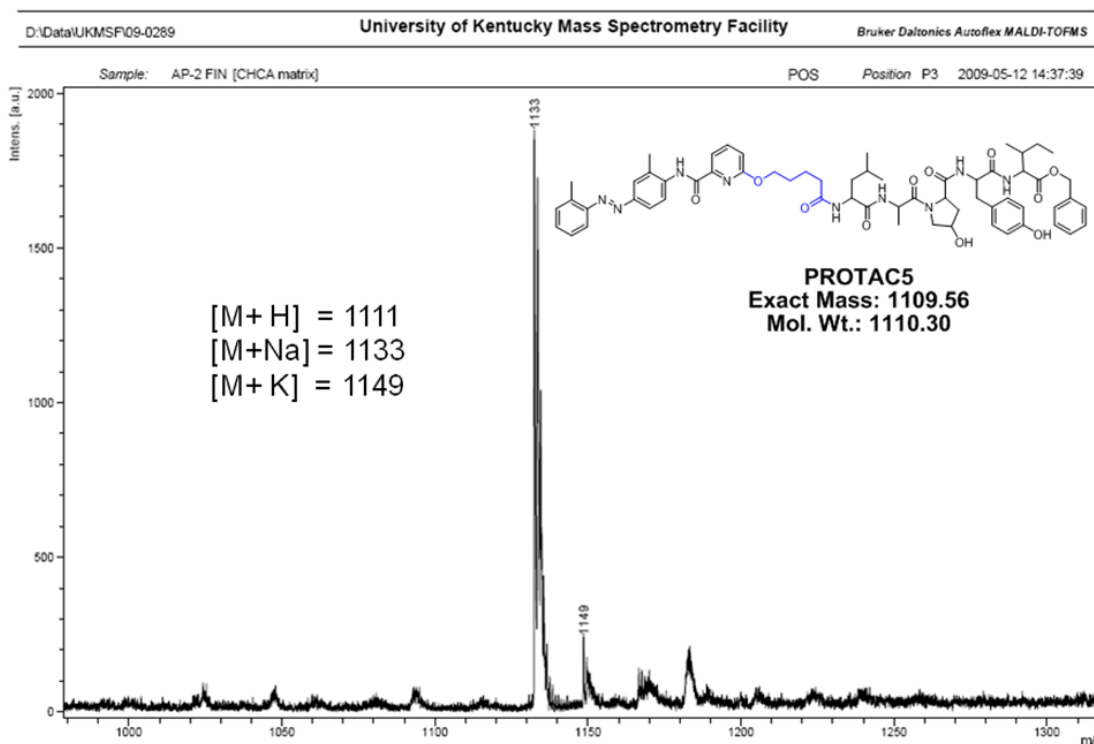


Figure 5.7 Mass spectrum for PROTAC5

PROTAC6 (**86**)

To a solution of **80** (1.0 mg, 0.0022 mmol) in methylene chloride (CH_2Cl_2 ; 0.5 ml) was added HBTU (1.3 mg, 0.0033 mmol), HOBt (0.5 mg, 0.0033 mmol), DIPEA

(1.4 mg, 0.0110 mmol) and 84 (2.6 mg, 0.0033 mmol). After stirring at room temperature for 2 h, the resulting mixture was concentrated under vacuum and subjected to flash column chromatography (CH₂Cl₂:MeOH = 9:1) to yield a fully assembled product (2.1 mg, 78 %) as a yellowish solid.

¹H NMR: δ = 8.57 (d, *J* = 8.5 Hz, 1H), 7.86 (m, 2H), 7.75 (m, 2H), 7.56 (d, *J* = 8.0 Hz, 1H), 7.35 (m, 5H), 7.27 (s, 2H), 7.20 (s, 1H), 7.08 (d, *J* = 8.5 Hz, 2H), 6.90 (m, 3H), 5.13 (s, 2H), 4.42 (m, 9H), 3.69 (s, 3H), 3.09 (m, 1H), 2.89 (m, 1H), 2.73 (s, 3H), 2.52 (s, 3H), 2.44 (t, *J* = 7.0 Hz, 2H), 1.93 (m, 2H), 1.91-1.89 (m, 4H), 1.55 (m, 2H), 1.45 (m, 1H), 1.28 (s, 9H), 1.25 (s, 6H), 1.17 (m, 1H), 1.09-0.85 (m, 12H) ppm.

To a solution of the fully assembled product (2.1 mg, 0.0017 mmol) in CH₂Cl₂ (0.2 ml) was added trifluoroacetic acid (100 μl, 0.87 mmol) at room temperature for 15 min to deprotect *t*-butyl residue of tyrosine within the fully assembled compound. Subsequently, the concentrated mixture was dried under high vacuum to remove trifluoroacetic acid. The resulting crude product was subjected to flash column chromatography (CH₂Cl₂/MeOH, 9:1) to yield 86 (2.0 mg, 100 %) as a yellowish solid.

¹H NMR: δ = 8.57 (d, *J* = 8.5 Hz, 1H), 7.86 (m, 2H), 7.75 (m, 2H), 7.56 (d, *J* = 8.0 Hz, 1H), 7.35 (m, 5H), 7.27 (s, 2H), 7.20 (s, 1H), 7.08 (d, *J* = 8.5 Hz, 2H), 6.90 (m, 3H), 5.13 (s, 2H), 4.42 (m, 9H), 3.69 (s, 3H), 3.09 (m, 1H), 2.89 (m, 1H), 2.73 (s, 3H), 2.52 (s, 3H), 2.44 (t, *J* = 7.0 Hz, 2H), 1.93 (m, 2H), 1.91-1.89 (m, 4H), 1.55 (m, 2H), 1.45 (m, 1H), 1.25 (s, 6H), 1.17 (m, 1H), 1.10-0.85 (m, 12H) ppm.

Mass calcd. for [M] 1166.58, found (MALDI) [M] 1166.71.

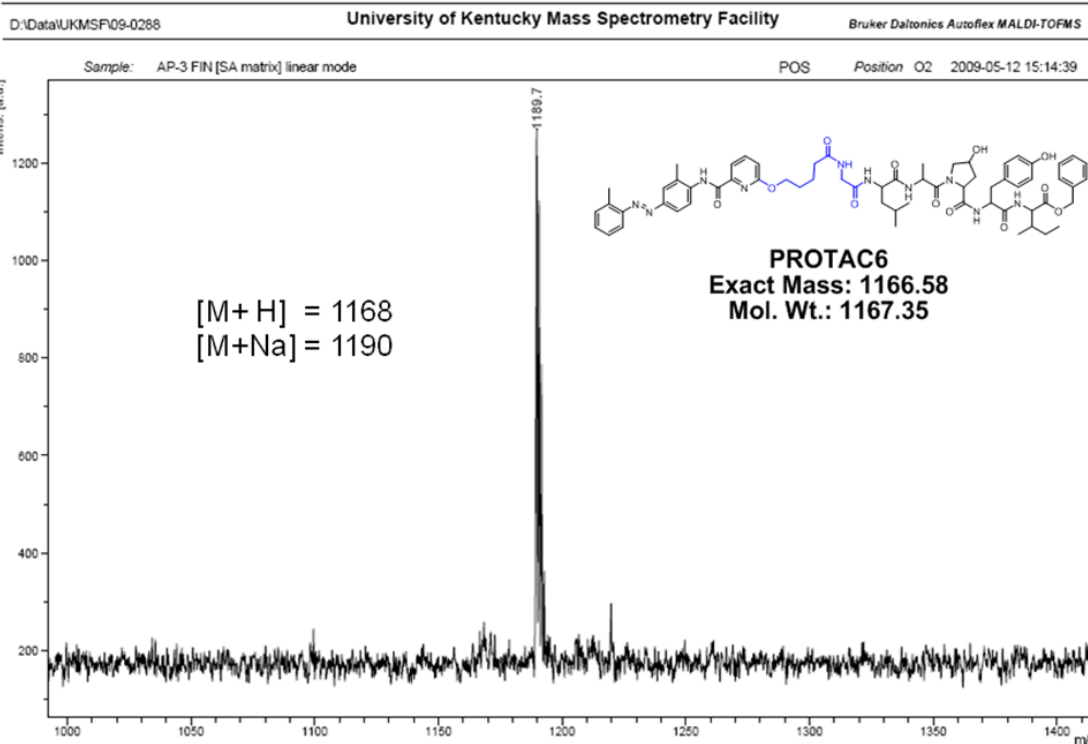


Figure 5.8 Mass spectrum for PROTAC6

PROTAC7 (87)

To a solution of 81 (1.0 mg, 0.0022 mmol) in methylene chloride (CH_2Cl_2 ; 0.5 ml) was added HBTU (1.3 mg, 0.0030 mmol), HOBt (0.5 mg, 0.0030 mmol), DIPEA (1.4 mg, 0.0110 mmol) and E3 ligase recognition motif (2.2 mg, 0.0030 mmol). After stirring at room temperature for 2 h, the resulting mixture was concentrated under vacuum and subjected to flash column chromatography (CH_2Cl_2 :MeOH = 9:1) to yield a fully assembled product (2.2 mg, 90 %) as a yellowish solid.

^1H NMR: δ = 8.66 (d, J = 8.5 Hz, 1H), 7.91 (m, 2H), 7.82 (m, 2H), 7.63 (d, J = 8.0 Hz, 1H), 7.35 (m, 7H), 7.27 (s, 1H), 7.08 (d, J = 8.5 Hz, 2H), 6.96 (d, J = 8.5 Hz, 3H), 5.13 (s, 2H), 4.40 (m, 7H), 3.76 (s, 3H), 3.09 (m, 1H), 2.89 (m, 1H), 2.73 (s, 3H), 2.52 (s, 3H), 2.33 (m, 3H), 1.93 (m, 2H), 1.87 (m, 2H), 1.63 (m, 3H), 1.55 (m, 2H), 1.48 (m, 2H), 1.45 (m, 1H), 1.38-1.24 (m, 23H), 1.17 (m, 1H), 0.83-1.00 (m, 12H) ppm.

To a solution of the fully assembled product (2.2 mg, 0.0017 mmol) in CH₂Cl₂ (0.2 ml) was added trifluoroacetic acid (100 μl, 0.87 mmol) at room temperature for 15 min to deprotect *t*-butyl residue of tyrosine within the fully assembled compound. Subsequently, the concentrated mixture was dried under high vacuum to remove trifluoroacetic acid. The resulting crude product was subjected to flash column chromatography (CH₂Cl₂/MeOH, 9:1) to yield **87** (2.1 mg, 100 %) as a yellowish solid.

¹H NMR: δ = 8.66 (d, *J* = 8.5 Hz, 1H), 7.91 (m, 2H), 7.82 (m, 2H), 7.63 (d, *J* = 8.0 Hz, 1H), 7.35 (m, 7H), 7.27 (s, 1H), 7.08 (d, *J* = 8.5 Hz, 2H), 6.96 (d, *J* = 8.5 Hz, 3H), 5.13 (s, 2H), 4.40 (m, 7H), 3.76 (s, 3H), 3.09 (m, 1H), 2.89 (m, 1H), 2.73 (s, 3H), 2.52 (s, 3H), 2.33 (m, 3H), 1.93 (m, 2H), 1.87 (m, 2H), 1.63 (m, 3H), 1.55 (m, 2H), 1.48 (m, 2H), 1.45 (m, 1H), 1.38-1.24 (m, 14H), 1.17 (m, 1H), 0.83-1.00 (m, 12H) ppm.

Mass calcd. for [M] 1193.65, found (MALDI) [M] 1193.81.

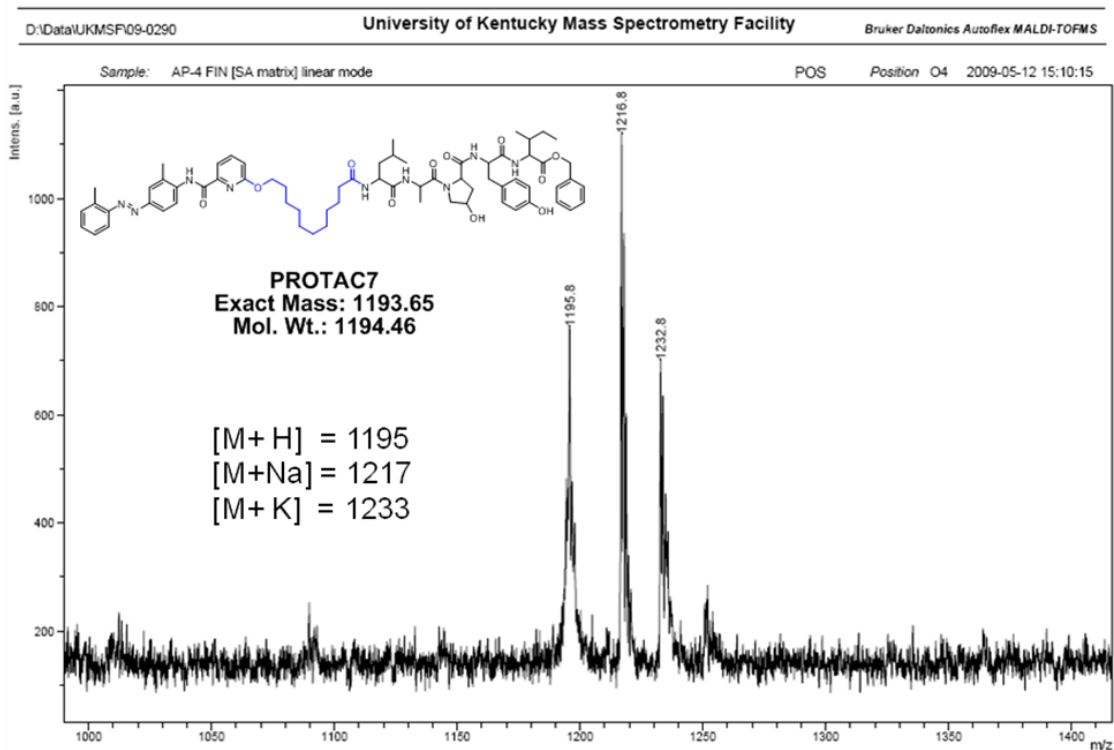


Figure 5.9 Mass spectrum for PROTAC7

PROTAC8 (88)

To a solution of 81 (1.1 mg, 0.0022 mmol) in methylene chloride (CH₂Cl₂; 0.5 ml) was added HBTU (1.3 mg, 0.0030 mmol), HOBt (0.5 mg, 0.0030 mmol), DIPEA (1.4 mg, 0.0110 mmol) and 84 (2.6 mg, 0.0033 mmol). After stirring at room temperature for 2 h, the resulting mixture was concentrated under vacuum and subjected to flash column chromatography (CH₂Cl₂:MeOH = 9:1) to yield a fully assembled product (2.1 mg, 73 %) as a yellowish solid.

¹H NMR: δ = 8.66 (d, *J* = 8.5 Hz, 1H), 7.91 (m, 2H), 7.82 (m, 2H), 7.63 (d, *J* = 8.0 Hz, 1H), 7.35 (s, 7H), 7.27 (s, 1H), 7.08 (d, *J* = 8.5 Hz, 2H), 6.96 (m, 3H), 5.13 (s, 2H), 4.40 (m, 9H), 3.76 (s, 3H), 3.09 (m, 1H), 2.89 (m, 1H), 2.73 (s, 3H), 2.52 (s, 3H), 2.33 (m, 3H), 1.93 (m, 2H), 1.87 (m, 2H), 1.63(m 3H), 1.55 (m, 2H), 1.47 (m, 3H), 1.38-1.25 (m, 14H), 1.10-0.83 (m, 13H) ppm.

To a solution of the fully assembled product (2.1 mg, 0.0017 mmol) in CH₂Cl₂ (0.2 ml) was added trifluoroacetic acid (100 μl, 0.87 mmol) at room temperature for 15 min to deprotect *t*-butyl residue of tyrosine within the fully assembled compound. Subsequently, the concentrated mixture was dried under high vacuum to remove trifluoroacetic acid. The resulting crude product was subjected to flash column chromatography (CH₂Cl₂/MeOH, 9:1) to yield 87 (2.0 mg, 100 %) as a yellowish solid.

¹H NMR: δ = 8.66 (d, *J* = 8.5 Hz, 1H), 7.91 (m, 2H), 7.82 (m, 2H), 7.63 (d, *J* = 8.0 Hz, 1H), 7.35 (s, 7H), 7.27 (s, 1H), 7.08 (d, *J* = 8.5 Hz, 2H), 6.96 (m, 3H), 5.13 (s, 2H), 4.40 (m, 9H), 3.76 (s, 3H), 3.09 (m, 1H), 2.89 (m, 1H), 2.73 (s, 3H), 2.52 (s, 3H), 2.33 (m, 3H), 1.93 (m, 2H), 1.87 (m, 2H), 1.63(m 3H), 1.55 (m, 2H), 1.47 (m, 3H), 1.38-1.25 (m, 23H), 1.10-0.83 (m, 13H) ppm.

Mass calcd. for [M] 1250.67, found (MALDI) [M] 1250.61.

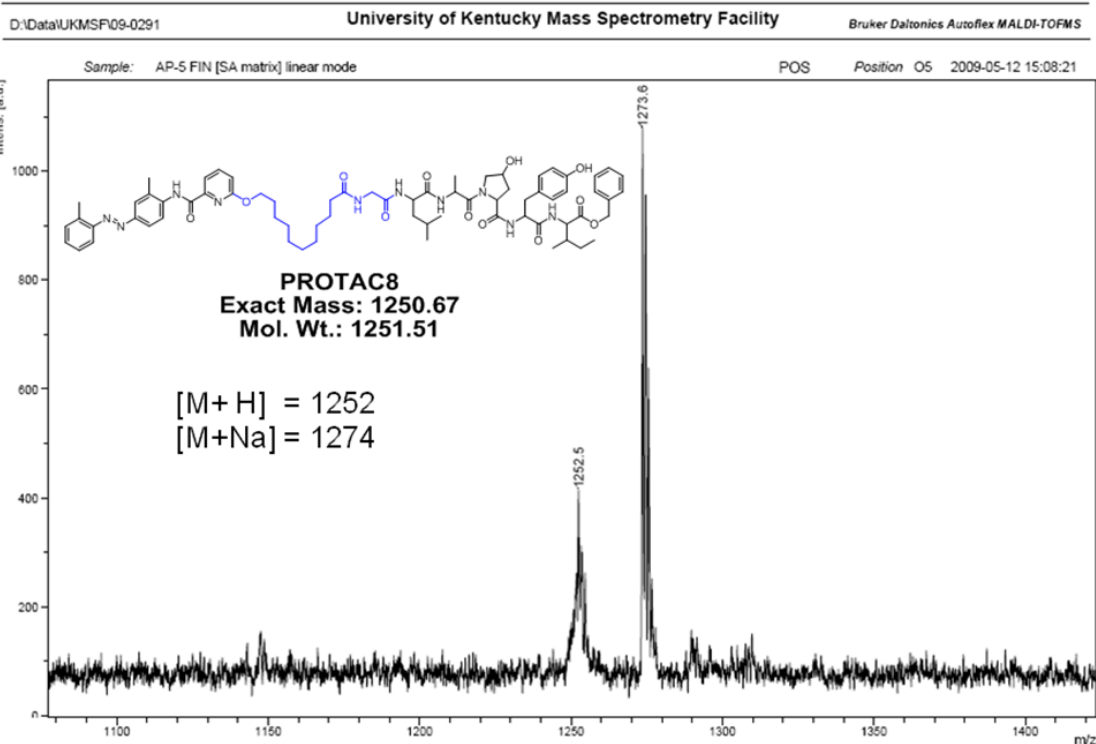


Figure 5.10 Mass spectrum for PROTAC8

PROTAC9 (89)

To a solution of 82 (1.2 mg, 0.0020 mmol) in methylene chloride (CH_2Cl_2 ; 0.5 ml) was added HBTU (1.3 mg, 0.0033 mmol), HOBt (0.5 mg, 0.0033 mmol), DIPEA (1.4 mg, 0.0110 mmol) and E3 ligase recognition motif (2.4 mg, 0.0033 mmol). After stirring at room temperature for 2 h, the resulting mixture was concentrated under vacuum and subjected to flash column chromatography (CH_2Cl_2 :MeOH = 9:1) to yield a fully assembled product (2.1 mg, 80 %) as a yellowish solid.

^1H NMR: δ = 8.66 (d, J = 8.5 Hz, 1H), 7.91 (m, 2H), 7.82 (m, 2H), 7.63 (d, J = 8.0 Hz, 1H), 7.35 (m, 7H), 7.27 (s, 1H), 7.08 (d, J = 8.5 Hz, 2H), 6.96 (m, 3H), 5.13 (s, 2H), 4.41 (m, 7H), 3.76 (s, 3H), 3.09 (m, 1H), 2.89 (m, 1H), 2.73 (s, 3H), 2.52 (s, 3H), 2.33 (m, 3H), 1.93 (m, 2H), 1.87 (m, 2H), 1.63 (m, 3H), 1.55 (m, 2H), 1.47 (m, 3H), 1.38-1.25 (m, 24H), 1.12-0.83 (m, 13H) ppm.

To a solution of the fully assembled product (2.1 mg, 0.0016 mmol) in CH₂Cl₂ (0.2 ml) was added trifluoroacetic acid (100 μl, 0.87 mmol) at room temperature for 15 min to deprotect *t*-butyl residue of tyrosine within the fully assembled compound. Subsequently, the concentrated mixture was dried under high vacuum to remove trifluoroacetic acid. The resulting crude product was subjected to flash column chromatography (CH₂Cl₂/MeOH, 9:1) to yield **89** (1.8 mg, 89 %) as a yellowish solid.

¹H NMR: δ = 8.66 (d, *J* = 8.5 Hz, 1H), 7.91 (m, 2H), 7.82 (m, 2H), 7.63 (d, *J* = 8.0 Hz, 1H), 7.35 (m, 7H), 7.27 (s, 1H), 7.08 (d, *J* = 8.5 Hz, 2H), 6.96 (m, 3H), 5.13 (s, 2H), 4.41 (m, 7H), 3.76 (s, 3H), 3.09 (m, 1H), 2.89 (m, 1H), 2.73 (s, 3H), 2.52 (s, 3H), 2.33 (m, 3H), 1.93 (m, 2H), 1.87 (m, 2H), 1.63 (m, 3H), 1.55 (m, 2H), 1.47 (m, 3H), 1.38-1.25 (m, 33H), 1.12-0.83 (m, 13H) ppm.

Mass calcd. for [M] 1263.73, found (MALDI) [M] 1263.71.

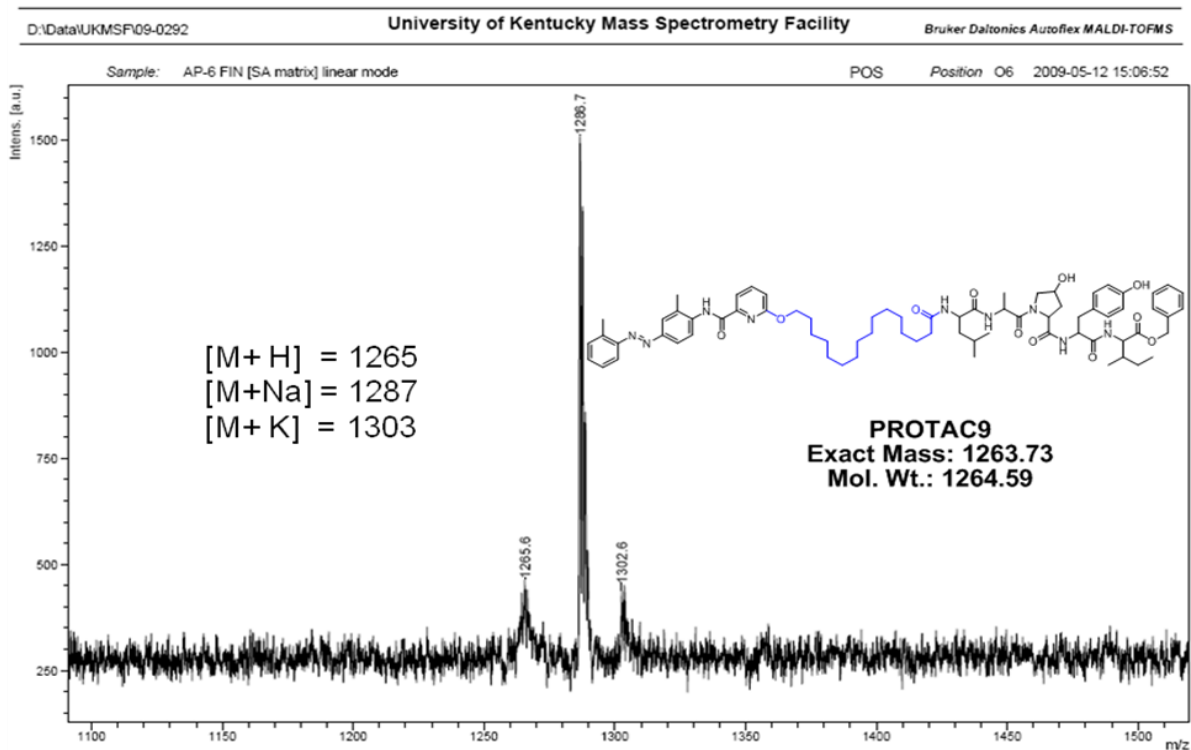


Figure 5.11 Mass spectrum for PROTAC9

PROTAC10 (90)

To a solution of 82 (1.2 mg, 0.0020 mmol) in methylene chloride (CH₂Cl₂; 0.5 ml) was added HBTU (1.3 mg, 0.0033 mmol), HOBt (0.5 mg, 0.0033 mmol), DIPEA (1.4 mg, 0.0110 mmol) and 84 (2.6 mg, 0.0033 mmol). After stirring at room temperature for 2 h, the resulting mixture was concentrated under vacuum and subjected to flash column chromatography (CH₂Cl₂:MeOH = 9:1) to yield a fully assembled product (2.0 mg, 73 %) as a yellowish solid.

¹H NMR: δ = 8.66 (d, *J* = 8.5 Hz, 1H), 7.91 (m, 2H), 7.82 (m, 2H), 7.63 (d, *J* = 8.0 Hz, 1H), 7.35 (m, 7H), 7.27 (s, 1H), 7.08 (d, *J* = 8.5 Hz, 2H), 6.96 (m, 3H), 5.13 (s, 2H), 4.41 (m, 9H), 3.76 (s, 3H), 3.09 (m, 1H), 2.89 (m, 1H), 2.73 (s, 3H), 2.52 (s, 3H), 2.33 (m, 3H), 1.93 (m, 2H), 1.87 (m, 2H), 1.63(m 3H), 1.55 (m, 2H), 1.47 (m, 3H), 1.38-1.25 (m, 33H), 1.12-0.83 (m, 13H) ppm.

To a solution of the fully assembled product (2.0 mg, 0.0015 mmol) in CH₂Cl₂ (0.2 ml) was added trifluoroacetic acid (100 μl, 0.87 mmol) at room temperature for 15 min to deprotect *t*-butyl residue of tyrosine within the fully assembled compound. Subsequently, the concentrated mixture was dried under high vacuum to remove trifluoroacetic acid. The resulting crude product was subjected to flash column chromatography (CH₂Cl₂/MeOH, 9:1) to yield 90 (1.9 mg, 99 %) as a yellowish solid.

¹H NMR: δ = 8.66 (d, *J* = 8.5 Hz, 1H), 7.91 (m, 2H), 7.82 (m, 2H), 7.63 (d, *J* = 8.0 Hz, 1H), 7.35 (m, 7H), 7.27 (s, 1H), 7.08 (d, *J* = 8.5 Hz, 2H), 6.96 (m, 3H), 5.13 (s, 2H), 4.41 (m, 9H), 3.76 (s, 3H), 3.09 (m, 1H), 2.89 (m, 1H), 2.73 (s, 3H), 2.52 (s, 3H), 2.33 (m, 3H), 1.93 (m, 2H), 1.87 (m, 2H), 1.63(m 3H), 1.55 (m, 2H), 1.47 (m, 3H), 1.38-1.25 (m, 24H), 1.12-0.83 (m, 13H) ppm.

Mass calcd. for [M] 1320.75, found (MALDI) [M] 1320.81.

CHAPTER 6 CONCLUSION

6.1 Discussion

AHR is a ligand-activated transcription factor regulating the expression of a number of genes by an agonist. The AHR signaling pathway is triggered by the activation of the receptor. In the traditional methodology, the study on a signaling pathway involves identification of the initiation signal. The study also includes an understanding of the cellular events caused by the affected signal transduction and gene regulations. For the AHR signaling pathway, the endogenous ligands that trigger the activation of signaling pathway are not yet well known and the corresponding function of the receptor is not yet fully understood. Recent studies suggest that the role of AHR may not be limited to the classical role as a regulator of xenobiotic metabolism. In addition, the findings that the AHR crosstalks with a number of other transcriptional factors further indicate the complexity of AHR signaling pathway. To dissect these complex signaling networks, the functional modulators specific for each signaling molecule provide powerful molecular tools. A number of potent AHR agonists are currently available for signaling studies. However, most AHR antagonists previously identified also function as partial agonists, limiting their use as molecular probes.

AHR binds to a large number of aromatic hydrocarbons of diverse. In order to maintain an "inactive" conformation of the receptor while it is interacting with ligand, one of the major concerns was the structural flexibility of AHR antagonist. It is because that the structures of strong AHR agonists are rigid and mono-planar in general, whereas those of newly identified antagonists are relatively flexible. Taken together, it was hypothesized that a multi-planar and flexible aromatic structure may provide pure antagonistic activity. Consistent with the hypothesis, a number of the flexible compounds developed in this study are pure antagonists.

The use of chemical library for ligand moiety of PROTAC is anticipated to provide a potential platform for the systemic development of appropriate molecular probes for the wider applications. In the present study, we hypothesized that AHR can be targeted though PROTAC approach. Once apigenin based PROTAC provided the proof

of principle, we then constructed a small focused library based on CH-223191. To this end, we optimized the ligand structure for antagonistic activity and prepared PROTACS based on the antagonist. To the best of my knowledge, this is the first trial to develop a small molecule targeting a protein of interest via the combinatorial methodology of PROTAC and chemical library.

The overall goal of this study was the development of novel AHR antagonist without agonistic potency. In accordance with the goal, a series of works were set forth as specific aims and performed. The followings are the summary of the accomplishments and the general conclusions drawn based on the results.

6.2 Summary

1. The PROTAC based on apigenin was successfully synthesized.
2. The PROTAC based on an exogenous ligand, apigenin, successfully induced degradation of AHR and effectively blocked TCDD-induced activation of AHR.
3. A Chemical library based on the structure of CH-223191 was constructed and screened for AHR antagonistic activity.
4. N-[2-Methyl-4-[(2-methylphenyl)diazenyl]phenyl]-2-pyridine carboxamide (36), N-[2-methyl-4-[(2-methylphenyl)diazenyl]phenyl]-2-pyrazine carboxamide (37) and N-[2-methyl-4-[(2-methylphenyl)diazenyl]phenyl]-2-furan carboxamide (31) were identified as antagonists of AHR.
5. *p*-(*p*-tolyl diazenyl)-*o*-toluidine exhibited synergistic activity for AHR activation in concert with TCDD in prolonged incubation.
6. The PROTACs based on the compound 36 was successfully prepared through A ring or C ring modification.
7. The PROTACs based on synthetic structure did not exhibit antagonistic activity in the initial experimental condition.

6.3 Conclusions

1. AHR can be targeted through the PROTAC approach.
2. PROTAC based on apigenin (PROTAC2) induces degradation of AHR and suppresses TCDD-induced activation of AHR without agonistic activity.
3. The structure of CH-223191 was optimized for AHR antagonistic activity by positional scanning identifying N-[2-Methyl-4-[(2-methylphenyl)diazanyl]phenyl]-2-pyridinecarboxamide (36) as the optimal AHR antagonist.
4. PROTAC based on synthetic ligand showed a modest antagonistic activity. Further characterization and optimization may be required

6.4. Future directions

The process of the development of PROTAC generated a number of useful research tools for studying or probing AHR biology such as agonist and antagonists targeting AHR including the PROTACs. Further, the findings and analyses described herein proposed a number of valuable insights that will likely be useful for further optimization of PROTACs targeting AHR.

The two functional heads are the primary targets for the optimization. In spite of optimization of the CH-223191 structure for antagonistic activity, we still do not have full understanding of the ligand structure required for pure antagonistic activity. Since an increasing number of building blocks for each position are made available, the ligand structure can be optimized further. On the other hand, the E3 ligase recognition motif moiety eliciting proteolysis is the key component for PROTAC development as well. This head has been evolved from diphospho-I κ B fragment into E3 ligase recognition motif exhibiting excellent activity. However, the PROTAC equipped with the small molecule, nutlin, has been reported, suggesting that non-peptidyl structures may also be useful in design of PROTACs. The investigation on the linker length described herein

did not reveal the optimal distance. Nonetheless, the linker moiety should be considered for improving the PROTAC activity since it serves as a spacer providing appropriate distance between two heads for the proper interaction.

It is also suggested that the effect on the each stage of signaling pathway as shown in the study on apigenin based PROTAC be investigated. In addition, the investigation on the specificity of future PROTACs is strongly suggested. With the further efforts to develop PROTACs of higher potency, the PROTAC technology will be validated as a generally applicable chemical approach to biology.

REFERENCES

1. Sakamoto, K. M., Kim, K. B., Kumagai, A., Mercurio, F., Crews, C. M., and Deshaies, R. J. (2001) Protacs: chimeric molecules that target proteins to the Skp1-Cullin-F box complex for ubiquitination and degradation, *Proc Natl Acad Sci U S A* 98, 8554-8559.
2. Sakamoto, K. M., Kim, K. B., Verma, R., Ransick, A., Stein, B., Crews, C. M., and Deshaies, R. J. (2003) Development of Protacs to target cancer-promoting proteins for ubiquitination and degradation, *Mol Cell Proteomics* 2, 1350-1358.
3. Zhang, D., Baek, S. H., Ho, A., Lee, H., Jeong, Y. S., and Kim, K. (2004) Targeted degradation of proteins by small molecules: a novel tool for functional proteomics, *Comb Chem High Throughput Screen* 7, 689-697.
4. Lee, H., Puppala, D., Choi, E. Y., Swanson, H., and Kim, K. B. (2007) Targeted degradation of the aryl hydrocarbon receptor by the PROTAC approach: a useful chemical genetic tool, *Chembiochem* 8, 2058-2062.
5. Schneekloth, A. R., Pucheault, M., Tae, H. S., and Crews, C. M. (2008) Targeted intracellular protein degradation induced by a small molecule: En route to chemical proteomics, *Bioorg Med Chem Lett* 18, 5904-5908.
6. Bacsi, S. G., Reisz-Porszasz, S., and Hankinson, O. (1995) Orientation of the heterodimeric aryl hydrocarbon (dioxin) receptor complex on its asymmetric DNA recognition sequence, *Mol Pharmacol* 47, 432-438.
7. Burbach, K. M., Poland, A., and Bradfield, C. A. (1992) Cloning of the Ah-receptor cDNA reveals a distinctive ligand-activated transcription factor, *Proc Natl Acad Sci U S A* 89, 8185-8189.
8. DeVito, M. J., Ma, X., Babish, J. G., Menache, M., and Birnbaum, L. S. (1994) Dose-response relationships in mice following subchronic exposure to 2,3,7,8-tetrachlorodibenzo-p-dioxin: CYP1A1, CYP1A2, estrogen receptor, and protein tyrosine phosphorylation, *Toxicol Appl Pharmacol* 124, 82-90.
9. Okey, A. B., Riddick, D. S., and Harper, P. A. (1994) Molecular biology of the aromatic hydrocarbon (dioxin) receptor, *Trends Pharmacol Sci* 15, 226-232.
10. Fernandez-Salguero, P. M., Hilbert, D. M., Rudikoff, S., Ward, J. M., and Gonzalez, F. J. (1996) Aryl-hydrocarbon receptor-deficient mice are resistant to 2,3,7,8-tetrachlorodibenzo-p-dioxin-induced toxicity, *Toxicol Appl Pharmacol* 140, 173-179.

11. Sogawa, K., and Fujii-Kuriyama, Y. (1997) Ah receptor, a novel ligand-activated transcription factor, *J Biochem* 122, 1075-1079.
12. Mimura, J., and Fujii-Kuriyama, Y. (2003) Functional role of AhR in the expression of toxic effects by TCDD, *Biochim Biophys Acta* 1619, 263-268.
13. Bock, K. W., and Kohle, C. (2005) Ah receptor- and TCDD-mediated liver tumor promotion: clonal selection and expansion of cells evading growth arrest and apoptosis, *Biochem Pharmacol* 69, 1403-1408.
14. Ma, C., Marlowe, J. L., and Puga, A. (2009) The aryl hydrocarbon receptor at the crossroads of multiple signaling pathways, *EXS* 99, 231-257.
15. Mason, G. G., Wilhelmsson, A., Cuthill, S., Gillner, M., Poellinger, L., and Gustafsson, J. A. (1988) The dioxin receptor: characterization of its DNA-binding properties, *J Steroid Biochem* 30, 307-310.
16. Denison, M. S., Fisher, J. M., and Whitlock, J. P., Jr. (1989) Protein-DNA interactions at recognition sites for the dioxin-Ah receptor complex, *J Biol Chem* 264, 16478-16482.
17. Swanson, H. I., and Bradfield, C. A. (1993) The AH-receptor: genetics, structure and function, *Pharmacogenetics* 3, 213-230.
18. Whitelaw, M. L., Gottlicher, M., Gustafsson, J. A., and Poellinger, L. (1993) Definition of a novel ligand binding domain of a nuclear bHLH receptor: co-localization of ligand and hsp90 binding activities within the regulable inactivation domain of the dioxin receptor, *EMBO J* 12, 4169-4179.
19. Jain, S., Dolwick, K. M., Schmidt, J. V., and Bradfield, C. A. (1994) Potent transactivation domains of the Ah receptor and the Ah receptor nuclear translocator map to their carboxyl termini, *J Biol Chem* 269, 31518-31524.
20. Reisz-Porszasz, S., Probst, M. R., Fukunaga, B. N., and Hankinson, O. (1994) Identification of functional domains of the aryl hydrocarbon receptor nuclear translocator protein (ARNT), *Mol Cell Biol* 14, 6075-6086.
21. Kronenberg, S., Esser, C., and Carlberg, C. (2000) An aryl hydrocarbon receptor conformation acts as the functional core of nuclear dioxin signaling, *Nucleic Acids Res* 28, 2286-2291.
22. McGuire, J., Coumailleau, P., Whitelaw, M. L., Gustafsson, J. A., and Poellinger, L. (1995) The basic helix-loop-helix/PAS factor Sim is associated with hsp90.

- Implications for regulation by interaction with partner factors, *J Biol Chem* 270, 31353-31357.
23. Li, H., Dong, L., and Whitlock, J. P., Jr. (1994) Transcriptional activation function of the mouse Ah receptor nuclear translocator, *J Biol Chem* 269, 28098-28105.
 24. Yamaguchi, Y., and Kuo, M. T. (1995) Functional analysis of aryl hydrocarbon receptor nuclear translocator interactions with aryl hydrocarbon receptor in the yeast two-hybrid system, *Biochem Pharmacol* 50, 1295-1302.
 25. Eguchi, H., Ikuta, T., Tachibana, T., Yoneda, Y., and Kawajiri, K. (1997) A nuclear localization signal of human aryl hydrocarbon receptor nuclear translocator/hypoxia-inducible factor 1beta is a novel bipartite type recognized by the two components of nuclear pore-targeting complex, *J Biol Chem* 272, 17640-17647.
 26. Ikuta, T., Eguchi, H., Tachibana, T., Yoneda, Y., and Kawajiri, K. (1998) Nuclear localization and export signals of the human aryl hydrocarbon receptor, *J Biol Chem* 273, 2895-2904.
 27. Ikuta, T., Tachibana, T., Watanabe, J., Yoshida, M., Yoneda, Y., and Kawajiri, K. (2000) Nucleocytoplasmic shuttling of the aryl hydrocarbon receptor, *J Biochem* 127, 503-509.
 28. Carlson, D. B., and Perdew, G. H. (2002) A dynamic role for the Ah receptor in cell signaling? Insights from a diverse group of Ah receptor interacting proteins, *J Biochem Mol Toxicol* 16, 317-325.
 29. Kanno, Y., Miyama, Y., Takane, Y., Nakahama, T., and Inouye, Y. (2007) Identification of intracellular localization signals and of mechanisms underlining the nucleocytoplasmic shuttling of human aryl hydrocarbon receptor repressor, *Biochem Biophys Res Commun* 364, 1026-1031.
 30. Hankinson, O. (1994) The role of the aryl hydrocarbon receptor nuclear translocator protein in aryl hydrocarbon receptor action, *Trends Endocrinol Metab* 5, 240-244.
 31. Boutros, P. C., Moffat, I. D., Franc, M. A., Tijet, N., Tuomisto, J., Pohjanvirta, R., and Okey, A. B. (2004) Dioxin-responsive AHRE-II gene battery: identification by phylogenetic footprinting, *Biochem Biophys Res Commun* 321, 707-715.

32. Long, W. P., Pray-Grant, M., Tsai, J. C., and Perdew, G. H. (1998) Protein kinase C activity is required for aryl hydrocarbon receptor pathway-mediated signal transduction, *Mol Pharmacol* 53, 691-700.
33. Schrenk, D. (1998) Impact of dioxin-type induction of drug-metabolizing enzymes on the metabolism of endo- and xenobiotics, *Biochem Pharmacol* 55, 1155-1162.
34. Choi, E. J., Toscano, D. G., Ryan, J. A., Riedel, N., and Toscano, W. A., Jr. (1991) Dioxin induces transforming growth factor-alpha in human keratinocytes, *J Biol Chem* 266, 9591-9597.
35. Levine-Fridman, A., Chen, L., and Elferink, C. J. (2004) Cytochrome P4501A1 promotes G1 phase cell cycle progression by controlling aryl hydrocarbon receptor activity, *Mol Pharmacol* 65, 461-469.
36. Puga, A., Hoffer, A., Zhou, S., Bohm, J. M., Leikauf, G. D., and Shertzer, H. G. (1997) Sustained increase in intracellular free calcium and activation of cyclooxygenase-2 expression in mouse hepatoma cells treated with dioxin, *Biochem Pharmacol* 54, 1287-1296.
37. Corchero, J., Martin-Partido, G., Dallas, S. L., and Fernandez-Salguero, P. M. (2004) Liver portal fibrosis in dioxin receptor-null mice that overexpress the latent transforming growth factor-beta-binding protein-1, *Int J Exp Pathol* 85, 295-302.
38. Guo, J., Sartor, M., Karyala, S., Medvedovic, M., Kann, S., Puga, A., Ryan, P., and Tomlinson, C. R. (2004) Expression of genes in the TGF-beta signaling pathway is significantly deregulated in smooth muscle cells from aorta of aryl hydrocarbon receptor knockout mice, *Toxicol Appl Pharmacol* 194, 79-89.
39. Yang, F., and Bleich, D. (2004) Transcriptional regulation of cyclooxygenase-2 gene in pancreatic beta-cells, *J Biol Chem* 279, 35403-35411.
40. Ikegwuonu, F. I., Christou, M., and Jefcoate, C. R. (1999) Regulation of cytochrome P4501B1 (CYP1B1) in mouse embryo fibroblast (C3H10T1/2) cells by protein kinase C (PKC), *Biochem Pharmacol* 57, 619-630.
41. Tan, Z., Chang, X., Puga, A., and Xia, Y. (2002) Activation of mitogen-activated protein kinases (MAPKs) by aromatic hydrocarbons: role in the regulation of aryl hydrocarbon receptor (AHR) function, *Biochem Pharmacol* 64, 771-780.

42. Chen, S., Nguyen, N., Tamura, K., Karin, M., and Tukey, R. H. (2003) The role of the Ah receptor and p38 in benzo[a]pyrene-7,8-dihydrodiol and benzo[a]pyrene-7,8-dihydrodiol-9,10-epoxide-induced apoptosis, *J Biol Chem* 278, 19526-19533.
43. Ohtake, F., Baba, A., Takada, I., Okada, M., Iwasaki, K., Miki, H., Takahashi, S., Kouzmenko, A., Nohara, K., Chiba, T., Fujii-Kuriyama, Y., and Kato, S. (2007) Dioxin receptor is a ligand-dependent E3 ubiquitin ligase, *Nature* 446, 562-566.
44. Stevens, E. A., Mezrich, J. D., and Bradfield, C. A. (2009) The aryl hydrocarbon receptor: a perspective on potential roles in the immune system, *Immunology* 127, 299-311.
45. Ho, P. P., and Steinman, L. (2008) The aryl hydrocarbon receptor: a regulator of Th17 and Treg cell development in disease, *Cell Res* 18, 605-608.
46. Veldhoen, M., Hirota, K., Westendorf, A. M., Buer, J., Dumoutier, L., Renauld, J. C., and Stockinger, B. (2008) The aryl hydrocarbon receptor links TH17-cell-mediated autoimmunity to environmental toxins, *Nature* 453, 106-109.
47. Walker, M. K., Pollenz, R. S., and Smith, S. M. (1997) Expression of the aryl hydrocarbon receptor (AhR) and AhR nuclear translocator during chick cardiogenesis is consistent with 2,3,7,8-tetrachlorodibenzo-p-dioxin-induced heart defects, *Toxicol Appl Pharmacol* 143, 407-419.
48. Fernandez-Salguero, P. M., Ward, J. M., Sundberg, J. P., and Gonzalez, F. J. (1997) Lesions of aryl-hydrocarbon receptor-deficient mice, *Vet Pathol* 34, 605-614.
49. Schmidt, J. V., Su, G. H., Reddy, J. K., Simon, M. C., and Bradfield, C. A. (1996) Characterization of a murine Ahr null allele: involvement of the Ah receptor in hepatic growth and development, *Proc Natl Acad Sci U S A* 93, 6731-6736.
50. Williamson, M. A., Gasiewicz, T. A., and Opanashuk, L. A. (2005) Aryl hydrocarbon receptor expression and activity in cerebellar granule neuroblasts: implications for development and dioxin neurotoxicity, *Toxicol Sci* 83, 340-348.
51. Lahvis, G. P., Lindell, S. L., Thomas, R. S., McCuskey, R. S., Murphy, C., Glover, E., Bentz, M., Southard, J., and Bradfield, C. A. (2000) Portosystemic shunting and persistent fetal vascular structures in aryl hydrocarbon receptor-deficient mice, *Proc Natl Acad Sci U S A* 97, 10442-10447.

52. Mullins, C. E. (2006) *Cardiac catheterization in congenital heart disease : pediatric and adult*, Blackwell Futura, Malden, Mass.
53. Walisser, J. A., Bungler, M. K., Glover, E., Harstad, E. B., and Bradfield, C. A. (2004) Patent ductus venosus and dioxin resistance in mice harboring a hypomorphic Arnt allele, *J Biol Chem* 279, 16326-16331.
54. Fahy, O., Tscopoulos, A., Hammad, H., Pestel, J., Tonnel, A. B., and Wallaert, B. (1999) Effects of diesel organic extracts on chemokine production by peripheral blood mononuclear cells, *J Allergy Clin Immunol* 103, 1115-1124.
55. Abbott, B. D., and Birnbaum, L. S. (1989) TCDD alters medial epithelial cell differentiation during palatogenesis, *Toxicol Appl Pharmacol* 99, 276-286.
56. Thackaberry, E. A., Bedrick, E. J., Goens, M. B., Danielson, L., Lund, A. K., Gabaldon, D., Smith, S. M., and Walker, M. K. (2003) Insulin regulation in AhR-null mice: embryonic cardiac enlargement, neonatal macrosomia, and altered insulin regulation and response in pregnant and aging AhR-null females, *Toxicol Sci* 76, 407-417.
57. Fernandez-Salguero, P., Pineau, T., Hilbert, D. M., McPhail, T., Lee, S. S., Kimura, S., Nebert, D. W., Rudikoff, S., Ward, J. M., and Gonzalez, F. J. (1995) Immune system impairment and hepatic fibrosis in mice lacking the dioxin-binding Ah receptor, *Science* 268, 722-726.
58. Abbott, B. D., Perdew, G. H., and Birnbaum, L. S. (1994) Ah receptor in embryonic mouse palate and effects of TCDD on receptor expression, *Toxicol Appl Pharmacol* 126, 16-25.
59. Boffetta, P. (2004) Risk of acute myeloid leukemia after exposure to diesel exhaust: a review of the epidemiologic evidence, *J Occup Environ Med* 46, 1076-1083.
60. Duan, R., Porter, W., Samudio, I., Vyhlidal, C., Kladde, M., and Safe, S. (1999) Transcriptional activation of c-fos protooncogene by 17beta-estradiol: mechanism of aryl hydrocarbon receptor-mediated inhibition, *Mol Endocrinol* 13, 1511-1521.
61. Landi, M. T., Bertazzi, P. A., Baccarelli, A., Consonni, D., Masten, S., Lucier, G., Mocarelli, P., Needham, L., Caporaso, N., and Grassman, J. (2003) TCDD-mediated alterations in the AhR-dependent pathway in Seveso, Italy, 20 years after the accident, *Carcinogenesis* 24, 673-680.

62. Mathieu, M. C., Lapierre, I., Brault, K., and Raymond, M. (2001) Aromatic hydrocarbon receptor (AhR). AhR nuclear translocator- and p53-mediated induction of the murine multidrug resistance *mdr1* gene by 3-methylcholanthrene and benzo(a)pyrene in hepatoma cells, *J Biol Chem* 276, 4819-4827.
63. Kondraganti, S. R., Fernandez-Salguero, P., Gonzalez, F. J., Ramos, K. S., Jiang, W., and Moorthy, B. (2003) Polycyclic aromatic hydrocarbon-inducible DNA adducts: evidence by 32P-postlabeling and use of knockout mice for Ah receptor-independent mechanisms of metabolic activation in vivo, *Int J Cancer* 103, 5-11.
64. van den Berg, M., van Wijnen, J., Wever, H., and Seinen, W. (1989) Selective retention of toxic polychlorinated dibenzo-p-dioxins and dibenzofurans in the liver of the rat after intravenous administration of a mixture, *Toxicology* 55, 173-182.
65. Denison, M. S., and Nagy, S. R. (2003) Activation of the aryl hydrocarbon receptor by structurally diverse exogenous and endogenous chemicals, *Annu Rev Pharmacol Toxicol* 43, 309-334.
66. Backlund, M., and Ingelman-Sundberg, M. (2004) Different structural requirements of the ligand binding domain of the aryl hydrocarbon receptor for high- and low-affinity ligand binding and receptor activation, *Mol Pharmacol* 65, 416-425.
67. Nagy, S. R., Liu, G., Lam, K. S., and Denison, M. S. (2002) Identification of novel Ah receptor agonists using a high-throughput green fluorescent protein-based recombinant cell bioassay, *Biochemistry* 41, 861-868.
68. Sweatlock, J. A., and Gasiewicz, T. A. (1986) The Interaction of 1,3-Diaryltriazenes with the Ah Receptor, *Chemosphere* 15, 1687-1690.
69. Bradshaw, T. D., Stone, E. L., Trapani, V., Leong, C. O., Matthews, C. S., te Poele, R., and Stevens, M. F. (2008) Mechanisms of acquired resistance to 2-(4-Amino-3-methylphenyl)benzothiazole in breast cancer cell lines, *Breast Cancer Res Treat* 110, 57-68.
70. Denison, M. S., Pandini, A., Nagy, S. R., Baldwin, E. P., and Bonati, L. (2002) Ligand binding and activation of the Ah receptor, *Chem Biol Interact* 141, 3-24.
71. Lee, I. J., Jeong, K. S., Roberts, B. J., Kallarakal, A. T., Fernandez-Salguero, P., Gonzalez, F. J., and Song, B. J. (1996) Transcriptional induction of the cytochrome P4501A1 gene by a thiazolium compound, YH439, *Mol Pharmacol* 49, 980-988.

72. Song, J., Clagett-Dame, M., Peterson, R. E., Hahn, M. E., Westler, W. M., Sicinski, R. R., and DeLuca, H. F. (2002) A ligand for the aryl hydrocarbon receptor isolated from lung, *Proc Natl Acad Sci U S A* 99, 14694-14699.
73. Cheung, Y. L., Lewis, D. F., Ridd, T. I., Gray, T. J., and Ioannides, C. (1997) Diaminonaphthalenes and related aminocompounds: mutagenicity, CYP1A induction and interaction with the Ah receptor, *Toxicology* 118, 115-127.
74. Lawrence, B. P., Denison, M. S., Novak, H., Vorderstrasse, B. A., Harrer, N., Neruda, W., Reichel, C., and Woisetschlager, M. (2008) Activation of the aryl hydrocarbon receptor is essential for mediating the anti-inflammatory effects of a novel low-molecular-weight compound, *Blood* 112, 1158-1165.
75. Platzer, B., Richter, S., Kneidinger, D., Waltenberger, D., Woisetschlager, M., and Strobl, H. (2009) Aryl hydrocarbon receptor activation inhibits in vitro differentiation of human monocytes and Langerhans dendritic cells, *J Immunol* 183, 66-74.
76. Backlund, M., Weidolf, L., and Ingelman-Sundberg, M. (1999) Structural and mechanistic aspects of transcriptional induction of cytochrome P450 1A1 by benzimidazole derivatives in rat hepatoma H4IIE cells, *Eur J Biochem* 261, 66-71.
77. Lemaire, G., Delescluse, C., Pralavorio, M., Ledirac, N., Lesca, P., and Rahmani, R. (2004) The role of protein tyrosine kinases in CYP1A1 induction by omeprazole and thiabendazole in rat hepatocytes, *Life Sci* 74, 2265-2278.
78. Negishi, T., Kato, Y., Ooneda, O., Mimura, J., Takada, T., Mochizuki, H., Yamamoto, M., Fujii-Kuriyama, Y., and Furusako, S. (2005) Effects of aryl hydrocarbon receptor signaling on the modulation of TH1/TH2 balance, *J Immunol* 175, 7348-7356.
79. Morales, J. L., Krzeminski, J., Amin, S., and Perdew, G. H. (2008) Characterization of the antiallergic drugs 3-[2-(2-phenylethyl) benzoimidazole-4-yl]-3-hydroxypropanoic acid and ethyl 3-hydroxy-3-[2-(2-phenylethyl)benzoimidazol-4-yl]propanoate as full aryl hydrocarbon receptor agonists, *Chem Res Toxicol* 21, 472-482.
80. Wang, B., and Zhou, S. F. (2009) Synthetic and natural compounds that interact with human cytochrome P450 1A2 and implications in drug development, *Curr Med Chem* 16, 4066-4218.

81. Heath-Pagliuso, S., Rogers, W. J., Tullis, K., Seidel, S. D., Cenijn, P. H., Brouwer, A., and Denison, M. S. (1998) Activation of the Ah receptor by tryptophan and tryptophan metabolites, *Biochemistry* 37, 11508-11515.
82. Rannug, U., Rannug, A., Sjoberg, U., Li, H., Westerholm, R., and Bergman, J. (1995) Structure elucidation of two tryptophan-derived, high affinity Ah receptor ligands, *Chem Biol* 2, 841-845.
83. Bergander, L., Wahlstrom, N., Alsberg, T., Bergman, J., Rannug, A., and Rannug, U. (2003) Characterization of in vitro metabolites of the aryl hydrocarbon receptor ligand 6-formylindolo[3,2-b]carbazole by liquid chromatography-mass spectrometry and NMR, *Drug Metab Dispos* 31, 233-241.
84. Adachi, J., Mori, Y., Matsui, S., Takigami, H., Fujino, J., Kitagawa, H., Miller, C. A., 3rd, Kato, T., Saeki, K., and Matsuda, T. (2001) Indirubin and indigo are potent aryl hydrocarbon receptor ligands present in human urine, *J Biol Chem* 276, 31475-31478.
85. Chen, I., Safe, S., and Bjeldanes, L. (1996) Indole-3-carbinol and diindolylmethane as aryl hydrocarbon (Ah) receptor agonists and antagonists in T47D human breast cancer cells, *Biochem Pharmacol* 51, 1069-1076.
86. Henry, E. C., Kende, A. S., Rucci, G., Totleben, M. J., Willey, J. J., Dertinger, S. D., Pollenz, R. S., Jones, J. P., and Gasiewicz, T. A. (1999) Flavone antagonists bind competitively with 2,3,7, 8-tetrachlorodibenzo-p-dioxin (TCDD) to the aryl hydrocarbon receptor but inhibit nuclear uptake and transformation, *Mol Pharmacol* 55, 716-725.
87. Ashida, H., Fukuda, I., Yamashita, T., and Kanazawa, K. (2000) Flavones and flavonols at dietary levels inhibit a transformation of aryl hydrocarbon receptor induced by dioxin, *FEBS Lett* 476, 213-217.
88. Fukuda, I., Mukai, R., Kawase, M., Yoshida, K., and Ashida, H. (2007) Interaction between the aryl hydrocarbon receptor and its antagonists, flavonoids, *Biochem Biophys Res Commun* 359, 822-827.
89. Reiners, J. J., Jr., Lee, J. Y., Clift, R. E., Dudley, D. T., and Myrand, S. P. (1998) PD98059 is an equipotent antagonist of the aryl hydrocarbon receptor and inhibitor of mitogen-activated protein kinase kinase, *Mol Pharmacol* 53, 438-445.
90. Kuo, S. M. (1997) Dietary flavonoid and cancer prevention: evidence and potential mechanism, *Crit Rev Oncog* 8, 47-69.

91. Birt, D. F., Hendrich, S., and Wang, W. (2001) Dietary agents in cancer prevention: flavonoids and isoflavonoids, *Pharmacol Ther* 90, 157-177.
92. Amakura, Y., Tsutsumi, T., Nakamura, M., Kitagawa, H., Fujino, J., Sasaki, K., Toyoda, M., Yoshida, T., and Maitani, T. (2003) Activation of the aryl hydrocarbon receptor by some vegetable constituents determined using in vitro reporter gene assay, *Biol Pharm Bull* 26, 532-539.
93. Zhang, S., Qin, C., and Safe, S. H. (2003) Flavonoids as aryl hydrocarbon receptor agonists/antagonists: effects of structure and cell context, *Environ Health Perspect* 111, 1877-1882.
94. Chen, I., McDougal, A., Wang, F., and Safe, S. (1998) Aryl hydrocarbon receptor-mediated antiestrogenic and antitumorigenic activity of diindolylmethane, *Carcinogenesis* 19, 1631-1639.
95. Anwar-Mohamed, A., and El-Kadi, A. O. (2009) Sulforaphane induces CYP1A1 mRNA, protein, and catalytic activity levels via an AhR-dependent pathway in murine hepatoma Hepa 1c1c7 and human HepG2 cells, *Cancer Lett* 275, 93-101.
96. Tutel'yan, V. A., Gapparov, M. M., Telegin, L. Y., Devichenskii, V. M., and Pevnitskii, L. A. (2003) Flavonoids and resveratrol as regulators of Ah-receptor activity: protection from dioxin toxicity, *Bull Exp Biol Med* 136, 533-539.
97. Casper, R. F., Quesne, M., Rogers, I. M., Shirota, T., Jolivet, A., Milgrom, E., and Savouret, J. F. (1999) Resveratrol has antagonist activity on the aryl hydrocarbon receptor: implications for prevention of dioxin toxicity, *Mol Pharmacol* 56, 784-790.
98. MacDonald, C. J., Ciolino, H. P., and Yeh, G. C. (2001) Dibenzoylmethane modulates aryl hydrocarbon receptor function and expression of cytochromes P50 1A1, 1A2, and 1B1, *Cancer Res* 61, 3919-3924.
99. Ciolino, H. P., Wang, T. T., and Yeh, G. C. (1998) Diosmin and diosmetin are agonists of the aryl hydrocarbon receptor that differentially affect cytochrome P450 1A1 activity, *Cancer Res* 58, 2754-2760.
100. Rinaldi, A. L., Morse, M. A., Fields, H. W., Rothas, D. A., Pei, P., Rodrigo, K. A., Renner, R. J., and Mallery, S. R. (2002) Curcumin activates the aryl hydrocarbon receptor yet significantly inhibits (-)-benzo(a)pyrene-7R-trans-7,8-dihydrodiol bioactivation in oral squamous cell carcinoma cells and oral mucosa, *Cancer Res* 62, 5451-5456.

101. Schaldach, C. M., Riby, J., and Bjeldanes, L. F. (1999) Lipoxin A4: a new class of ligand for the Ah receptor, *Biochemistry* 38, 7594-7600.
102. Savouret, J. F., Antenos, M., Quesne, M., Xu, J., Milgrom, E., and Casper, R. F. (2001) 7-ketocholesterol is an endogenous modulator for the arylhydrocarbon receptor, *J Biol Chem* 276, 3054-3059.
103. Seidel, S. D., Winters, G. M., Rogers, W. J., Ziccardi, M. H., Li, V., Keser, B., and Denison, M. S. (2001) Activation of the Ah receptor signaling pathway by prostaglandins, *J Biochem Mol Toxicol* 15, 187-196.
104. Oesch-Bartlomowicz, B., Huelster, A., Wiss, O., Antoniou-Lipfert, P., Dietrich, C., Arand, M., Weiss, C., Bockamp, E., and Oesch, F. (2005) Aryl hydrocarbon receptor activation by cAMP vs. dioxin: divergent signaling pathways, *Proc Natl Acad Sci U S A* 102, 9218-9223.
105. Gradelet, S., Astorg, P., Leclerc, J., Chevalier, J., Vernevaut, M. F., and Siess, M. H. (1996) Effects of canthaxanthin, astaxanthin, lycopene and lutein on liver xenobiotic-metabolizing enzymes in the rat, *Xenobiotica* 26, 49-63.
106. Gradelet, S., Astorg, P., Pineau, T., Canivenc, M. C., Siess, M. H., Leclerc, J., and Lesca, P. (1997) Ah receptor-dependent CYP1A induction by two carotenoids, canthaxanthin and beta-apo-8'-carotenal, with no affinity for the TCDD binding site, *Biochem Pharmacol* 54, 307-315.
107. Phelan, D., Winter, G. M., Rogers, W. J., Lam, J. C., and Denison, M. S. (1998) Activation of the Ah receptor signal transduction pathway by bilirubin and biliverdin, *Arch Biochem Biophys* 357, 155-163.
108. Togawa, H., Shinkai, S., and Mizutani, T. (2008) Induction of human UGT1A1 by bilirubin through AhR dependent pathway, *Drug Metab Lett* 2, 231-237.
109. Blank, J. A., Tucker, A. N., Sweatlock, J., Gasiewicz, T. A., and Luster, M. I. (1987) Alpha-Naphthoflavone Antagonism of 2,3,7,8-Tetrachlorodibenzo-Para-Dioxin-Induced Murine Lymphocyte Ethoxyresorufin-O-Deethylase Activity and Immunosuppression, *Molecular Pharmacology* 32, 168-172.
110. Reiners, J. J., Jr., Clift, R., and Mathieu, P. (1999) Suppression of cell cycle progression by flavonoids: dependence on the aryl hydrocarbon receptor, *Carcinogenesis* 20, 1561-1566.
111. Davis, J. W., Jr., Burdick, A. D., Lauer, F. T., and Burchiel, S. W. (2003) The aryl hydrocarbon receptor antagonist, 3-methoxy-4-nitroflavone, attenuates 2,3,7,8-

tetrachlorodibenzo-p-dioxin-dependent regulation of growth factor signaling and apoptosis in the MCF-10A cell line, *Toxicol Appl Pharmacol* 188, 42-49.

112. Lu, Y. F., Santostefano, M., Cunningham, B. D., Threadgill, M. D., and Safe, S. (1995) Identification of 3'-methoxy-4'-nitroflavone as a pure aryl hydrocarbon (Ah) receptor antagonist and evidence for more than one form of the nuclear Ah receptor in MCF-7 human breast cancer cells, *Arch Biochem Biophys* 316, 470-477.
113. Lee, J. E., and Safe, S. (2000) 3',4'-dimethoxyflavone as an aryl hydrocarbon receptor antagonist in human breast cancer cells, *Toxicol Sci* 58, 235-242.
114. Lu, Y. F., Santostefano, M., Cunningham, B. D., Threadgill, M. D., and Safe, S. (1996) Substituted flavones as aryl hydrocarbon (Ah) receptor agonists and antagonists, *Biochem Pharmacol* 51, 1077-1087.
115. Cunningham, B. D., Threadgill, M. D., Groundwater, P. W., Dale, I. L., and Hickman, J. A. (1992) Synthesis and biological evaluation of a series of flavones designed as inhibitors of protein tyrosine kinases, *Anticancer Drug Des* 7, 365-384.
116. Kim, S. H., Henry, E. C., Kim, D. K., Kim, Y. H., Shin, K. J., Han, M. S., Lee, T. G., Kang, J. K., Gasiewicz, T. A., Ryu, S. H., and Suh, P. G. (2006) Novel compound 2-methyl-2H-pyrazole-3-carboxylic acid (2-methyl-4-o-tolylazophenyl)-amide (CH-223191) prevents 2,3,7,8-TCDD-induced toxicity by antagonizing the aryl hydrocarbon receptor, *Mol Pharmacol* 69, 1871-1878.
117. Sakamoto, K. M. (2005) Chimeric molecules to target proteins for ubiquitination and degradation, *Methods Enzymol* 399, 833-847.
118. Schneekloth, J. S., Jr., Fonseca, F. N., Koldobskiy, M., Mandal, A., Deshaies, R., Sakamoto, K., and Crews, C. M. (2004) Chemical genetic control of protein levels: selective in vivo targeted degradation, *J Am Chem Soc* 126, 3748-3754.
119. Rodriguez-Gonzalez, A., Cyrus, K., Salcius, M., Kim, K., Crews, C. M., Deshaies, R. J., and Sakamoto, K. M. (2008) Targeting steroid hormone receptors for ubiquitination and degradation in breast and prostate cancer, *Oncogene* 27, 7201-7211.
120. Tang, Y. Q., Han, B. M., Yao, X. Q., Hong, Y., Wang, Y., Zhao, F. J., Yu, S. Q., Sun, X. W., and Xia, S. J. (2009) Chimeric molecules facilitate the degradation of androgen receptors and repress the growth of LNCaP cells, *Asian J Androl* 11, 119-126.

121. Kaelin, W. G., Jr. (2002) How oxygen makes its presence felt, *Genes Dev* 16, 1441-1445.
122. Kaelin, W. G., Jr. (2002) Molecular basis of the VHL hereditary cancer syndrome, *Nat Rev Cancer* 2, 673-682.
123. Puppala, D., Gairola, C. G., and Swanson, H. I. (2007) Identification of kaempferol as an inhibitor of cigarette smoke-induced activation of the aryl hydrocarbon receptor and cell transformation, *Carcinogenesis* 28, 639-647.
124. Lepley, D. M., Li, B., Birt, D. F., and Pelling, J. C. (1996) The chemopreventive flavonoid apigenin induces G2/M arrest in keratinocytes, *Carcinogenesis* 17, 2367-2375.
125. Birt, D. F., Pelling, J. C., Nair, S., and Lepley, D. (1996) Diet intervention for modifying cancer risk, *Prog Clin Biol Res* 395, 223-234.
126. Lepley, D. M., and Pelling, J. C. (1997) Induction of p21/WAF1 and G1 cell-cycle arrest by the chemopreventive agent apigenin, *Mol Carcinog* 19, 74-82.
127. Havsteen, B. H. (2002) The biochemistry and medical significance of the flavonoids, *Pharmacol Ther* 96, 67-202.
128. Puppala, D., Lee, H., Kim, K. B., and Swanson, H. I. (2008) Development of an aryl hydrocarbon receptor antagonist using the proteolysis-targeting chimeric molecules approach: a potential tool for chemoprevention, *Mol Pharmacol* 73, 1064-1071.
129. Chen, D., Chen, M. S., Cui, Q. C., Yang, H., and Dou, Q. P. (2007) Structure-proteasome-inhibitory activity relationships of dietary flavonoids in human cancer cells, *Front Biosci* 12, 1935-1945.
130. Mak, P., Leung, Y. K., Tang, W. Y., Harwood, C., and Ho, S. M. (2006) Apigenin suppresses cancer cell growth through ERbeta, *Neoplasia* 8, 896-904.
131. Puppala, D., Gairola, C. G., and Swanson, H. I. (2006) Identification of kaempferol as an inhibitor of cigarette smoke induced activation of the aryl hydrocarbon receptor and cell transformation, *Carcinogenesis*.
132. Chiang, L. C., Ng, L. T., Lin, I. C., Kuo, P. L., and Lin, C. C. (2006) Anti-proliferative effect of apigenin and its apoptotic induction in human Hep G2 cells, *Cancer Lett* 237, 207-214.

133. Shukla, S., Mishra, A., Fu, P., MacLennan, G. T., Resnick, M. I., and Gupta, S. (2005) Up-regulation of insulin-like growth factor binding protein-3 by apigenin leads to growth inhibition and apoptosis of 22Rv1 xenograft in athymic nude mice, *Faseb J* 19, 2042-2044.
134. Fukuda, I., Kaneko, A., Nishiumi, S., Kawase, M., Nishikiori, R., Fujitake, N., and Ashida, H. (2009) Structure-activity relationships of anthraquinones on the suppression of DNA-binding activity of the aryl hydrocarbon receptor induced by 2,3,7,8-tetrachlorodibenzo-p-dioxin, *J Biosci Bioeng* 107, 296-300.
135. Wang, M. X., Funabiki, K., and Matsui, M. (2003) Synthesis and properties of bis(hetaryl)azo dyes, *Dyes and pigments* 57, 77-86.
136. Azumaya, I., Okamoto, T., Imabeppu, F., and Takayanagi, H. (2003) Simple and convenient synthesis of tertiary benzanilides using dichlorotriphenylphosphorane, *Tetrahedron* 59, 2325-2331.
137. Rauch, P., Puttmann, M., Oesch, F., Okamoto, Y., and Robertson, L. W. (1987) Differential induction of cytochrome P-450 by the enantiomers of trans-stilbene oxide, *Biochem Pharmacol* 36, 4355-4359.
138. Cikryt, P., Gottlicher, M., and Neumann, H. G. (1990) Competitive binding affinity of carcinogenic aromatic amines to the rat hepatic aromatic hydrocarbon (Ah) receptor in vitro and potency to induce monooxygenase activity in vivo, *Carcinogenesis* 11, 1359-1366.
139. Poland, A., Clover, E., Kende, A. S., DeCamp, M., and Giandomenico, C. M. (1976) 3,4,3',4'-Tetrachloro azoxybenzene and azobenzene: potent inducers of aryl hydrocarbon hydroxylase, *Science* 194, 627-630.
140. Kirby, A. H. (1947) Studies in carcinogenesis with azo compounds; the action of four azo compounds in Wistar rats fed restricted diets; N,N-diethyl-p-aminoazobenzene in mice, *Cancer Res* 7, 333-341.
141. Kato, T. A., Matsuda, T., Matsui, S., Mizutani, T., and Saeki, K. (2002) Activation of the aryl hydrocarbon receptor by methyl yellow and related congeners: structure-activity relationships in halogenated derivatives, *Biol Pharm Bull* 25, 466-471.
142. Yuta, K., and Jurs, P. C. (1981) Computer-assisted structure-activity studies of chemical carcinogens. Aromatic amines, *J Med Chem* 24, 241-251.

VITA

HYOSUNG LEE

BIRTH

January 03, 1972

Seoul, Republic of Korea (South Korea)

EDUCATION

1998-2000 Master of Science, Biotechnology, Organic & Natural Product Chemistry,
Yonsei University, College of Engineering, Seoul, Korea

Thesis: Synthesis of N-substituted tyramine derivatives as aldose reductase inhibitors.

1992-1998 Bachelor of Science, Biotechnology, Yonsei University, College of
Engineering, Seoul, Korea

Thesis: Synthesis of isoguanosine derivatives as anticancer agents.

SCHOLASTIC AND PROFESSIONAL HONORS

1995-1996 Yonsei Fellowship, Yonsei University

1998-1999 Graduate Fellowship, Yonsei graduate school

2010~ Rho Chi Honor Society membership, Alpha Xi Chapter

PROFESSIONAL POSITIONS

- 2003-2005 Researcher, University of Kentucky, College of Pharmacy
 Project: Synthesis of proteolysis inducing small molecule
- 2002 Researcher, STC Institute for life science
 Project: Screening for anti-wrinkle agent from medicinal plant
- 2001 Researcher, Medical Research Center, Yonsei Medical School.
 Project: Bone Analysis by EXAFS, development of embolizer
- 2000 Researcher, Green Biotech Co. LTD., R&D Center
 Project: Screening for anticoagulants from *Ginkgo biloba*
- 1998-2000 Research Assistant, Department of biotechnology, Yonsei University
 Project: Synthesis of analogues of microbial anti-diabetic agent
- 1995-1998 Undergraduate Lab-tech, Department of biotechnology, Yonsei University
 Project: Synthesis of isogunosine analogues as anticancer agent

PROFESSIONAL PUBLICATIONS

1. Cyrus, Kedra; Wehenkel, Marie; Choi, Eun-Young; **Lee, Hyosung**; Kim, Kyung Bo. Jostling for position; optimizing linker location in the design of Estrogen Receptor-targeting PROTACs. *Journal of the American Chemical Society*. (submitted in 2010 Apr.)
2. Ban, Jung Ok; Oh, Ju Hoon; Hwang, Bang Yeon; Moon, Dong Cheul; Jeong, Heon-Sang; Lee, Seram; Kim, Soyoun; **Lee, Hyosung**; Kim, Kyung-Bo; Han, Sang Bae; Hong, Jin Tae. Inflexinol inhibits colon cancer cell growth through inhibition of nuclear factor- κ B activity via direct interaction with p50. *Molecular Cancer Therapeutics*, June 1, 2009, 8, 1613
3. Dinesh Puppala, **Hyosung Lee**, Kyung Bo Kim, Hollie I. Swanson. Development of an AHR antagonist using the Protacs Approach: A potential tool for chemoprevention. *Molecular Pharmacology*, 73, 2008 Jan, 4, 1064-1071

4. **Lee, Hyosung**; Puppala, Dinesh; Choi, Eun-Young; Swanson, Hollie I; Kim, Kyung-Bo, Targeted degradation of the aryl hydrocarbon receptor by the PROTAC approach: a useful chemical genetic tool. *ChemBioChem: A European journal of chemical biology*. 2007 Dec; 8(17), 2058-2062.
5. Ho A, Kim YE, **Lee HyoSung**, Cyrus K, Baek SH, Kim KB.; SAR studies of 2-methoxyestradiol and development of its analogs as probes of anti-tumor mechanisms.; *Bioorganic & medicinal chemistry letters*. 2006 Jul; 1;16(13):3383-7
6. Bargagna-Mohan P, Baek SH, Lee Hyosung, Kim K, Mohan R.; Use of PROTACS as molecular probes of angiogenesis.; *Bioorganic & medicinal chemistry letters*. 2005 Jun; 2;15(11):2724-7
7. Zhang, D.; Baek, S.H.; Ho, A.; **Lee, Hyosung.**; Jeong, Y.S.; Kim, K.B. Targeted degradation of proteins by small molecules: a novel tool for functional proteomics. *Comb. Chem. High Throughput Screen*. 2004 Nov; 7(7):689-97
8. Sun WS, **Lee HyoSung**, Park JM, Kim SH, Yu JH, Kim JH.; YUA001, a novel aldose reductase inhibitor isolated from alkalophilic *Corynebacterium* sp. YUA25. II. Chemical modification and biological activity. *The journal of antibiotics*. 2001 Oct; 54(10):857-30

SCIENTIFIC MEETINGS/PRESENTATIONS

Hyosung Lee, Eun-Young Choi, RW Cameron Dingle, Hollie I. Swanson, Kyung Bo Kim. Development of novel AHR antagonists using PROTAC technology: A potential tool for chemoprevention. Cancer Research day, Markey Cancer center, University of Kentucky, Lexington KY, USA, Apr 14, 2010

Hyosung Lee, Eun-Young Choi, Hollie I. Swanson, Kyung Bo Kim. Targeted degradation of Aryl Hydrocarbon Receptor (AHR) by PROTAC: A potential approach to chemoprevention. Cancer Research day, Markey Cancer center, University of Kentucky, Lexington KY, USA, Oct 30, 2008

Lee, Hyosung. Chemical approach to biology. Korean Biomedical Association at the University of Kentucky seminar series, Mar 2008.

Dinesh Puppala, **Hyosung Lee**, Kyung Bo Kim, Hollie I. Swanson. Development of an AHR antagonist using the PROTACS Approach: A potential tool for chemoprevention. Cancer Research day. Markey Cancer center, University of Kentucky, Lexington KY, United States, Sep 27, 2007.

Lee, Hyosung; Puppala, Dinesh; Choi, Eun-Young; Swanson, Hollie I.; Kim, Kyung Bo, Targeted degradation of aryl hydrocarbon receptor via the PROTAC approach: A chemical genetic tool for AHR biology. Ohio Valley Society of Toxicology Annual meeting, Eli Lilly and Company, Indianapolis, IN United States, Nov 02, 2007.

Lee, Hyosung; Puppala, Dinesh; Choi, Eun-Young; Swanson, Hollie I.; Kim, Kyung Bo, Targeted degradation of aryl hydrocarbon receptor via the PROTAC approach: A chemical genetic tool for AHR biology. 39th Central Regional Meeting of the American Chemical Society, Covington, KY, United States, May 20-23, 2007.

Lee, Hyosung; Puppala, Dinesh; Choi, Eun-Young; Swanson, Hollie I; Kim, KyungBo, Targeted degradation of aryl hydrocarbon receptor via the PROTAC approach: A chemical genetic tool for AHR biology. 233rd American Chemical Society National Meeting Chicago, IL, United States, March 25-29, 2007.

Lee, Hyosung. Chemical genetic approach to biology. Korean Biomedical Association at the University of Kentucky, seminar series, Apr 2007.

Lee, Hyosung. Chemical genetic approach to natural product. Korean Biomedical Association at the University of Kentucky, seminar series, Nov 2005.

Lee, Hyosung. Target oriented organic synthesis. Korean Biomedical Association in University of Kentucky seminar series, Sep 2003.

Jin Hang Huh, Jin Suk Choi, Sang Eun Lee, **Hyosung Lee**, Geum Hee Hwang; Screening for anti-wrinkle agent from the oriental medicinal plants. Korean Society of Food Science and technology, 69th annual meeting and symposium, Muju, Rep. of Korea, Oct 2002

Sung Han Kim, Won Suk Sun, Jung Ae Jun, **Hyosung Lee**, Jung Han Kim; Synthesis of Berberine derivatives as anticancer agents. Korean Chemical Society, 81st national meeting and symposia. Ewha Womans University Seoul, Korea, Apr 1998

Sung Han Kim, Won Suk Sun, Sung Wook Oh, Sang Jun Lee, **Hyosung Lee**, Jung Han Kim; Synthesis of Isoguanosine derivatives as anticancer agents. International Union of Pure & Applied Chemistry, 36th general Congress and symposium. Geneva, Switzerland, Aug 1997